Wireless Communications and Mobile Computing

Full-Duplex and Cognitive Radio Networking for the Emerging 5G Systems

Lead Guest Editor: Mohammad Shikh-Bahaei
Guest Editors: Yang-seok Choi and Daesik Hong

Full-Duplex and Cognitive Radio Networking for the Emerging 5G Systems

Wireless Communications and Mobile Computing

Full-Duplex and Cognitive Radio Networking for the Emerging 5G Systems

Lead Guest Editor: Mohammad Shikh-Bahaei
Guest Editors: Yang-seok Choi and Daesik Hong

Editorial Board

Contents

Hindawi
Wireless Communications and Mobile Computing
Volume 2018, Article ID 8752749, 2 pages
https://doi.org/10.1155/2018/8752749

Editorial

Full-Duplex and Cognitive Radio Networking for the Emerging 5G Systems

M. Shikh-Bahaei,[1] **Y.-S. Choi**,[2] **and D. Hong**[3]

[1]*Department of Informatics, King's College London, 30 Aldwych, London WC2B 4BG, UK*
[2]*Intel Labs, Hillsboro, OR, USA*
[3]*Department of Electrical and Electronic Engineering, Yonsei University, 134 Sinchon-dong, Seodaemun-gu, Seoul 120-749, Republic of Korea*

Correspondence should be addressed to M. Shikh-Bahaei; m.sbahaei@kcl.ac.uk

Received 4 February 2018; Accepted 6 February 2018; Published 4 March 2018

Full duplex and cognitive radio technologies have paved the way to enormous advances in wireless communications. Cognitive radio, since 1990s, has predicted transceivers that can be aware of their surroundings and be able to detect and exploit underutilized frequency bands licensed to other users. With half duplex radios, sensing the primary channels, detecting spectrum holes, and accessing the idle or underutilized channels according to certain algorithms are performed *sequentially* by cognitive (secondary) users. This can inherently cause interfering with primary users in the licensed bands, as secondary users cannot hear the return of primary users while transmitting data.

With full duplex radio, on the other hand, the users can transmit data and sense/receive data *simultaneously*. This can potentially improve the throughput of the secondary network and at the same time provide better protection to the primary users. Since the secondary users can sense the primary channel(s) whilst transmitting over the primary's idle channel, they can detect return of primary users and would immediately stop transmission over the respective frequency band. End to end delay reduction is also another major benefit of full duplex communication, as some of the above sequential processes can be made concurrent with full duplex radio.

Potential benefits of full duplex communication, specifically in enhancing spectral efficiency, have also been known since 1960s. However, hardware and system complexities hindered wide use of these technologies in realistic conditions; substantial effect of self-interference in full duplex radio and practical difficulties in cancelling it were the prime reasons for the five-decade delay in serious attention to this technology. Recent advances in self-interference cancellation, through cutting edge digital and analog signal processing techniques, have brought full duplex communication closer to reality. At the same time, remarkable advances in centralized and distributed signal processing, machine to machine communication, deep learning methods, and cloud/edge computing have spurred a major shift in cognitive radio paradigm and realized many early promises of this technology.

Applications of these two technologies, in the future wireless networks, can be vast, and the potentials for improving network performance, for example, in terms of delay and throughput, are promising. As said above, by combining the two technologies, that is, cognitive and full duplex radio, even further benefits can be achieved, for instance, offering higher secondary user throughput and concurrently protecting the primary users through parallel sensing and transmitting data by the secondary users.

However, when we deal with 4th and 5th generation dense networks and apply full duplex and cognitive radio technologies in the emerging Internet of Things, new challenges will arise. For instance, multiuser interference is increased when full duplex communication is exploited in multiuser scenarios, and especially in dense environments. This will necessitate new cognitive and full duplex MAC- and Network-layer protocols to tackle these problems in multiuser and multihop scenarios. Such new MAC and Network layer protocols can be far more efficient than the respective standard protocols, as the users can *learn* the

environment through cognitive radio and can *transmit while sensing* through full duplex radio.

Security is another concern in wireless networks with potentially large number of users/machines competing for limited shared pool of resources, specifically in shared spectrum cognitive network conditions.

The present special issue of this journal is dedicated to addressing some of the challenges in cognitive and full duplex networking. The first paper "Cognitive Security of Wireless Communication Systems in the Physical Layer" by M. H. Yilmaz et. al. looks into so-called "cognitive security" and proposes new physical layer measures for enhancing security in cognitive wireless networks. This paper specifically suggests employing an adaptive radio that adapts to the network condition and accordingly takes necessary precautions before security attack takes place.

The second paper, "Fast Cooperative Energy Detection under Accuracy Constraints in Cognitive Radio Networks" by S. Peng et al., studies minimizing the delay incurred in finding and accessing frequency holes in cognitive networks. Service latency is a critical constraint in many of the applications in the 5th generation wireless systems. The proposed technique in this work is based on cooperative energy detection by the secondary (i.e., cognitive) users.

The third paper, "Coexistence of Cognitive Small Cell and WiFi System: A Traffic Balancing Dual-Access Resource Allocation Scheme" by X. Huang et al., touches upon optimization of heterogeneous cognitive networks, comprising (licensed) small cells and (unlicensed) wifi constituents. 5G networks are envisaged to corroborate the idea of cognitive networking in heterogeneous conditions; hence optimal allocation of resources in such networks is essential for achieving fair and high quality of service provisioning to various applications. New power allocation algorithms are presented by the authors to achieve traffic balance between licensed and unlicensed users in a cognitive networking setup.

The 4th paper, "Distributed Schemes for Crowdsourcing-based Sensing Task Assignment in Cognitive Radio Networks" by L. Zhai et al. studies crowdsourcing by exploiting spectrum sensing in cognitive wireless networks. This paper considers the scenario where spectrum sensing is assigned to mobile terminals and tablets as a distributed task. The authors propose a number of algorithms in order to optimize this assignment.

The last paper, "Cooperative Full-Duplex Physical and MAC Layer Design in Asynchronous Cognitive Networks" by T. Febrianto et. al., studies an asynchronous cognitive network (i.e., no synchronicity between primary and secondary users), where the nodes are also capable of full duplex communication. Full duplex radio in cognitive users has been exploited for enhancing the sum-throughput of the network. The users can simultaneously transmit and sense channel/receive data. This paper also proposes a new full duplex MAC protocol for the case where multiple secondary users cooperatively sense the primary channels. This paper considers the case where a cognitive full duplex user can sense multiple channels and studies the effect of the number of sensed channels on the MAC throughput.

M. Shikh-Bahaei
Y.-S. Choi
D. Hong

Hindawi
Wireless Communications and Mobile Computing
Volume 2018, Article ID 4092681, 17 pages
https://doi.org/10.1155/2018/4092681

Research Article

Coexistence of Cognitive Small Cell and WiFi System: A Traffic Balancing Dual-Access Resource Allocation Scheme

Xiaoge Huang, Yangyang Li, She Tang, and Qianbin Chen

Chongqing Key Laboratory of Mobile Communication Technology, Chongqing University of Posts and Telecommunications, Chongqing, China

Correspondence should be addressed to Yangyang Li; lyyhenan@163.com

Received 26 May 2017; Revised 17 November 2017; Accepted 11 December 2017; Published 8 January 2018

Academic Editor: Yang-Seok Choi

We consider a holistic approach for dual-access cognitive small cell (DACS) networks, which uses the LTE air interface in both licensed and unlicensed bands. In the licensed band, we consider a sensing-based power allocation scheme to maximize the sum data rate of DACSs by jointly optimizing the cell selection, the sensing operation, and the power allocation under the interference constraint to macrocell users. Due to intercell interference and the integer nature of the cell selection, the resulting optimization problems lead to a nonconvex integer programming. We reformulate the problem to a nonconvex power allocation game and find the relaxed equilibria, quasi-Nash equilibrium. Furthermore, in order to guarantee the fairness of the whole system, we propose a dynamic satisfaction-based dual-band traffic balancing (SDTB) algorithm over licensed and unlicensed bands for DACSs which aims at maximizing the overall satisfaction of the system. We obtain the optimal transmission time in the unlicensed band to ensure the proportional fair coexistence with WiFi while guaranteeing the traffic balancing of DACSs. Simulation results demonstrate that the SDTB algorithm could achieve a considerable performance improvement relative to the schemes in literature, while providing a tradeoff between maximizing the total data rate and achieving better fairness among networks.

1. Introduction

Recently, the rapid progress and pleasant experience of smart Internet based devices lead to an increasing demand for high data rate in wireless communication systems, which cause the growth of mobile traffic over thousands of times in the next decade [1]. However, since the licensed spectrum is limited, the new available licensed spectrum is becoming rare and expensive. To respond to increasing wireless communication capacity demand, new technologies have been proposed for cellular networks, such as small cells, microwave, massive *multiple-input multiple-output* (MIMO). Small cells as parts of the second tier in multitiered cellular networks have been considered as an effective means to boost the capacity and expand the coverage [2]. The incorporation of massive MIMO techniques into cellular networks can boost the channel throughput by transmitting independent data streams simultaneously over different antennas. However, the scarcity of the licensed spectrum is still the major block to further improve the data rate. The innovations that focus on the techniques that enable better utilization of the spectrum, including unlicensed bands, are an urgent issue. Specifically, it is assumed that up to 30% of the broadband access in cellular networks can be offloaded to the unlicensed spectrum occupied by WiFi networks [3].

Cognitive radio is able to enhance the spectrum efficiency by allowing cognitive radio users (CRs) to access the resources owned by primary users (PUs) in an opportunistic manner. In order to minimize the performance degradation caused to PUs, CRs perform spectrum sensing to determine the status of the spectrum [4]. In this paper, we define a dual-access cognitive small cell (DACS) network which takes the advantage of CRs and small cell networks. The DACS network could reuse the spectrum over small regions, which is regarded as one of the promising solutions for expanding the coverage and boosting the capacity of wireless networks. In addition, cognitive small cell base stations (CSBSs) can coexist with macrocell base stations (MBSs) by using the unoccupied licensed spectrum based on sensing results. One of the primary tasks of the DACS is to find a proper

selection mechanism for cognitive small cell users (CSUs) and the associated CSBSs based on the sensing performance. However, the reliability of the sensing result is limited by several factors; thus the influence of the sensing accuracy should be taken into account.

Particularly, the unlicensed spectrum is considered as a solution of disposing the scarcity and valuableness of the licensed spectrum in Rel. 13, which supports the LTE system to offload the traffic to the unlicensed spectrum used by WiFi network, namely, LTE-*unlicensed* (LTE-U) [5]. The extension of LTE over 5 GHz spectrum requires providing fair coexistence of LTE-U with already existing WiFi systems. A feasible way to use both the licensed and unlicensed band simultaneously through the carrier aggregation feature (CA) is investigated in [6, 7]. On the one hand, allowing cellular networks to share the unlicensed band could mitigate spectrum scarcity in the licensed spectrum, while improving spectrum efficiency in the unlicensed band. Literature [8] investigated traffic load offloading from LTE-U to WiFi and aims to maximize the throughput of LTE-U with the minimum throughput requirement of WiFi networks. On the other hand, the impact of the cellular network on the WiFi system is not negligible; for example, the transmission of LTE users could increase the collision probability to WiFi systems. Therefore, there comes a critical challenge for designers to ensure that the LTE-U can coexist with WiFi fairly and friendly in the unlicensed band while guaranteeing regulatory requirement of the local government policy.

1.1. Related Work. In the licensed band, resource allocation problems are discussed in [9–13]. The power allocation problem in cognitive small cell networks (CSNs) leads to a noncooperative game (NCG) which was discussed in [11]. In addition, the sensing information was addressed in [12] as a part of the game, and the analysis of the equilibria is based on a concept called quasi-Nash equilibrium (QNE) [13].

The current researches focus on the coexistence of LTE-U and WiFi in the unlicensed band based on different deployment scenarios [14–18]. In [14], the authors proposed a time-domain resource separation method based on almost blank subframes (ABSs). In this scenario, LTE users stop transmitting in ABSs, whereas WiFi users have the opportunity to access the channel without interference. A similar coexistence scheme was proposed in [15], where LTE users allocate silent gaps with a predefined duty cycle to facilitate better coexistence with WiFi users. However, those schemes cannot achieve the optimal performance of LTE-U operation due to its discontinuous transmission. In [16], Zhang et al. proposed an enhanced static ABSs scheme to mitigate the cochannel interference between small cells and WiFi systems. The authors in [17] specially aim to optimize the transmission QoS of LTE users with the minimum transmission requirement of WiFi users, while it does not meet QoS requirement of all the LTE users by the designed mechanism. Based on the decision tree and the game theory, [18] presented a flexible architecture decoupling control plane from data plane which could improve throughput and spectrum efficiency.

Listen-before-talk (LBT) scheme is a another way to enable the coexistence of LTE-U and WiFi in the unlicensed band [19–22]. In [19], the authors proposed a LBT scheme by enabling carrier sensing at each LTE-eNB. Although the scheme can enable fair coexistence between LTE-U and WiFi, it results in spectrum underutilization due to the carrier sense operation in the LBT scheme. The fair coexistence between LTE-U and WiFi in the unlicensed band has been investigated by a stochastic geometry modeling approach where the LBT scheme is applied at SBSs [20]. A channel access framework based on LBT mechanism in LTE-U systems was proposed in [21], without the consideration of the licensed and the unlicensed spectrum management. In [22], the authors introduced a new time-frequency structure with a modified LBT scheme.

Traffic balancing scheme between licensed and unlicensed bands was proposed in [23–25]. The authors in [23] presented traffic balancing scheme in the licensed and unlicensed band by controlling the transmission power in the licensed band and the fraction of transmission time in the unlicensed band, respectively. However, the analysis in [23] was limited to the single user case, which can not be easily extended to the case with multiple users. For the downlink traffic balancing between licensed and unlicensed bands, [24] proposed a regret-based learning aided downlink traffic balancing scheme to ensure fair coexistence between LTE-U and WiFi. Jointly considering the power control and spectrum allocation in licensed/unlicensed bands to maximize the spectrum efficiency while guaranteeing the QoS of small cell users and WiFi users was discussed in [25].

1.2. Contributions. In this study, dual-access cognitive small cell (DACS) refers to the cognitive small cell with LTE technologies which can access both licensed and unlicensed bands simultaneously. The transmission model is based on the current wireless transmission system, in which the licensed spectrum is scarce and UEs have ever increasing data rate requirements, especially for downlink transmission. Thus, the supplemental downlink (SDL) model is suggested in [17, 26]; in this model LTE could offload parts of the traffic load to the unlicensed band and coexist with the WiFi user while taking into account the WiFi transmission requirements. In addition, in order to ensure the transmission QoS, the control information will still use the licensed band. Therefore, we use the licensed band to support the uplink transmission and use the unlicensed band to support the downlink transmission. Assume there are two sets of antennas for each CSBS; A_L is used for the licensed band and A_u for the unlicensed band. The DACS can access both licensed and unlicensed bands simultaneously; in the licensed band, CSUs are considered as the secondary users which work based on the mechanism of cognitive radio (CR) technologies. It could reuse the licensed spectrum when the macrocell users (MUs) are absent. In the unlicensed band, CSUs share the unlicensed spectrum with WiFi users by adjusting the transmission time. The objective is to maximize the utility of the whole system (including macrocell system, DACS system, and WiFi system), which could evaluate the satisfaction of the whole system, while guaranteeing the coexistence between CSUs and WiFi users in the unlicensed band. The main contributions can be summarized as follows:

(i) Firstly, CSU defined in this paper is based on CR technologies in which the licensed band could be reused when the MBS is absent. In addition, SDL model is considered for the transmission scheme, and parts of the downlink traffic load could be offloaded to the unlicensed band while the control information still uses the licensed band to ensure the transmission QoS. We propose a sensing-based power allocation scheme to maximize the total data rate of the whole network (LTE and WiFi) by jointly optimizing the cell selection, the sensing operation, and the power allocation as well as the unlicensed band transmission time.

(ii) Secondly, in the licensed band, we aim at maximizing the total data rate of DACSs by jointly optimizing the CSU-CSBS assignment, the detection operation, and the power allocation under the interference constraint to MUs. Due to the nonconvexity of the optimization problem, we reformulate the problem to a nonconvex power allocation game and find the quasi-Nash equilibrium (QNE) of the nonconvex game. The sufficient conditions for the existence and the uniqueness of a QNE are given by theoretical prove.

(iii) Thirdly, in the unlicensed band, taking into account the dynamic WiFi traffic load with varying transmission probability, we propose a dynamic channel access scheme for CSUs based on enhanced-LBT (E-LBT) scheme which could increase the spectrum efficiency and guarantee the transmission QoS of WiFi networks in the unlicensed band. Specifically, we analyze the WiFi traffic load by a statistical method, which could calculate the optimal transmission time of CSU based on the transmission probability of WiFi users.

(iv) Finally, we propose a satisfaction-based dual-band traffic balancing (SDTB) algorithm over the licensed and the unlicensed band which aims at maximizing the overall utility of DACSs and WiFi networks by jointly optimizing the cell selection, detection operation, and power allocation in the licensed band and transmission time in the unlicensed band. Furthermore, we calculate the computation complexity and evaluate the performance of the proposed SDTB scheme in the realistic channel status with multi-CSBS and multi-AP.

In the rest of this paper, we describe the system model in Section 2 and formulate the optimization problem in Section 3. The optimal satisfaction-based dual-band traffic balancing scheme is shown in Section 4. The simulation results are discussed in Section 5 and Section 6 finally concludes the paper.

Notations. Matrices and vectors are indicated in boldface. $\mathbb{C}^{m\times n}$ denotes that the space size of matrix is $m \times n$. $\mathrm{Tr}(\cdot)$ and $(\cdot)^H$ stand for trace and Hermitian transpose, respectively. $[\cdot]^+$ denotes $\max(0, \cdot)$. $\nabla^2_{\mathbf{x}} R(\mathbf{x})$ is the Hessian matrix of function $R(\mathbf{x})$; $\nabla_{\mathbf{x}} R(\mathbf{x})$ is the gradient of function $R(\mathbf{x})$ at point $\mathbf{x}$.

2. System Model

As shown in Figure 1, we consider a DACS system which could transmit and receive signals in both licensed and unlicensed bands simultaneously. There are M CSBSs, J CSUs, one MBS, K MUs, one WiFi-AP, and N WiFi users. In the licensed band, we consider the uplink transmission of CSBSs based on sensing results from antennas A_L while sharing the unlicensed band with WiFi systems for downlink transmission based on sensing results from antennas A_u. Due to the limited coverage radius of CSBSs, the number of CSUs and CSBSs is in an order of magnitude. Assuming both the CSBSs and the MBS are equipped with N_r antennas (including A_L and A_u), WiFi-AP and various users (CSUs, MUs, and WiFi users) are equipped with N_t antennas (including A_L and A_u). There is no cooperation within the heterogeneous network (macrocell network, DACS network, and WiFi network). Each user can simultaneously communicate over multiple channels; thus, multiuser interference (MUI) in the same channel must be taken into account.

2.1. Resource Allocation for CSUs with MUs in the Licensed Band. In the licensed band, we consider the uplink transmission under OFDMA technology where CSUs could control the emitted antenna pattern and the power allocation of each subchannel through the precoding matrices. We aim at maximizing the sum rate of overall DACSs with proper precoding matrix, as well as the best assignment between CSU j ($j = 1, 2, \ldots, J$) and the associated CSBS i ($i = 1, 2, \ldots, M$). The binary incidence matrix is $\mathbf{A}$, whose coefficients a^{ij} shows the status between CSBS i and CSU j. If $a^{ij} = 1$, it denotes that CSU j and CSBS i are associated; otherwise $a^{ij} = 0$. The binary incidence matrix a^{ij} should satisfy the following conditions:

(1) For CSU j, $\sum_{i=1}^{M} a^{ij} = 1$ means that CSU j can only connect to one CSBS;

(2) For CSBS i, $\sum_{j=1}^{J} a^{ij} \le D$, where D is the maximum acceptable number of CSUs for CSBS i.

The value D is derived from zero-forcing (ZF) decoding to eliminate the interference; thus, $D \le N_r/N_t$. Based on this assumption, CSUs connected to the same CSBS do not have interference, while there is intercell interference between DACSs and macrocell networks. The frame structure of CSU j consists of a sensing slot of duration t_s and a data transmission slot of duration $T_L - t_s$ over k ($k = 1, 2, \ldots, K$) spatial subchannels. In the sensing slot, if MU is detected absent, CSUs start transmitting in the transmission slot. We assume that simultaneous spectrum sensing of each licensed subchannel is performed by the set of antennas A_L at each CSBS under energy detection scheme, where the MU signal is modeled as a complex Gaussian random signal in the presence of an additive white Gaussian noise. The detection problem on subchannel k can be formulated as a hypothesis test, where hypothesis $H_{0,k}$ represents the absence of a MU in subchannel k, and hypothesis $H_{1,k}$ represents the presence of

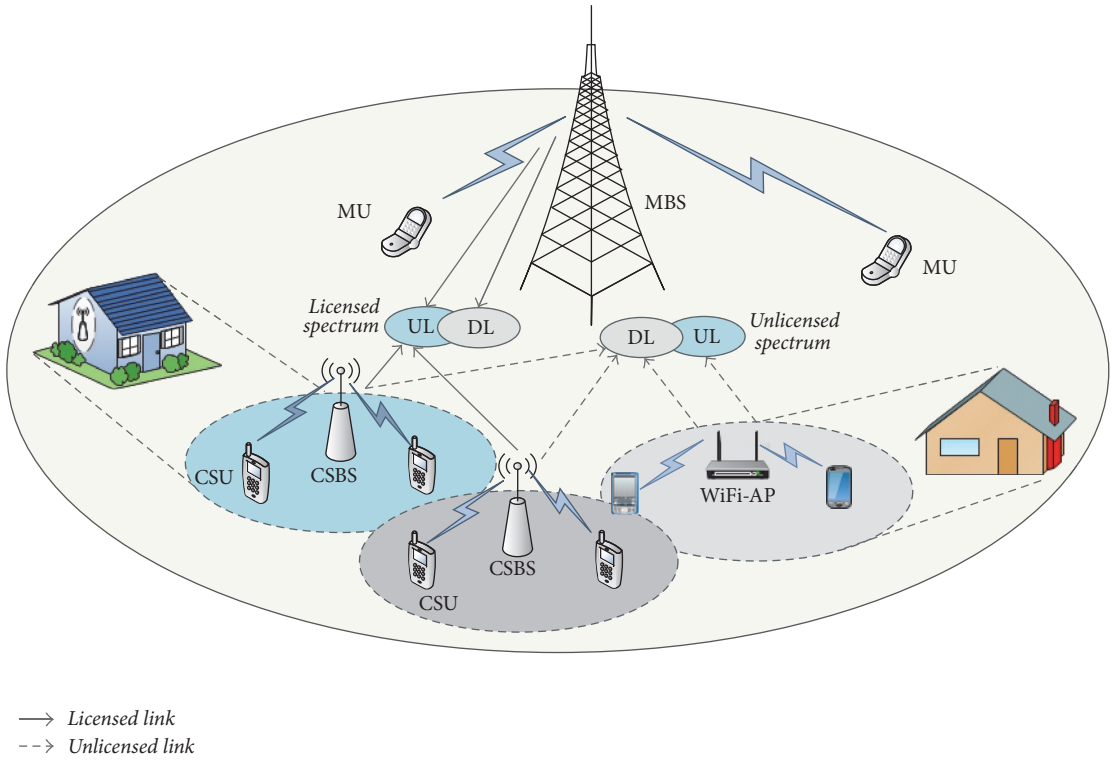

Figure 1: Network model. Illustration of DACSs shares licensed bands with the macrocell network and unlicensed bands with the WiFi network.

a MU in subchannel k. Specifically, for channel k, the received signal $\mathbf{y}_k^i$ at CSBS i can be formulated as

$$\begin{aligned} H_{0,k} &: \mathbf{y}_k^i(t) = \mathbf{n}_k(t) \\ H_{1,k} &: \mathbf{y}_k^i(t) = \mathbf{S}_k^i(t) + \mathbf{n}_k(t), \end{aligned} \tag{1}$$

where $\mathbf{y}_k^i(t) \in \mathbb{C}^{N_r \times 1}$ denotes the received signal, $\mathbf{n}_k(t) \in \mathbb{C}^{N_r \times 1}$ denotes the i.i.d noise on subchannel k with zero mean and variance $(\delta_{k,n}^i)^2$, that is, $\mathcal{N}(0, (\delta_{k,n}^i)^2\mathbf{I})$, and $\mathbf{S}_k^i(t) = \mathbf{G}_k^i \mathbf{s}_k(t)$ stands for MU signals on subchannel k, where $\mathbf{s}_k(t) \in \mathbb{C}^{N_t \times 1} \sim \mathcal{N}(0, \gamma_k \mathbf{I})$ is a column vector of N_t information symbols, γ_k is the variance of symbol $\mathbf{s}_k$, and $\mathbf{G}_k^i \in \mathbb{C}^{N_r \times N_t}$ is the channel matrix on subchannel k between MU and CSBS i. $L_s = t_s f_s$ denotes the number of detection samples. Under an energy detection scheme the decision is based on [27]:

$$\sum_{l=1}^{L_s} \mathrm{Tr}\left(\mathbf{Y}_k^i\right) \underset{H_{0,k}}{\overset{H_{1,k}}{\gtrless}} \tau_k, \quad k = 1, 2, \ldots, K, \tag{2}$$

where τ_k denote the decision thresholds. According to the Central Limit Theorem, for large L_s, $\mathbf{Y}_k$ are approximately normally distributed: $\mathbf{Y}_k^i \sim \mathcal{N}(\mu_{k,0}^i, (\sigma_{k,0}^i)^2)$ for $H_{0,k}$, and $\mathbf{Y}_k^i \sim \mathcal{N}(\mu_{k,1}^i, (\sigma_{k,1}^i)^2)$ for $H_{1,k}$, where

$$\begin{aligned} \mu_{k,0}^i &= L_s N_r \left(\delta_{k,n}^i\right)^2 \\ \left(\delta_{k,0}^i\right)^2 &= L_s N_r^2 \left(\delta_{k,n}^i\right)^4 \\ \mu_{k,1}^i &= L_s \left(N_r \left(\delta_{k,n}^i\right)^2 + \gamma_k \mathrm{Tr}\left(\mathbf{G}_k^i \left(\mathbf{G}_k^i\right)^H\right)\right) \\ \left(\delta_{k,1}^i\right)^2 &= L_s \left(N_r \left(\delta_{k,n}^i\right)^2 + \gamma_k \mathrm{Tr}\left(\mathbf{G}_k^i \left(\mathbf{G}_k^i\right)^H\right)\right)^2. \end{aligned} \tag{3}$$

The probabilities of detection $\mathscr{P}_{k,d}^i$ and false alarm $\mathscr{P}_{k,\mathrm{fa}}^i$ for the kth channel for CSBS i are expressed in closed forms as

$$\begin{aligned} \mathscr{P}_{k,\mathrm{fa}}^i(\tau_k, t_s) &= \mathcal{Q}\left(\frac{\left(\tau_k - \mu_{k,0}^i\right)}{\delta_{k,0}^i}\right) \\ \mathscr{P}_{k,d}^i(\tau_k, t_s) &= \mathcal{Q}\left(\frac{\left(\tau_k - \mu_{k,1}^i\right)}{\delta_{k,1}^i}\right). \end{aligned} \tag{4}$$

2.2. Resource Allocation for CSUs with WiFi Users in the Unlicensed Band. In the unlicensed band, the coexistence of DACS and WiFi is based on LTE-Release 10–12 by using specific techniques such as Carrier Sense Adaptive Transmission (CSAT) with LTE air interface protocol, which performs Clear Channel Assessment (CCA) before transmitting data [5]. CCA may potentially degrade the channel utilization and lose the access opportunities in unlicensed spectrum channel to other systems. In LTE-Release 13, LBT mechanism is required which needs to change LTE air interface [22]. The performance of WiFi systems will be significantly affected due to the CSMA/CA mechanism, while the performance of DACS system was almost unchanged based on the LTE

protocol. The main challenge for the coexistence of DACS and WiFi is to ensure the fairness between two systems.

Two guidelines are followed in the design of the access scheme in the unlicensed band: (1) the CSBS senses the unlicensed band in order to avoid interference from ongoing transmission by other users; (2) the access scheme aligns with LTE frame structure.

In order to access the unlicensed band while guaranteeing the fairness for WiFi users, in this paper, we develop a channel access scheme that aligns with LTE frame structure, namely, Enhanced-LBT (E-LBT) scheme. The proposed E-LBT is based on the 3GPP definition. Instead of fixing the data transmission and detection duration, the transmission duration for DACSs will be adaptively adjusted with respected to the available licensed bandwidth as well as the WiFi traffic load. The frame structure of CSBS i consists of the detection duration and the data transmission duration in the unlicensed band.

Assume that spectrum sensing in the unlicensed band is performed by the set of antennas A_u at each CSBS by energy detection scheme. If the unlicensed band is regarded as clear (no WiFi users or other CSBSs occupying the band), the CSBS i will start transmitting for time duration T^i according to the channel condition as well as the WiFi traffic load.

Due to the randomness of the locations of WiFi-AP/CSBS, as well as the time-varying channel conditions, the detection results depended on the current traffic load of WiFi users. For the simplicity and without loss of generality, we define the probability of a WiFi user continuing to transmit data in the next slot (after accessing the unlicensed band) as λ.

In the E-LBT scheme, there are the five following cases in the unlicensed band transmission.

Case 1. WiFi and CSBS i occupy the unlicensed band simultaneously with cochannel interference. For instance, the WiFi user is transmitting in the unlicensed band while CSBS i accesses the band under error detection results, namely, miss detection with probability $1 - \mathscr{P}_d^i$.

Case 2. CSBS i and CSBS $i + 1$ are transmitting in the unlicensed band simultaneously with cochannel interference. For instance, CSBS i decides to access the unlicensed band which is occupied by other CSBSs due to miss detection results.

Case 3. WiFi is absent, and CSBS i occupies the unlicensed band without false alarm.

Case 4. WiFi occupies the unlicensed band, without interference from CSBSs. For instance, all the CSBSs detect the WiFi signal correctly.

Case 5. WiFi and all the CSBSs are absent; thus the channel is idle.

The details of E-LBT scheme are shown in Figure 2. According to above cases, the detection problem in the unlicensed band can be formulated as a hypothesis test. We denote the hypotheses as H_{XY}, where $X \in \{0, 1, 2\}$, $Y \in \{0, 1\}$ represent the activity of CSBSs and WiFi users, respectively. $X = 0$ represents all the CSBSs being absent; $X = 1$ represents only one CSBS transmitting; $X = 2$ represents more than one CSBS transmitting at the same time. Similarly, $Y = 0$ represents the WiFi user being absent, while $Y = 1$ represents the WiFi user transmitting. For instance, hypothesis H_{20} represents more than one CSBS occupying the channel without the WiFi user; thus there is interference between CSBSs in the unlicensed band. Specifically, the received signal at CSBS i under each hypothesis can be written as

$$\mathbf{y}^i(t) = \begin{cases} \mathbf{S}^i(t) + \mathbf{n}(t) & H_{10} \\ \mathbf{S}^i(t) + \mathbf{W}^i(t) + \mathbf{n}(t) & H_{11} \\ \mathbf{S}^{i+1}(t) + \mathbf{n}(t) & H_{20} \\ \mathbf{W}^i(t) + \mathbf{n}(t) & H_{01} \\ \mathbf{n}(t) & H_{00}, \end{cases} \tag{5}$$

where $\mathbf{y}^i(t) \in \mathbb{C}^{N_r \times 1}$ denotes the received signal, $\mathbf{n}(t) \in \mathbb{C}^{N_r \times 1}$ denotes the additive background noise with zero mean and variance $(\delta_n)^2$, that is, $\mathcal{N}(0, (\delta_n)^2\mathbf{I})$, $\{\mathbf{S}^i(t) = \mathbf{H}_u^i\mathbf{s}(t), \mathbf{W}^i(t) = \mathbf{G}_w^i\mathbf{w}(t)\} \in \mathbb{C}^{N_r \times 1}$ stand for the receive signals at CSBS i from other CSBSs, and WiFi in the unlicensed band, respectively. Specially, for H_{20}, $\mathbf{S}^{i+1}(t)$ represents the received signals from multi-CSBSs. $\mathbf{s}(t) \in \mathbb{C}^{N_r \times 1} \sim \mathcal{N}(0, \gamma_u\mathbf{I})$ is a column vector of N_r information symbols, γ_u is the variance of $\mathbf{s}(t)$, and $\mathbf{H}_u^i \in \mathbb{C}^{N_r \times N_r}$ is the channel matrix in the unlicensed band from other CSBSs to CSBS i. $\mathbf{w}(t) \in \mathbb{C}^{N_t \times 1}$ is a column vector of N_t information symbols, and $\mathbf{G}_w^i \in \mathbb{C}^{N_r \times N_t}$ is the channel matrix in the unlicensed band from WiFi user to CSBS i. By the similar process to (4), the probabilities of detection $\mathscr{P}_d^i$ and false alarm $\mathscr{P}_{\text{fa}}^i$, with the threshold τ_u in the unlicensed band are given, respectively, by

$$\begin{aligned} \mathscr{P}_{\text{fa}}^i(\tau_u, t_u) &= \mathcal{Q}\left(\frac{\left(\tau_u - \mu_0^i\right)}{\delta_0^i}\right) \\ \mathscr{P}_d^i(\tau_u, t_u) &= \mathcal{Q}\left(\frac{\left(\tau_u - \mu_1^i\right)}{\delta_1^i}\right), \end{aligned} \tag{6}$$

where

$$\begin{aligned} \mu_0^i &= L_u N_r (\delta_n)^2 \\ \left(\delta_0^i\right)^2 &= L_u N_r^2 (\delta_n)^4 \\ \mu_1^i &= L_u \Big(N_r (\delta_n)^2 \\ &\quad + \gamma_u \left(\text{Tr}\left(\mathbf{G}_w^i \left(\mathbf{G}_w^i\right)^H\right) + \text{Tr}\left(\mathbf{H}_u^i \left(\mathbf{H}_u^i\right)^H\right)\right)\Big) \\ \left(\delta_1^i\right)^2 &= L_u \Big(N_r (\delta_n)^2 \\ &\quad + \gamma_u \left(\text{Tr}\left(\mathbf{G}_w^i \left(\mathbf{G}_w^i\right)^H\right) + \text{Tr}\left(\mathbf{H}_u^i \left(\mathbf{H}_u^i\right)^H\right)\right)\Big)^2. \end{aligned} \tag{7}$$

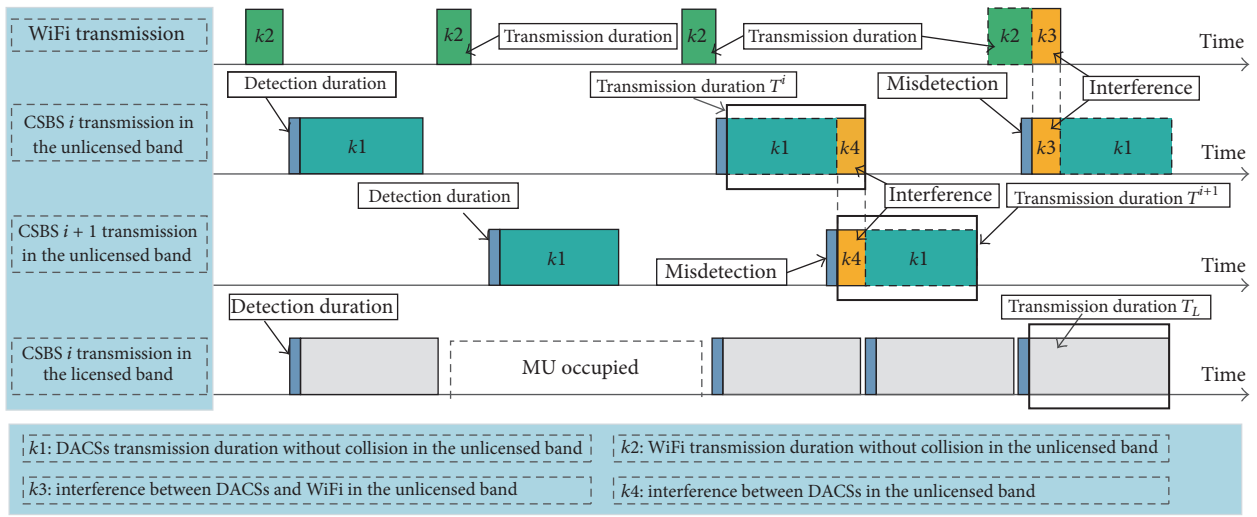

Figure 2: Data transmission in the unlicensed band.

Based on the above discussion, there is cochannel interference in Cases 1 and 2, whereas Cases 3 and 4 referred to the scene without cochannel interference; if the unlicensed band is idle, we obtain Case 5. Before discussion, we give the definition of the following parameters. In Figure 2, k_1 represents the average transmission time of DACSs without interference; k_2 represents the average transmission time of WiFi without interference; k_3 represents the average interference time between DACSs and WiFi; k_4 represents the average interference time between DACSs under miss detection; k_t represents the average backoff time and detection time.

(i) Cases with Interference

Case 1 (t_1). Let $t_1 = k_3/k_{\text{tol}}$ denote the final interference ratio between DACSs and WiFi in the unlicensed band, where $k_{\text{tol}} = k_L + k_w + k_t$ is the total available transmission time, including the average transmission time of DACSs, $k_L = (1 - \mathscr{P}_{\text{fa}}^i)T^i$, and the average transmission time of WiFi based on the traffic load λ (k represents the time slot index), $k_w = \sum_{k=1}^{\infty} k \cdot \lambda^{k-1} = 1/(1-\lambda)^2$. Furthermore, taking into account the idle time, we have $k_t = d \cdot (k_L + k_w)$, which depends on the detection and backoff time before occupying the unlicensed band, where d is idle time factor. $k_3 = (1 - (\mathscr{P}_d^i)^M)(k_w - k_2)$ is the average interference time between DACSs and WiFi, where $k_2 = \sum_{k=1}^{\infty} k \cdot (\lambda \mathscr{P}_d^i)^{k-1} = 1/(1 - \lambda \mathscr{P}_d^i)^2$ represents the WiFi average transmission time without interference.

Case 2 (t_2). The interference ratio between DACSs is denoted as $t_2 = k_4/k_{\text{tol}}$, where $k_4 = k_L \cdot (1 - (\mathscr{P}_d^i)^{M-1})$ is the average interference time between DACSs, under miss detection.

(ii) Cases without Interference

Case 3 (t_3). The transmission ratio of DACSs in the unlicensed band without interference is denoted as $t_3 = k_1/k_{\text{tol}}$, where $k_1 = k_L \cdot (\mathscr{P}_d^i)^{M-1}$ is the average transmission time without interference.

Case 4 (t_4). The WiFi transmission ratio is given by $t_4 = k_2/k_{\text{tol}}$.

(iii) Spectrum Idle

Case 5 (t_5). Due to the backoff time and detection time before accessing the channel, the idle ratio is $t_5 = k_t/k_{\text{tol}}$.

According to the above analysis, we obtain that the transmission ratio of DACSs and WiFi in the unlicensed band can be represented as η and Φ, respectively:

$$\begin{aligned} \eta &= t_1 + t_2 + t_3 \\ \Phi &= t_1 + t_4. \end{aligned} \tag{8}$$

3. Problem Formulation

Table 1 describes the users' transmission data rate in the licensed and unlicensed band. The transmission data rate of DACSs consists of the uplink transmission rate R_L in the licensed band and the downlink transmission rate R_u in the unlicensed band, and the transmission data rate of WiFi user n ($n = 1, 2, \ldots, N$) is expressed as $R_{w,n}$.

3.1. In the Licensed Band. In this work, the data rate of the DACS consists of two parts: uplink transmission in the licensed band and downlink transmission in the unlicensed band. In the licensed subchannel k, the received signal $\mathbf{z}_k^i \in \mathbb{C}^{N_r \times 1}$ at the CSBS i from CSU j is given by

$$\mathbf{z}_k^i = \sum_{j=1}^{J} a^{ij} \mathbf{H}_k^{ij} \mathbf{q}_k^j + \sum_{j=1}^{J} \left(1 - a^{ij}\right) \mathbf{H}_k^{ij} \mathbf{q}_k^j + \mathbf{n}_k, \tag{9}$$

Table 1: The relationship between five cases and transmission data rate.

User type	Cases	1	2	3	4	5	Average transmission rate
	Hypothesis	H_{11}	H_{20}	H_{10}	H_{01}	H_{00}	
	Transmission ratio	t_1	t_2	t_3	t_4	t_5	
DACS	Licensed band			R_L			R_L
	Unlicensed band	R_U^{01}	R_U^{10}	R_U^{00}			$R_U = t_1 R_U^{01} + t_2 R_U^{10} + t_3 R_U^{00}$
WiFi		$R_{w,n}^{01}$			$R_{w,n}^{11}$		$R_{w,n} = t_4 R_{w,n}^{11} + t_1 R_{w,n}^{01}$

where $\mathbf{q}_k^j$ denotes the transmission data from CSU j; $\mathbf{H}_k^{ij} \in \mathbb{C}^{N_r \times N_t}$ is the cross-channel matrix on channel k from CSU j to CSBS i. The first term on the right-hand side is the desired signals sent from intracell CSU j; the second term represents the intercell interference from other CSUs that share the subchannel k. The achievable sum rate of DACS i for a given set of user's covariance matrices $\mathbf{Q}_{L,k}^1, \mathbf{Q}_{L,k}^2, \ldots, \mathbf{Q}_{L,k}^J$, is denoted as $R_L^i(\mathbf{Q}_L^j, \mathbf{a}^j, \boldsymbol{\tau}, t_s)$, $\mathbf{Q}_L^j = (\mathbf{Q}_{L,k}^j)_{k=1}^K$, $\mathbf{a}^j = (a^{ij})_{i=1}^M$, and $\boldsymbol{\tau} = (\tau_k)_{k=1}^K$ and formulated as

$$R_L^i\left(\mathbf{Q}_L^j, \mathbf{a}^j, \boldsymbol{\tau}, t_s\right) = T_s \sum_{k=1}^{K} \left(1 - \mathscr{P}_{k,\mathrm{fa}}^i\left(\tau_k, t_s\right)\right) B_{L,k} \cdot \log\det\left(\mathbf{I} + \left(\mathbf{C}_k^j\right)^{-1} \sum_{j=1}^{J} a^{ij} \mathbf{Q}_{L,k}^{j,H}\right), \tag{10}$$

where $B_{L,k} = B_L/K$ is the bandwidth, $\mathbf{Q}_{L,k}^{j,H} = \mathbf{H}_k^{ij} \mathbf{Q}_{L,k}^j (\mathbf{H}_k^{ij})^H$, $T_s = 1 - t_s/T_L$, and $\mathbf{Q}_{L,k}^j$ denote the covariance matrix of the symbols transmitted by CSU j in subchannel k. $\mathbf{C}_k^j$ is the noise-plus-interference covariance:

$$\mathbf{C}_k^j = \mathbf{I} + \sum_{j=1}^{J} \left(1 - a^{ij}\right) \mathbf{H}_k^{ij} \mathbf{Q}_{L,k}^j \left(\mathbf{H}_k^{ij}\right)^H. \tag{11}$$

For CSU j, the total transmission power over all licensed subchannels should not exceed its budget power $P_{\max}^j$. Consequently, the power budget constraint is denoted as

$$\sum_{k=1}^{K} \mathrm{Tr}\left(\mathbf{Q}_{L,k}^j\right) \le P_{\max}^j. \tag{12}$$

Considering that the sensing information is not always reliable, to guarantee the QoS of MUs, the cochannel interference from CSUs should not exceed an interference mask. Thus the individual soft-shaping constraint to effectively protect the MU is denoted as

$$\left(1 - \mathscr{P}_{k,d}^i\left(\tau_k, t_s\right)\right) \mathrm{Tr}\left(\mathbf{G}_k^j \mathbf{Q}_{L,k}^j \left(\mathbf{G}_k^j\right)^H\right) \le P_{\mathrm{mask},k}, \tag{13}$$

where $\mathbf{G}_k^j \in \mathbb{C}^{N_t \times N_t}$ is the channel matrix from CSU j to the MU in subchannel k and $\mathbf{P}_{\mathrm{mask}} = [P_{\mathrm{mask},k}]_{k=1}^K$ denotes the interference mask on all subchannels. In addition, from the target sensing accuracy, the following linear constraint should be satisfied:

$$\tau_{k,\min} \le \tau_k \le \tau_{k,\max}, \tag{14}$$

where $\tau_{k,\min} = (\mu_{k,0}^i)_{\max}$ and $\tau_{k,\max} = (\mu_{k,1}^i)_{\min}$, denoted as $\boldsymbol{\tau} \in \mathscr{T}$. For the convenience of reading, we enable the a^{ij} to the following convex set:

$$\mathscr{A} = \left\{ \sum_{i=1}^{M} a^{ij} = 1, \sum_{j=1}^{J} a^{ij} \le D, a^{ij} \in \{0,1\} \right\}. \tag{15}$$

Therefore, the sum data rate of DACSs over all licensed subchannels can be written as

$$R_L = \sum_{i \in M} R_L^i. \tag{16}$$

3.2. In the Unlicensed Band. DACSs and WiFi coexist in the unlicensed band, sharing the unlicensed band under the E-LBT mechanism. Based on the E-LBT, the CSBS detects the channel condition before transmitting data and determines the transmission time according to the channel condition (e.g., WiFi traffic load). Thus, DACSs transmission data rate is associated with WiFi real-time traffic load. According to Table 1, the data rate of DACSs and WiFi networks is composed of several parts:

(i) For Case 1 $(R_u^{01}, R_{w,n}^{01})$, the data rate of DACS i with interference from WiFi is given by

$$R_u^{01} = \sum_{j=1}^{J} B_u \log\det\left(\mathbf{I} + \left(\mathbf{C}_u^{j.1}\right)^{-1} \mathbf{H}_u^{ij} \mathbf{Q}_u^i \left(\mathbf{H}_u^{ij}\right)^H\right), \tag{17}$$

where B_u is the unlicensed bandwidth, $\mathbf{H}_u^{ij}$ is the channel matrix in the unlicensed band from CSBS i to CSU j, and $\mathbf{Q}_u^i$ represents the covariance matrix of CSBS i in the unlicensed band. $\mathbf{C}_u^{j.1} = \delta_n^2 \mathbf{I} + \mathbf{G}_u^j \mathbf{Q}_w (\mathbf{G}_u^j)^H$ denotes the noise-plus-interference covariance matrix of WiFi networks, $\mathbf{G}_u^j$ is the channel matrix in the unlicensed band of CSU j, and $\mathbf{Q}_w$ is the covariance matrix of WiFi networks. Moreover, the data rate of WiFi user n with interference from DACSs is given by

$$R_{w,n}^{01} = B_u \log\det\left(\mathbf{I} + \left(\mathbf{C}_u^0\right)^{-1} \mathbf{H}_w \mathbf{Q}_w \left(\mathbf{H}_w\right)^H\right) \tag{18}$$

where $\mathbf{C}_u^0 = \delta_n^2 \mathbf{I} + \mathbf{G}_u^i \mathbf{Q}_u^i (\mathbf{G}_u^i)^H$ denotes the noise-plus-interference covariance matrix from DACSs in the unlicensed band; $\mathbf{G}_u^i$ represents the channel matrix in the unlicensed band from DACS i to WiFi users.

(ii) For Case 2 (R_u^{10}), the data rate of DACS i with interference from other DACSs is given by

$$R_u^{10} = \sum_{j=1}^{J} B_u \log\det\left(\mathbf{I} + \left(\mathbf{C}_u^{j.2}\right)^{-1} \mathbf{H}_u^{ij} \mathbf{Q}_u^i \left(\mathbf{H}_u^{ij}\right)^H\right), \quad (19)$$

where $\mathbf{C}_u^{j.2} = \delta_n^2 \mathbf{I} + \sum_{i=1}^{M} (1 - a^{ij}) \mathbf{H}_u^{ij} \mathbf{Q}_u^i (\mathbf{H}_u^{ij})^H$ denotes the noise-plus-interference covariance matrix from nonassociated DACSs in the unlicensed band.

(iii) For Case 3 (R_u^{00}), the data rate of DACS i without interference from other users is given by

$$R_u^{00} = \sum_{j=1}^{J} B_u \log\det\left(\mathbf{I} + \left(\mathbf{C}_u^{j.0}\right)^{-1} \mathbf{H}_u^{ij} \mathbf{Q}_u^i \left(\mathbf{H}_u^{ij}\right)^H\right), \quad (20)$$

where $\mathbf{C}_u^{j.0} = \delta_n^2 \mathbf{I}$ is the additive background noise covariance matrix in the unlicensed band.

(iv) For Case 4 ($R_{w,n}^{11}$), the data rate of WiFi user n is denoted as

$$R_{w,n}^{11} = B_u \log\det\left(\mathbf{I} + \frac{\mathbf{H}_w \mathbf{Q}_w \left(\mathbf{H}_w\right)^H}{\delta_n^2}\right), \quad (21)$$

where $\mathbf{H}_w$ is the WiFi channel matrix in the unlicensed band.

Consequently, we obtain the achievable total data rate of DACSs in the unlicensed band as

$$R_u = t_1 R_u^{01} + t_2 R_u^{10} + t_3 R_u^{00} \quad (22)$$

and the achievable data rate of WiFi user n as

$$R_{w,n} = t_1 R_{w,n}^{01} + t_4 R_{w,n}^{11}. \quad (23)$$

In the unlicensed band, all the CSUs and WiFi users share the same spectrum band. Therefore, there is not only the interference between CSUs, but also the interference between CSUs and WiFi users. According to Figure 2, CSUs decide to access the unlicensed band based on the results from E-LBT scheme. However, due to the variable channel state, the detection accuracy of a DACS is fluctuant; thus the detection results are not always reliable: (1) WiFi user is transmitting in the channel, but DACSs detect that the channel is idle (with misdetection). Consequently, there is interference between CSUs and WiFi users due to misdetection. Specially, when users are closer to each other, the interference is serious. (2) WiFi users are not transmitting in the channel, but DACSs detect that the channel is busy (with false alarm), resulting in a waste of available spectrum resource.

In the licensed band, in order to share the spectrum with MUs, power control for CSUs is needed to ensure the interference from CSUs to MUs below a given interference mask. Due to different government regulation requirements, we assign separated power budgets to the licensed and unlicensed band.

We adopt a utility function $U(R)$ to evaluate user's satisfaction about an achieved data rate R. The widely used logarithmic utility function is considered to guarantee the proportional fair coexistence between CSUs and WiFi,

$$U(R) = \ln(R), \quad (24)$$

where $\ln(\cdot)$ is natural logarithm function. It could capture the typical user satisfaction about data rate—as data rate increases, user utility grows faster when data rate is low than when it is high.

Since CSUs have the ability to access both the licensed and unlicensed bands simultaneously, the CSUs will generate interference to the cochannel users (MUs, WiFi users) during the transmission process. Therefore, in this paper, we focus on the harmonious coexistence mechanism between CSUs and WiFi users, while ensuring the communication performances of MUs and WiFi users in the licensed and unlicensed band, respectively. According to the above analysis, the optimization problem of maximizing the total utility of DACSs and WiFi networks by jointly optimizing the cell selection, detection operation, power allocation, and transmission time in the licensed and unlicensed band can be formulated as $P1$:

$$\begin{aligned}
\max_{\mathbf{Q}_L^j, \mathbf{a}^j, \boldsymbol{\tau}, t_s, T^i} \quad & U\left(\mathbf{Q}_L^j, \mathbf{a}^j, \boldsymbol{\tau}, t_s, T^i\right) \\
& = \ln\left(R_L\left(\mathbf{Q}_L^j, \mathbf{a}^j, \boldsymbol{\tau}, t_s\right) + R_u\left(T^i\right)\right) \\
& \quad + \sum_{n=1}^{N} \ln\left(R_{w,n}\left(T^i\right)\right) \\
\text{s.t.} \quad & (c1)\left(1 - \mathscr{P}_{k,d}^i\left(\tau_k, t_s\right)\right) \mathrm{Tr}\left(\mathbf{G}_k^j \mathbf{Q}_{L,k}^j \left(\mathbf{G}_k^j\right)^H\right) \\
& \le P_{\mathrm{mask},k} \\
& (c2) \sum_{k=1}^{K} \mathrm{Tr}\left(\mathbf{Q}_{L,k}^j\right) \le P_{\max}^j \\
& (c3)\, \mathbf{a} \in \mathscr{A} \\
& (c4)\, \boldsymbol{\tau} \in \mathscr{T} \\
& (c5)\, 0 \le t_s \le T_L \\
& (c6)\, 0 \le T^i \le \frac{\left(k_{\mathrm{tol}} - k_w\right)}{\left(1 - \mathscr{P}_{\mathrm{fa}}^i\right)}, \quad \forall i, j, k,
\end{aligned} \quad (25)$$

where $(c1)$ is the nonconvex individual soft-shaping constraint to effectively protect MUs from harmful interference by CSUs transmission. $(c2)$–$(c6)$ are the convex constraint sets. $(c2)$ ensures that the total transmission power of CSU j should not exceed its power budget. In addition, due to the integer nature of the element a^{ij} of the incidence matrix, the problem $P1$ is an integer programming which is NP-hard. Furthermore, constraint $(c6)$ shows that the transmission time of CSUs in the unlicensed band must be no more than the total transmission time except the WiFi transmission time based on the correct detection, so that the harmonious coexistence between CSUs and WiFi users can be achieved. In

order to find the optimal solution of problem $P1$, we propose a dual-band (licensed and unlicensed bands) traffic balancing scheme to simplify the original problem and find equivalent solutions.

4. Satisfaction-Based Dual-Band Traffic Balancing Scheme

The optimization problem can be divided into two suboptimization problems and solved separately. Firstly, we maximize the data rate R_L of CSU in the licensed band by optimizing the cell selection, detection operation, and power allocation, which results in the maximum utility of the licensed band. Secondly, we maximize the utility $U(\cdot)$ of whole networks by optimizing the transmission time in the unlicensed band. Specifically, the alternative direction optimization method is used to obtain the optimal solution of $P1$:

(i) Suboptimization 1: sensing-based power allocation (SBPA): for CSU j, the status a^{ij} can be considered as a constant with the initial assignment and the optimal sensing time t_s can be found by exhaustive search. Thus, we start from the two multidimensional variables $\mathbf{Q}_L^j$ and τ_k to maximize the data rata $R_L^\star$ of DACSs. Due to the inherently competitive nature of distributed multiuser DACSs, we adopt the game theory to solve the nonconvex noncooperative problem for DACSs.

(ii) Suboptimization 2: dual-band traffic balancing (DBTB): based on the solution from SBPA, we obtained the optimal $R_L^\star$ in the licensed band. In the following step, the $R_L^\star$ as well as the associated parameters $\mathbf{Q}_L^{j\star}, \mathbf{a}^{j\star}, \boldsymbol{\tau}^\star, t_s^\star$ are considered as constant and the original optimization problem can be formulated as maximizing the utility $U(\cdot)$ in (25). The suboptimization problem DBTB aims at optimizing the transmission time T^i based on WiFi real-time traffic load, that is, λ, to maximize the total utility of whole networks, while guaranteeing the coexistence between CSUs and WiFi users.

4.1. Suboptimization Problem 1: SBPA. According to the inherently competitive nature of distributed multiuser DACSs, game theory is adopted to solve the nonconvex noncooperative problem for DACSs. The resource allocation problem among CSUs is reformulated as a strategic noncooperative game. In order to simplify the game, we consider the problem equal to maximizing the individual rate of CSU j. For CSU j, the variable $\mathbf{a}^j$ can be considered as a constant and the optimal sensing time t_s can be finally optimized by exhaustive search. Collaborative spectrum sensing can improve the performance of spectrum sensing in cognitive radio networks [28]. Furthermore, we assume that the sensing results from CSBS i are shared with CSU j in this cell, with the initial assignment based $\mathbf{a}^j$, we have $\mathscr{P}_{k,\mathrm{fa}}^j = \mathscr{P}_{k,\mathrm{fa}}^i$ and $\mathscr{P}_{k,d}^j = \mathscr{P}_{k,d}^i$. We start from the two multidimensional variables case, that is, $\mathbf{Q}_L^j$ and $\boldsymbol{\tau}$. Assume that there are J players, corresponding to the J CSUs, each one controlling the variables $\mathbf{x}^j = (\mathbf{Q}^j, \boldsymbol{\tau})$, $j = 1, \ldots, J$. Let $\mathbf{x}^{-j} = (\mathbf{x}^1, \ldots, \mathbf{x}^{j-1}, \mathbf{x}^{j+1}, \ldots, \mathbf{x}^J)$ be the set of strategies from all the CSUs, except CSU j. The optimization function $R_L^j(\mathbf{Q}_L^j, \boldsymbol{\tau})$ for CSU j is the data rate over channels, given by

$$R_L^j\left(\mathbf{Q}_L^j, \boldsymbol{\tau}\right) = T_s \sum_{k=1}^{K} \left(1 - \mathscr{P}_{k,\mathrm{fa}}^j B_{L,k}\left(\tau_k\right)\right) \cdot \log\det\left(\mathbf{I} + \left(\mathbf{C}_k^j\right)^{-1} \mathbf{Q}_{L,k}^{j,H}\right), \tag{26}$$

where T_s is considered as a constant to be optimized at a later step. Each CSU competes against the others by choosing the transmit covariance matrix $\mathbf{Q}^j$ and the associated threshold $\boldsymbol{\tau}$ to maximize its own rate with the given certain constraints. The noncooperative power allocation game of CSU j can be formulated as problem $P2$:

$$\begin{aligned} \max_{\mathbf{Q}_L^j, \boldsymbol{\tau}} \quad & R_L^j\left(\mathbf{Q}_L^j, \boldsymbol{\tau}\right) \\ \text{s.t.} \quad & \left(1 - \mathscr{P}_{k,d}^j\left(\tau_k\right)\right) \mathrm{Tr}\left(\mathbf{G}_k^j \mathbf{Q}_{L,k}^j \left(\mathbf{G}_k^j\right)^H\right) \le P_{\mathrm{mask},k}, \\ & \sum_{k=1}^{K} \mathrm{Tr}\left(\mathbf{Q}_{L,k}^j\right) \le P_{\max}^j, \\ & \boldsymbol{\tau} \in \mathscr{T}, \ \forall i, j, k. \end{aligned} \tag{27}$$

The resulting game $P2$ is nonconvex, we analyze the proposed nonconvex game based on a relaxed equilibrium concept introduced in [13], namely, the QNE, and prove that the proposed nonconvex game in DACSs always admits a unique QNE, which coincides with the NE. We denote the nonconvex individual constraints $(c1)$ as $\mathbf{H}_{\mathbb{C}}(\mathbf{x}) = [h_{\mathbb{C}}^j(\mathbf{x}^j)]_{j=1}^J$. The convex individual constraints $(c2)$–$(c5)$ are denoted as $\widetilde{\mathbf{G}}_{\mathbb{C}}(\mathbf{x}) = [(\widetilde{g}_k^j(\mathbf{x}^j))_{k=1}^K]_{j=1}^J$, and embedded in the definition set of $\mathbf{x}^j = [\mathbf{Q}_L^j, \boldsymbol{\tau}]$, denoted as $\mathbf{X}_{\mathbb{C}}^j$. Thus, we can formulate the nonconvex game $\mathscr{G}_{\mathbb{C}}(\mathbf{H}_{\mathbb{C}}, \widetilde{\mathbf{G}}_{\mathbb{C}})$ as problem $P3$:

$$\begin{aligned} \max_{\mathbf{x}^j} \quad & R_L^j\left(\mathbf{x}^j\right) \\ \text{s.t.} \quad & h_{\mathbb{C}}^j\left(\mathbf{x}^j\right) \le 0, \quad \mathbf{x}^j \in \mathbf{X}_{\mathbb{C}}^j. \end{aligned} \tag{28}$$

Let $\mathscr{Y}_{\mathbb{C}}^j$ denote the feasible strategy set of CSU j, written as

$$\mathscr{Y}_{\mathbb{C}}^j = \left\{\mathbf{x}^j \in \mathbf{X}_{\mathbb{C}}^j \mid h_{\mathbb{C}}^j\left(\mathbf{x}^j\right) \le 0\right\}, \quad 1 \le k \le K. \tag{29}$$

Denoting by α_k^j the multipliers associated with the nonconvex constraints $h_{\mathbb{C}}^j(\mathbf{x}^j) \le 0$ of CSU j, the Lagrange function of the problem $P3$ can be written as

$$L^j\left(\mathbf{x}^j, \boldsymbol{\alpha}^j\right) = -R_L^j\left(\mathbf{x}^j\right) + \boldsymbol{\alpha}^j h_{\mathbb{C}}^j\left(\mathbf{x}^j\right). \tag{30}$$

The KKT conditions of CSU j are given by

$$\begin{aligned}
&\nabla_{\mathbf{Q}_L^j} R_L^j\left(\mathbf{Q}_L^j, \boldsymbol{\tau}\right) - \alpha_k^j\left(1 - \mathscr{P}_{k,d}^j\left(\tau_k\right)\right)\mathrm{Tr}\left(\mathbf{G}_k^j\left(\mathbf{G}_k^j\right)^H\right) \\
&\quad = 0 \\
&\nabla_{\boldsymbol{\tau}} R_L^j\left(\mathbf{Q}_L^j, \boldsymbol{\tau}\right) + \alpha_k^j \nabla_{\tau_k} \mathscr{P}_{k,d}^j\left(\tau_k\right)\mathrm{Tr}\left(\mathbf{G}_k^j \mathbf{Q}_{L,k}^i \left(\mathbf{G}_k^j\right)^H\right) \\
&\quad = 0 \\
&\alpha_k^j\left[\left(1 - \mathscr{P}_{k,d}^j\left(\tau_k\right)\right)\mathrm{Tr}\left(\mathbf{G}_k^j \mathbf{Q}_{L,k}^j \left(\mathbf{G}_k^j\right)^H\right) - P_{\mathrm{mask},k}\right] \\
&\quad = 0,
\end{aligned} \tag{31}$$

where $\nabla_{\mathbf{Q}_L^j} R_L^j(\mathbf{Q}_L^j, \boldsymbol{\tau}), \nabla_{\boldsymbol{\tau}} R_L^j(\mathbf{Q}_L^j, \boldsymbol{\tau})$ denote the complex matrix derivative of $R_L^j(\mathbf{x}^j)$ with respect to $\mathbf{Q}_L^j$ and $\boldsymbol{\tau}$, respectively. More specifically, if $\mathbf{x}^\star$ are the stationary solutions of game $\mathscr{G}_{\mathbb{C}}(\mathbf{H}_{\mathbb{C}}, \widetilde{\mathbf{G}}_{\mathbb{C}})$, the KKT conditions (31) can be reformulated to the equivalent form:

$$\begin{aligned}
&\left(\mathbf{x}^\star, \boldsymbol{\alpha}^\star\right)^{T_L} \\
&\cdot \underbrace{\begin{pmatrix}
\nabla_{\mathbf{Q}_L^j} R_L^j\left(\mathbf{Q}_L^j, \boldsymbol{\tau}\right) - \alpha_k^j\left(1 - \mathscr{P}_{k,d}^j\left(\tau_k\right)\right)\mathrm{Tr}\left(\mathbf{G}_k^j\left(\mathbf{G}_k^j\right)^H\right) \\
\nabla_{\boldsymbol{\tau}} R_L^j\left(\mathbf{Q}_L^j, \boldsymbol{\tau}\right) + \alpha_k^j \nabla_{\tau_k} \mathscr{P}_{k,d}^j\left(\tau_k\right)\mathrm{Tr}\left(\mathbf{G}_k^j \mathbf{Q}_{L,k}^j \left(\mathbf{G}_k^j\right)^H\right) \\
-P_{\mathrm{mask},k} + \left(1 - \mathscr{P}_{k,d}^j\left(\tau_k\right)\right)\mathrm{Tr}\left(\mathbf{G}_k^j \mathbf{Q}_{L,k}^j \left(\mathbf{G}_k^j\right)^H\right)
\end{pmatrix}_{j=1}^{J}}_{\boldsymbol{\Gamma}_{\mathbb{C}}(\mathbf{x}^\star, \boldsymbol{\alpha}^\star)} \\
&\leq 0, \quad \left(\mathbf{x}^j, \boldsymbol{\alpha}^j\right) \in \mathbf{Y}_{\mathbb{C}}.
\end{aligned} \tag{32}$$

Inequalities (32) define a VI problem with variables $(\mathbf{x}, \boldsymbol{\alpha})$, denoted as $\mathrm{VI}_{\mathbb{C}}(\mathbf{Y}_{\mathbb{C}}, \boldsymbol{\Gamma}_{\mathbb{C}})$, where the vector function $\boldsymbol{\Gamma}_{\mathbb{C}}$ is defined in (32), and feasible set $\mathbf{Y}_{\mathbb{C}} = \prod_{j=1}^{J} \mathbf{X}_{\mathbb{C}}^j \times \mathbb{R}_+^r$. The $\mathrm{VI}_{\mathbb{C}}(\mathbf{Y}_{\mathbb{C}}, \boldsymbol{\Gamma}_{\mathbb{C}})$ is an equivalent reformulation of the KKT conditions (31). The convex constraints ($c2$)–($c5$) are embedded in the complex defining set $\mathbf{Y}_{\mathbb{C}}$, $\mathbf{Y}_{\mathbb{C}} = \prod_{j=1}^{J} \mathbf{X}_{\mathbb{C}}^j \times \mathbb{R}_+^r$, where $\mathbf{X}_{\mathbb{C}}^j$ stands for the complex convex constraints ($c2$)–($c5$) defined in the problem $P1$, and r is the total number of multipliers $\boldsymbol{\alpha}$.

Definition 1. A quasi-Nash equilibrium of the game $\mathscr{G}_{\mathbb{C}}(\mathbf{H}_{\mathbb{C}}, \widetilde{\mathbf{G}}_{\mathbb{C}})$ is defined and formed by the solution tuple $(\mathbf{x}^\star, \boldsymbol{\alpha}^\star)$ of the equivalent $\mathrm{VI}_{\mathbb{C}}(\mathbf{Y}_{\mathbb{C}}, \boldsymbol{\Gamma}_{\mathbb{C}})$, which is obtained under the first-order optimality conditions of each player's problems, while retaining the convex constraints in the defined set $\mathbf{X}_{\mathbb{C}}^j$ [13].

Theorem 2. *The $VI_{\mathbb{C}}(\mathbf{Y}_{\mathbb{C}}, \boldsymbol{\Gamma}_{\mathbb{C}})$ has a solution; thus the game $\mathscr{G}_{\mathbb{C}}(\mathbf{H}_{\mathbb{C}}, \widetilde{\mathbf{G}}_{\mathbb{C}})$ has a QNE, which is nontrivial.*

The similar proof can be found in [12]. The uniqueness of the QNE for the problem $P3$ needs an appropriate second-order sufficiency condition. We provide the following theorem.

Theorem 3. *If the Hessian matrix of (30), denoted as $\nabla_{\mathbf{x}^j}^2 L^j(\mathbf{x}^j, \boldsymbol{\alpha}^j)$, is positive definite for all $\mathbf{x}^j \in \mathbf{X}_{\mathbb{C}}^j$ and $\boldsymbol{\alpha}^j \in \mathbb{R}_+^r$, then the nonconvex optimization problem $P3$ for each CSU j has a unique optimal solution $\mathbf{x}^{j,\star} \in \mathbf{X}_{\mathbb{C}}^j$. In addition, the $\nabla_{\mathbf{x}^j}^2 L^j(\mathbf{x}^j, \boldsymbol{\alpha}^j)$ is positive definite, if the following sufficient condition is satisfied:*

$$\begin{aligned}
&\frac{\max_{k=1,\ldots,K}\left(\boldsymbol{\alpha}^j/\sqrt{2\pi}\right)\mathrm{Tr}\left(\mathbf{G}_k^j\left(\mathbf{G}_k^j\right)^H\right)}{\min\left(\mathrm{Re}\left(\xi_{\min}\left(-\nabla_{\mathbf{Q}_L^j}^2 R_L^i\left(\mathbf{x}^j\right)\right), \xi_{\min}\left(-\nabla_{\boldsymbol{\tau}}^2 R_L^j\left(\mathbf{x}^j\right)\right)\right)\right)} \\
&\quad < 1.
\end{aligned} \tag{33}$$

Proof. The proof is provided in [29]. □

$\xi_{\min}(-\nabla_{\mathbf{Q}_L^j}^2 R_L^j(\mathbf{x}^j))$ and $\xi_{\min}(-\nabla_{\boldsymbol{\tau}}^2 R_L^j(\mathbf{x}^j))$ denote the minimum eigenvalues of matrices $-\nabla_{\mathbf{Q}_L^j}^2 R_L^j(\mathbf{x}^j)$ and $-\nabla_{\boldsymbol{\tau}}^2 R_L^j(\mathbf{x}^j)$, respectively. This condition quantifies how much MUI can be tolerated by the systems to guarantee the existence and the uniqueness of the QNE, meaning that when the interference from the CSU to the MU is sufficiently small (satisfying the condition (33)), the nonconvex problem $P3$ has a unique solution QNE, which coincides with the NE.

4.2. Suboptimization Problem 2: DBTB. Based on the optimal results $\mathbf{Q}_L^{j\star}, \mathbf{a}^{j\star}, \boldsymbol{\tau}^\star, t_s^\star$ obtained from SBPA, we obtain the achievable maximum sum data rate $R_L^\star$ of DACSs in the licensed band. In DBTB, we focus on maximizing the utility of whole networks while ensuring the traffic balancing between CSUs and WiFi users in the licensed and unlicensed band. Consequently, the original problem can be formulated as

$$\begin{aligned}
\max_{T^i} \quad & U\left(T^i\right) \\
& = \ln\left(R_L^\star + R_u\left(T^i\right)\right) + \sum_{n=1}^{N} \ln\left(R_{w,n}\left(T^i\right)\right)
\end{aligned} \tag{34}$$

$$\text{s.t.} \quad 0 \leq T^i \leq \frac{k_{\mathrm{tol}} - k_w}{1 - \mathscr{P}_{\mathrm{fa}}^i}, \quad \forall i, j, k. \tag{35}$$

The objective function of the above DBTB is only related to the DACS transmission time T^i in the unlicensed band. By the characteristics of the natural logarithm equation, when T^i is large, there are higher data rate and satisfaction of DACS, with lower WiFi users data rate and satisfaction; on the contrary, when T^i is small, the CSUs' data rate and satisfaction are lower, but those of WiFi users are higher.

Since the overall utility is composed of two parts: DACSs utility and WiFi networks utility, to achieve the maximum utility of whole networks, we need to balance the tradeoff between them. Therefore, we maximize the whole network utility by maximizing the data rate of DACSs while guaranteeing the WiFi users transmission quality. Equation (34) is a linear equation with respect to T^i. To get the optimal T^i, take the derivative of (34) with respect to T^i and set it to zero; we obtain that

$$T^\star = \frac{\widetilde{e} \cdot \widetilde{g} + \widetilde{f} - N \cdot \widetilde{g} \cdot \widetilde{b}}{2N \cdot \widetilde{g} \cdot \widetilde{a}}, \tag{36}$$

where the $\widetilde{a}, \widetilde{b}, \widetilde{c}, \widetilde{e}, \widetilde{f}, \widetilde{g}$ are expressed as follows:

$$\begin{aligned}
\widetilde{a} &= (1+d)\left(1-\mathscr{P}_{\mathrm{fa}}^{i}\right)^{2}(1-\lambda)^{4}T^{2}\left[(1+d)R_{L}^{\star}\right.\\
&\quad\left.+R_{u}^{0.0}\left(\mathscr{P}_{d}^{i}\right)^{n-1}+R_{u}^{1.0}\left(1-\left(\mathscr{P}_{d}^{i}\right)^{n-1}\right)\right]\\
\widetilde{b} &= \left(1-\mathscr{P}_{\mathrm{fa}}^{i}\right)(1-\lambda)^{2}T\left[2R_{L}^{\star}(1+d)^{2}\right.\\
&\quad+R_{u}^{0.1}(1+d)\left(1-\left(\mathscr{P}_{d}^{i}\right)^{n}\right)\left(1-\frac{(1-\lambda)^{2}}{\left(1-\lambda\mathscr{P}_{d}^{i}\right)^{2}}\right)\\
&\quad\left.+R_{u}^{0.0}\left(\mathscr{P}_{d}^{i}\right)^{n-1}+R_{u}^{1.0}\left(1-\left(\mathscr{P}_{d}^{i}\right)^{n-1}\right)\right]\\
\widetilde{c} &= R_{L}^{\star}(1+d)^{2}+R_{u}^{0.1}\left(1-\left(\mathscr{P}_{d}^{i}\right)^{n}\right)\left(1\right.\\
&\quad\left.-\frac{(1-\lambda)^{2}}{\left(1-\lambda\mathscr{P}_{d}^{i}\right)^{2}}\right)\\
\widetilde{e} &= \left(1-\mathscr{P}_{\mathrm{fa}}^{i}\right)(1-\lambda)^{2}(1+d)\left[R_{u}^{0.0}\left(\mathscr{P}_{d}^{i}\right)^{n-1}\right.\\
&\quad+R_{u}^{1.0}\left(1-\left(\mathscr{P}_{d}^{i}\right)^{n-1}\right)\\
&\quad\left.-\left(1-\frac{(1-\lambda)^{2}}{\left(1-\lambda\mathscr{P}_{d}^{i}\right)^{2}}\right)R_{u}^{0.1}\left(1-\left(\mathscr{P}_{d}^{i}\right)^{n}\right)\right]\\
\widetilde{f} &= \sqrt{\left(\widetilde{e}\cdot\widetilde{g}-N\widetilde{g}\cdot\widetilde{b}\right)^{2}-4N\widetilde{g}\cdot\widetilde{a}\left(N\widetilde{g}\cdot\widetilde{c}-\widetilde{e}\right)}\\
\widetilde{g} &= \left(1-\mathscr{P}_{\mathrm{fa}}^{i}\right)(1-\lambda)^{2}.
\end{aligned} \tag{37}$$

Considering the constraint (35) which restricts the transmission time T^i of DACS, we have

$$T^{\star}=\min\left(\left(\frac{\widetilde{e}\cdot\widetilde{g}+\widetilde{f}-N\cdot\widetilde{g}\cdot\widetilde{b}}{2N\cdot\widetilde{g}\cdot\widetilde{a}}\right)^{+},\frac{k_{\mathrm{tol}}-k_{w}}{1-\mathscr{P}_{\mathrm{fa}}^{i}}\right), \tag{38}$$

where $(x)^+ = \max(0, x)$. The optimal solutions (38) show that DACSs can adjust the transmission time based on the real-time WiFi users traffic load.

According to the above analysis, based on the SBPA, DACSs could get the maximum data rate $R_L^\star$ in the licensed band by optimizing the cell selection, detection operation, and power allocation. Furthermore, based on the DBTB, DACSs could adjust the amount of traffic assigned to the unlicensed band to decide the transmission time T^i in the unlicensed band.

Due to the nonconvexity of the problem, we propose a satisfaction-based dual-band traffic balancing (SDTB) algorithm for DACSs based on the IP method [30, 31], which is composed of two suboptimization problems: SBPA and DBTB. Suboptimization problem SBPA is composed of two steps: line search step and trust region step. We start from line searching to ensure that the search direction is a descent direction for the merit function, turning to the trust region step otherwise. The merit function of our problem is composed of an objective function component and a component comprising constraints of the problem. We outline the main steps of SDTB algorithm in Algorithm 1, where N_b is the maximum number of backtracking search steps. For our problem, we choose $\varepsilon = 10^{-7}$ and $N_b = 3$. The resulting algorithm is ensured to have global convergence, thus achieving a QNE of the game $P3$. For more details, we refer to [12, 29–31].

The complexity of the iterative SDTB algorithm relates to the procedure of line search iteration steps and trust region iteration steps, as well as the size of the DACS. The total complexity of the SDTB algorithm is given by $O_{\mathrm{SDTB}} = O(\ln(1/\varepsilon)J\sqrt{L(2K+J)}) \sim O(\ln(1/\varepsilon)J((N_b+1)\sqrt{L(2K+J)}+L(2K+J)))$.

5. Simulation Results

In this section, we evaluate the proposed satisfaction-based dual-band traffic balancing (SDTB) algorithm in practical deployment scenarios. We consider a DACS network with $M = 3$ CSBSs, $J = 8$ CSUs, and $K = 2$ MUs. All the MUs and CSUs are randomly placed in a 50 m × 50 m square. Assume CSBS, MU, and CSU are equipped with $N_r = 10$ and $N_t = 2$ antennas, respectively. All involved channels between CSUs, CSBSs, and MUs obey Rayleigh distribution as well as the channel gains being associated with distance.

Table 2 summarizes the path loss model and parameter used in the simulations. The path loss is based on the 3GPP Indoor scenario for LTE [32], where path loss (PL) is in dB, d_{ij} is the distances between user j and station i, and L_{ow} is the outer wall penetration loss. Log-normal shadowing is with variance 3 dB, $T_L = 50$ ms, $f_{\mathrm{ls}} = 2$ MHz in the licensed band, $f_{\mathrm{us}} = 5$ GHz in the unlicensed band, and $(\delta_{k,n}^{i})^2 = 1$, according to [33]. $P_{\mathrm{mu}} = 10$ dB is the transmission power of MU. The maximum power of CSU j is $P_{\max}^{j} = 5$ dB. LTE-Advanced is adopted as the cellular air interface while 802.11 with a frame aggregation level of 15 k Bytes is used for the WiFi air interface. The unlicensed bandwidth is set to 20 MHz. The calculated utility function described in Section 3 is used in the simulations.

Figure 3 represents the total data rate of DACSs in the licensed band R_L versus the sensing time $t_s^\star$ for different D. We can observe the optimal sensing time t_s from the figure. Based on the result, there exists a maximum data rate at the optimal sensing time $t_s^\star$ for different D. $D = 2$ represents the case without optimization, leading to the lower total data rate due to the CSBSs and CSUs being randomly associated compared with the proposed SDTB algorithm, in which CSUs could select the best CSBSs to maximize the total data rate. Notice that, for $D = 4$ and $D = 5$, the curves are overlapped, which means that there is no rate gain for $D \geq 4$; thus DACSs achieve the best performance.

Figure 4 shows the total utility of CSUs and WiFi users versus the WiFi traffic load λ for different DACS transmission

(1) Initialize $\mathbf{x}^j = (\mathbf{Q}_L^j, \boldsymbol{\tau})$, $\mathbf{z}^j = (\mathbf{x}^j, \mathbf{s}^j)$, λ. $\boldsymbol{\Psi}^j = (\boldsymbol{\alpha}^j, \boldsymbol{\beta}^j)$, T^i, Trust region radius $\Upsilon^j > 0$ and $\mathbf{v}^j > 0$.
(i) sub-optimal algorithm 1: SBPA
(2) **repeat**
(3) **for** $j = 1 : J$
(4) **repeat**; **repeat**
(5) Compute the number N_e^j, set LS = 0
(6) **if** $N_e^j \leq 3K$
(7) Get direction $\overrightarrow{dr}$ and step size ρ for $\mathbf{z}^j$ and $\boldsymbol{\Psi}^j$ by Newtons's method
(8) **if** Step size $\rho_{\min}^j > \varepsilon$, set $i = 0$, $\rho_{T_L}^j = 1$
(9) **repeat**
(10) **if** The merit function in search direction $\overrightarrow{dr}$ for
(11) $\boldsymbol{\Psi}^j$ this step ρ^j is decreased update ρ^j, $\mathbf{z}^j$
(12) Update Υ^j and set LS = 1
(13) **else** Update $i = i + 1$, choose a smaller $\rho_{T_L}^j$
(14) **endif**
(15) **until** $i > N_b$ Or $\rho_{T_L}^j < \varepsilon$ Or LS == 1
(16) **endif**; **endif**
(17) **if** LS == 0
(18) Compute $\mathbf{z}^j, \boldsymbol{\Psi}^j \Upsilon^j$ using the trust region method
(19) **endif**, Update $\mathbf{v}^j$
(20) **until** $\mathbf{x}^j$ and $\boldsymbol{\Psi}^j$ satisfy the stopping test
(21) Reset the barrier parameters, so that $\mathbf{v}^j$ is decreasing
(22) **until** $\mathbf{x}^j$ and $\boldsymbol{\Psi}^j$ satisfy the stopping test
(23) Update $\mathbf{x}^j$
(24) **endfor**
(25) **until** $\mathbf{x}^j$ achieve convergence
(ii) sub-optimal algorithm 2: DBTB
(26) Based on the optimal result $R_L^\star$
(27) Take the derivative of (34), set to zero, obtain T^i in (36)
(28) **if** $T^i < (k_{\text{tol}} - k_w)/(1 - \mathscr{P}_{\text{fa}}^i)$, then get optimal $T^\star$ in (36)
(29) **else** get the optimal $T^\star = (k_{\text{tol}} - k_w)/(1 - \mathscr{P}_{\text{fa}}^i)$
(30) **endif**
(31) End the SDTB algorithm

Algorithm 1: Satisfaction-based dual-band traffic balancing algorithm.

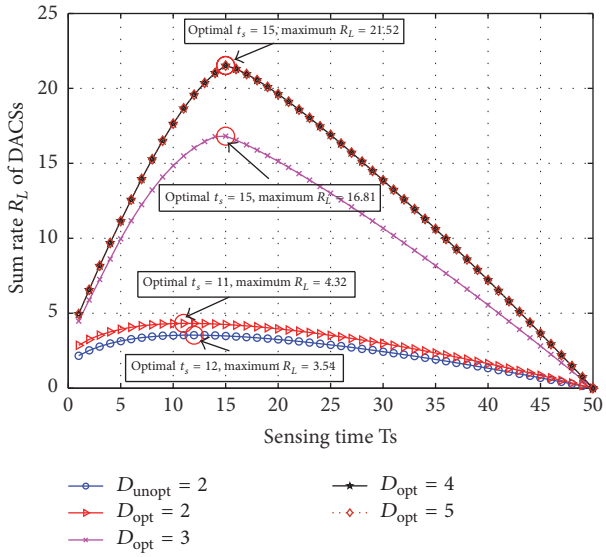

Figure 3: The sum rate R_L versus sensing time t for different D.

time T. We assume that the licensed bandwidth B_L = 1.4 MHZ and the WiFi users number $N = 1$. In this figure, we could observe that, with fixed T, the overall utility is not maximized with variational WiFi traffic load λ. The total utility increases with increasing λ at the beginning, that is, because the data rate of WiFi increases with increasing λ whereas there is only tiny influence on DACSs. The utility of whole networks achieves the maximum value at different T with dynamic traffic load λ, namely, traffic balance turning point, (e.g., $T = 5$, $\lambda = 0.56$, $R_L = 21.52$). After this point, the utility of whole networks decreases owing to the fact that the utility descending from DACSs is more than the utility ascending from WiFi with respect to the increasing traffic load λ. For larger T, the traffic balance turning point appears with larger λ. Furthermore, we compare the proposed SDTB algorithm with the ordinary scheme for fixed transmission time T. It is clear from the result that the proposed SDTB algorithm can obtain the optimal T under different WiFi traffic load λ and achieve the maximum utility of whole networks.

Table 2: Simulation parameters.

Parameter	Value
CSBS number	$M = 3$
CSU number	$J = 8$
CSU transmission duration in licensed bands	$T_L = 50$ ms
CSU transmission duration in unlicensed bands	$T \in (0, 30)$ ms
Licensed frequency	$f_{ls} = 2$ MHz
Unlicensed frequency	$f_{us} = 5$ GHz
Unlicensed bandwidth	$B_u = 20$ MHz
MU's transmission power	$P_{mu} = 10$ dB
CSU's maximum power budget	$P_{max} = 5$ dB
CSBS/WiFi-AP's transmission power	15 dBm
Path loss between MBS and CSU	$PL = 25.3 + 37.6\log_{10}(d^{ij})$
Path loss between CSBS and CSU	$PL = 38.46 + 20\log_{10}(d^{ij}) + 0.7d^{ij}$
Path loss between CSBS and WiFi	$PL = 35.3 + 37.6\log_{10}(d^{ij})$

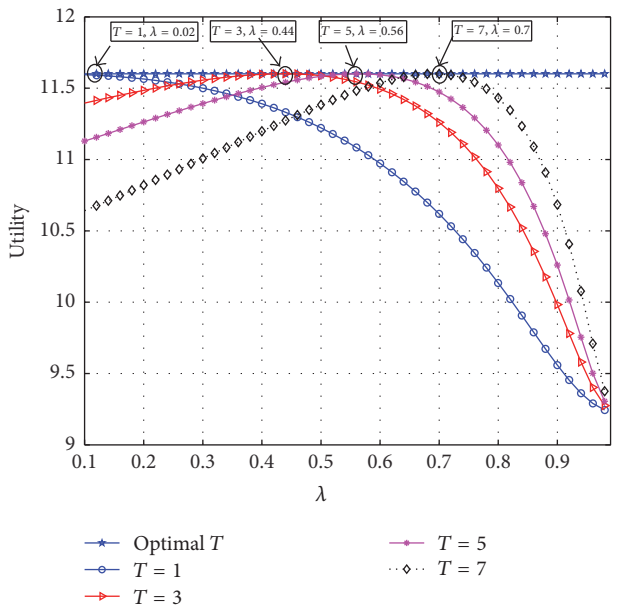

Figure 4: The utility versus the WiFi traffic load λ for different T.

Figure 5 shows the variability of utility for different data rate ratio R_L/R_u and transmission time T. Specifically, for fixed transmission time T, the bigger the data rate ratio R_L/R_u, the higher the utility of whole networks. This is because the increasing of R_L directly causes the increasing of whole networks, while the R_u does not change.

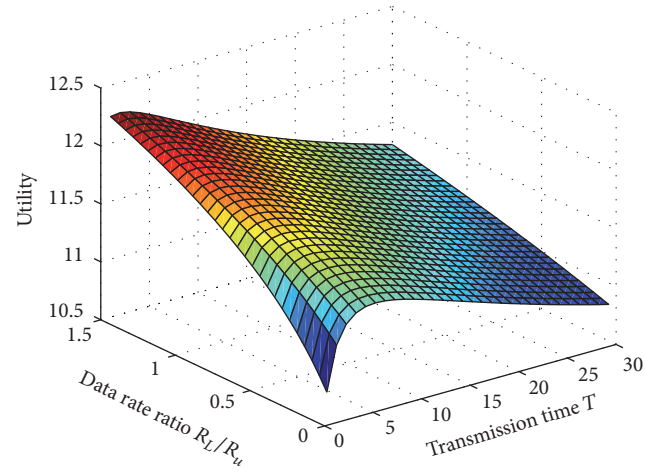

Figure 5: The utility versus data rate ratio R_L/R_u and transmission time T.

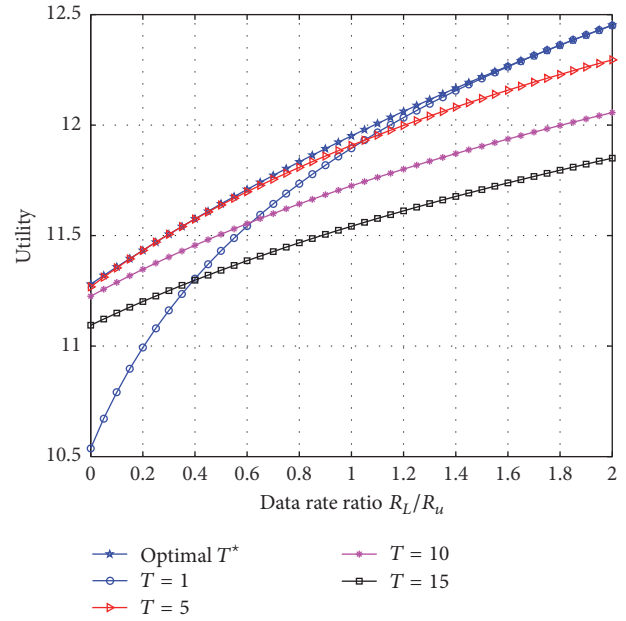

Figure 6: The utility versus the data rate ratio R_L/R_u for different T.

Figure 6 shows the utility versus the data rate ratio R_L/R_u for different T. Let $\lambda = 0.6$, $N = 1$. Based on the optimal power allocation and the optimal cell selection in the licensed band, for fixed T (e.g., $T = 10$), only the bandwidth of the licensed and unlicensed band will affect R_L and R_u, respectively. Furthermore, we fix the unlicensed bandwidth $B_u = 20$ MHz, and obtain different data rate R_L in the licensed band based on different licensed bandwidth (1.4, 3, 5, 10, 15, 20, and 30 MHz). Compare the curves of $T = 5, 10, 15$ with optimal T^*; we can see that with the same data rate ratio R_L/R_u, the larger the T is, the lower the utility could be. This is because larger T represents the larger traffic load of DACSs, which results in the WiFi performance decreasing due to the interference from DACSs. Notice that, for $T = 1$, the smaller

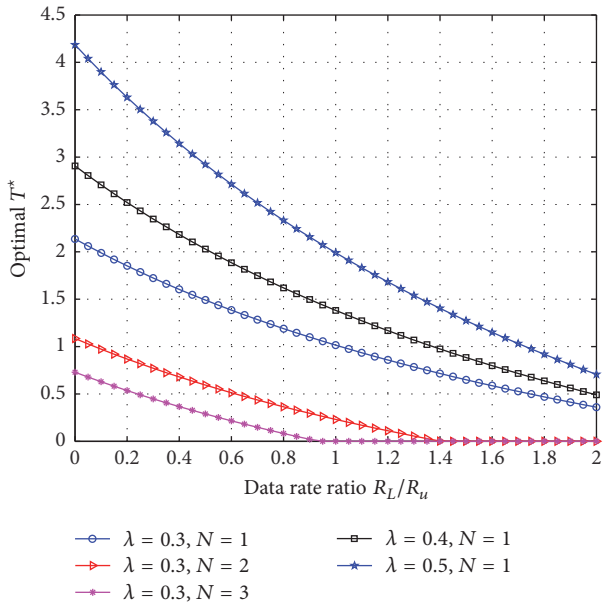

FIGURE 7: The optimal T^* versus the data rate ratio R_L/R_u for different WiFi users number N and λ.

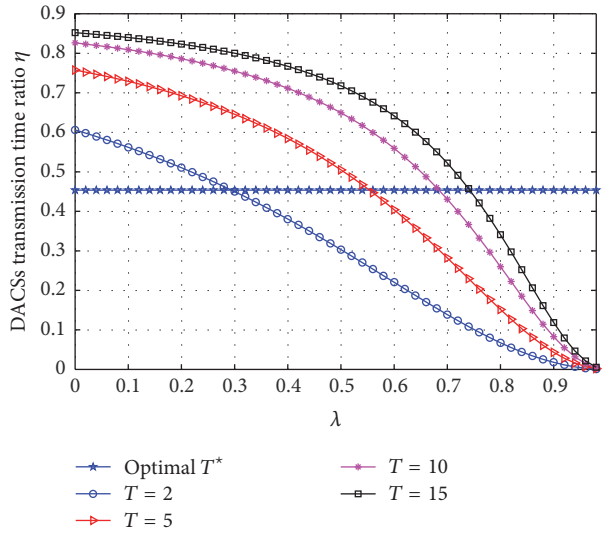

FIGURE 8: The DACSs transmission time ratio η versus the λ for different T.

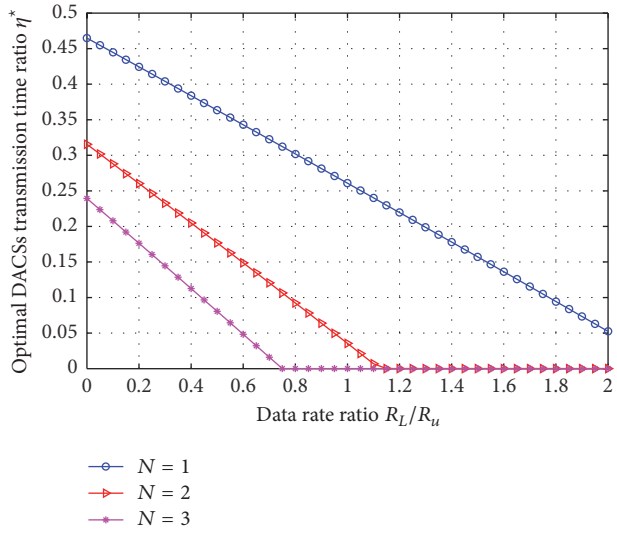

FIGURE 9: The optimal DACSs transmission time ratio η^* versus the data rate ratio R_L/R_u for different WiFi users number N.

the data rate ratio R_L/R_u, the lower the utility due to DACSs having a low satisfaction from the licensed band.

From Figure 7 we can observe that the optimal transmission time T depends on several parameters. For the fixed λ and N, the optimal T decreases when the data rate ratio R_L/R_u is increasing. That is because the licensed band could gradually ensure the QoS of DACSs while less resource is required from the unlicensed band. Moreover, when $\lambda = 0.3$, the optimal DACSs transmission time T is smaller with larger N. In addition, we can see that the larger the λ, the larger the optimal transmission time T of DACSs. Since larger traffic load of WiFi results in larger transmission time of DACS, guaranteeing the maximum utility of whole networks can be achieved.

From Figure 8, it is clear that the DACSs transmission time ratio $\eta = t_1 + t_2 + t_3$ is a decreasing function of λ, and an increasing function of transmission time T. Since the optimal T^* is influenced by λ, in order to keep the traffic balancing between DACSs and WiFi, and maximize the utility of whole systems, the ratio η is stable.

In Figure 9, we evaluate the optimal DACSs transmission time ratio η^* with $\lambda = 0.6$ and $k_w = 1/(1-\lambda)^2$. The optimal DACSs transmission time ratio η^* is decreasing with the increasing data rate ratio R_L/R_u for different WiFi users number N. η decreases to zero when ratio $R_L/R_u > 1.15$, $N = 2$, and $R_L/R_u > 0.75$, $N = 3$, respectively. In this case, DACSs can obtain enough resource in the licensed band and do not acquire additional resource from the unlicensed band. In addition, we also observe that the more the WiFi users, the lower the optimal DACS transmission time ratio η^*, since more WiFi users lead to fiercer competition and less available spectrum resource in unlicensed band.

In order to illustrate the dual-band access scheme based on sensing information in the licensed/unlicensed band and evaluate the performance of the proposed SDTB algorithm, we use the following schemes for simulation comparison: (1) Ergodic Capacity Resource Allocation (ECRA) algorithm which only accesses the licensed band; (2) Distributed Downlink Resource Allocation (DDRA-fixed T) algorithm which only uses the unlicensed band with fixed T; (3) Optimal Distributed Downlink Resource Allocation (DDRA-optimal T) algorithm which only uses the unlicensed band with optimal T^*; (4) Dual-Band Resource Allocation (DBRA-fixed T) algorithm which uses both licensed and unlicensed bands with fixed T; (5) SDTB algorithm which could access both licensed and unlicensed bands with optimal T^*. Generally, we set $T = 15$ and $\lambda = 0.6$, $B_L = 14$ MHz, and $N = 1$.

Figures 10 and 11 show the average data rate and the utility of different algorithms, respectively. We have the following

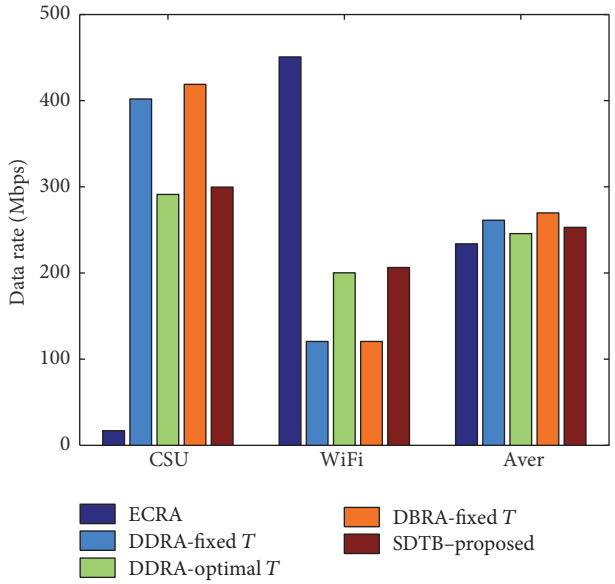

Figure 10: The average data rate for SDTB, ECRA, DDRA-fixed T, DDRA-optimal T, and DBRA-fixed T.

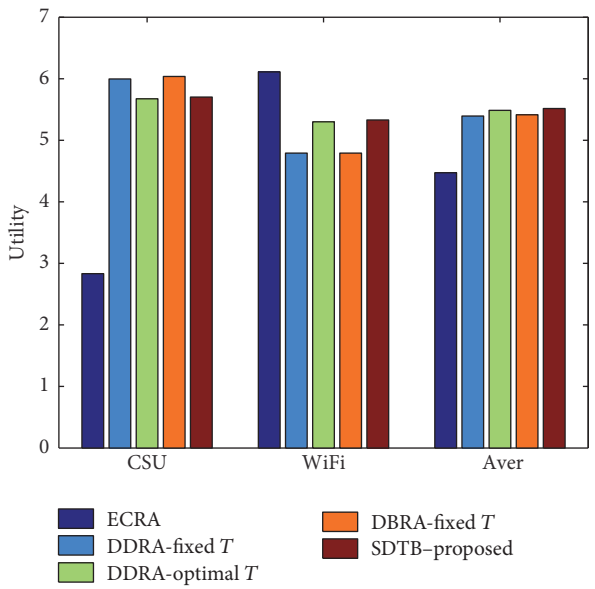

Figure 11: The average utility for SDTB, ECRA, DDRA-fixed T, DDRA-optimal T, and DBRA-fixed T.

observations from the figures. First of all, the proposed SDTB algorithm significantly improves the performance of DACSs, while it does not significantly affect the performance of WiFi network. Secondly, based on FDD, DACSs could access both licensed and unlicensed bands simultaneously, which improves the average utility and data rate compared with the Half-Duplex model. Obviously, the proposed SDTB algorithm obtains higher average utility than other schemes. Moreover, there is very little difference between the DDRA-fixed T and the DBRA-fixed T schemes, due to the small part of contributions from the licensed band to the final

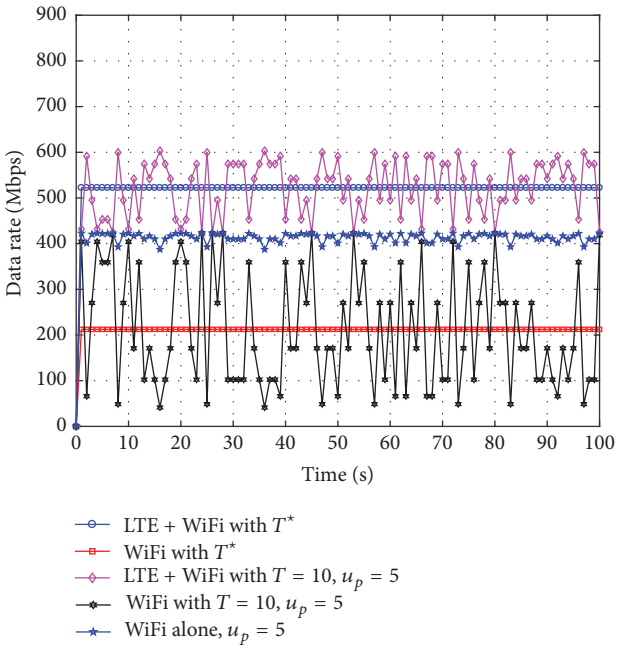

Figure 12: The data rate versus the time for different scenarios.

results. The proposed SDTB algorithm provides a better tradeoff between maximizing the total network data rate and obtaining fairness among different networks.

In this section, we evaluate the performance of the proposed SDTB scheme and the CSMA/CA scheme in realistic channel status with multi-CSBS and multi-AP. In the realistic scenarios, the traffic load of WiFi nodes is random and formulated by the Poisson-distribution with parameter u_p. In order to obtain the optimal transmission time for both LTE users and WiFi nodes we should predict the traffic load of WiFi nodes which is random. Thus, we consider the following three scenarios: CSBSs and one WiFi node scenario with optimal-T based on the SDTB algorithm, CSBSs and one WiFi node scenario with $T = 10$ based on the DBRA-fixed T algorithm, and WiFi nodes alone. Figures 12 and 13 show the data rate and the utility versus the time for different scenarios. Considering that WiFi nodes access the channel in a random fashion, the Poisson-distribution with parameter u_p is used in the simulation to present the random arrival of WiFi users traffic load and the number of the packet obeying exponential distribution. K_p is the number of WiFi packets according to the Poisson-distribution with mean rate u_p, and the probability of a WiFi user continuing to transmit data in the next slot is $\lambda = \sum_{k=0}^{K_p}((u_p)^k \cdot e^{-u_p})/(k!)$. The mean rate $u_p = 5$ in our simulation. Based on the simulation results, the data rate of the DBRA-fixed T algorithm and the WiFi-alone is not stable during the simulation time due to the random traffic load of WiFi, while the data rate of the proposed algorithm with optimal T could provide a stable performance, as well as the traffic balancing between the DACS system and the WiFi system. Clearly, the total data rate and the data rate of WiFi with optimal-T are not always larger than those of the algorithm with $T = 10$. This is because the main purpose

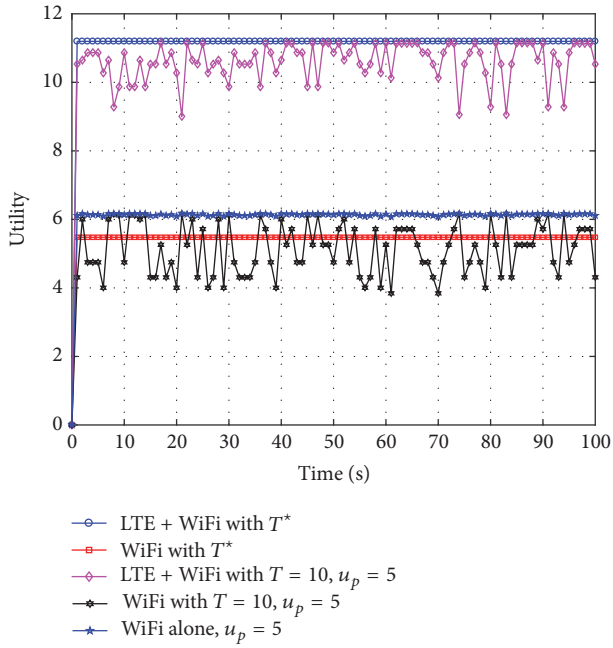

Figure 13: The utility versus the time for different scenarios.

is to maximize the total utility of the whole network. From Figure 13, we can observe that the total utility of LTE and WiFi and WiFi utility with optimal-T are stable which is in accordance with the result from the Figure 4. The proposed SDTB algorithm can obtain the optimal T under different WiFi traffic load λ and achieve the maximum utility of whole networks. Specially, the utility of WiFi-alone scenario is close to the number 6, since the WiFi access mechanism is based on the CSMA/CA protocol without the interference from LTE system. Moreover, Figure 13 shows that the proposed scheme in our paper can achieve higher and stable satisfaction.

6. Conclusion

In this paper, we have described the dual-access cognitive small cell (DACS) network that uses the LTE air interface to transmit and receive signals in the licensed and unlicensed band simultaneously. In order to maximize the total utility of the whole network, we jointly optimize the cell selection, the sensing operation, and the power allocation in the licensed band while optimizing the transmission time in the unlicensed band. A satisfaction-based dual-band traffic balancing (SDTB) algorithm over licensed and unlicensed bands for DACSs is proposed to improve the total utility of DACSs and WiFi systems. The optimization problem is divided into two suboptimization problems: sensing-based power allocation (SBPA) and dual-band traffic balancing (DBTB). The SBPA problem is formulated as a nonconvex game and it theoretically proved the existence and uniqueness of the QNE. In addition, based on the DBTB scheme, we could obtain the optimal transmission time in the unlicensed band and ensure the fairness coexistence between DACS and WiFi.

Conflicts of Interest

The authors declare that they have no conflicts of interest.

Acknowledgments

This work is supported by the National Natural Science Foundation of China (NSFC) (61401053), the 863 project (no. 2014AA01A701), Changjiang Scholars and Innovative Research Team in University (IRT1299), Special Fund of Chongqing Key Laboratory (CSTC), the Natural Science Foundation of Chongqing (CSTC2012JJA40043), and the Advanced and Applied Basic Research Projects of Chongqing (cstc2015jcyj40048).

References

[1] A. Bleicher, "A surge in small cells: mini cell ular base stations will blanket urban hot zones and rural dead zones," *IEEE Spectrum*, vol. 50, no. 1, pp. 38-39, 2013.

[2] N. I. A. Apandi, W. Hardjawana, and B. Vucetic, "Distributed transmit power management for small cell networks," in *Proceedings of the 25th IEEE Annual International Symposium on Personal, Indoor, and Mobile Radio Communication (IEEE PIMRC '14)*, pp. 1696–1700, Washington, Wash, USA, September 2014.

[3] A. K. Sadek, T. Kadous, K. Tang, H. Lee, and M. Fan, "Extending LTE to unlicensed band-merit and coexistence," in *Proceedings of the IEEE International Conference on Communication Workshop (ICCW '15)*, pp. 2344–2349, London, UK, June 2015.

[4] A. Ranjan, Anurag, and B. Singh, "Design and analysis of spectrum sensing in cognitive radio based on energy detection," in *Proceedings of the 2016 International Conference on Signal and Information Processing (IConSIP 16)*, Vishnupuri, India, October 2016.

[5] S.-Y. Lien, J. Lee, and Y.-C. Liang, "Random access or scheduling: optimum LTE licensed-assisted access to unlicensed spectrum," *IEEE Communications Letters*, vol. 20, no. 3, pp. 590–593, 2016.

[6] F. Liu, E. Bala, E. Erkip, and R. Yang, "A framework for femtocells to access both licensed and unlicensed bands," in *Proceedings of the 2011 International Symposium of on Modeling and Optimization of Mobile, Ad Hoc, and Wireless Networks (WiOpt '11)*, pp. 407–411, Princeton, NJ, USA, May 2011.

[7] G. Yuan, X. Zhang, W. Wang, and Y. Yang, "Carrier aggregation for LTE-advanced mobile communication systems," *IEEE Communications Magazine*, vol. 48, no. 2, pp. 88–93, 2010.

[8] Z. Li, C. Dong, A. Li, and H. Wang, "Traffic offloading from LTE-U to WiFi: A multi-objective optimization approach," in *Proceedings of the 2016 IEEE International Conference on Communication Systems (ICCS '16)*, Shenzhen, China, December 2016.

[9] R. Sun, M. Hong, and Z.-Q. Luo, "Optimal joint base station assignment and power allocation in a cellular network," in *Proceedings of the IEEE 13th International Workshop on Signal Processing Advances in Wireless Communications (SPAWC '12)*, pp. 234–238, Cesme, Turkey, June 2012.

[10] D. H. N. Nguyen and T. Le-Ngoc, "Joint beamforming design and base-station assignment in a coordinated multicell system," *IET Communications*, vol. 7, no. 10, pp. 942–949, 2013.

[11] Z. Han, D. Niyato, W. Saad, T. Basar, and A. Hjorungnes, *Game Theory in Wireless and Communication Networks*, Cambridge University Press, Cambridge, UK, 2011.

[12] X. Huang, B. Beferull-Lozano, and C. Botella, "Quasi-nash equilibria for non-convex distributed power allocation games in cognitive radios," *IEEE Transactions on Wireless Communications*, vol. 12, no. 7, pp. 3326–3337, 2013.

[13] J.-S. Pang and G. Scutari, "Joint sensing and power allocation in nonconvex cognitive radio games: Quasi-nash equilibria," *IEEE Transactions on Signal Processing*, vol. 61, no. 9, pp. 2366–2382, 2013.

[14] E. Almeida, A. M. Cavalcante, R. C. D. Paiva et al., "Enabling LTE/WiFi coexistence by LTE blank subframe allocation," in *Proceedings of the IEEE International Conference on Communications (ICC '13)*, pp. 5083–5088, IEEE, Budapest, Hungary, June 2013.

[15] CableLabs, "Cable Labs perspective on LTE-U coexistence with WiFi and operational modes for LTE-U, 3GPP RAN1 standard contribution-RWS-140004," Tech. Rep., CableLabs, Louisville, Colo, USA, 2014.

[16] H. Zhang, X. Chu, W. Guo, and S. Wang, "Coexistence of Wi-Fi and heterogeneous small cell networks sharing unlicensed spectrum," *IEEE Communications Magazine*, vol. 53, no. 3, pp. 158–164, 2015.

[17] A. K. Bairagi, N. H. Tran, and C. S. Hong, "LTE-U sum-rate maximization considering QoS and co-existence issue," in *Proceedings of the 2017 IEEE International Conference on Big Data and Smart Computing (BigComp '17)*, pp. 352–357, Jeju Island, South Korea, Feburary 2017.

[18] F. Cai, Y. Gao, L. Cheng, L. Sang, and D. Yang, "Spectrum sharing for LTE and WiFi coexistence using decision tree and game theory," in *Proceedings of the 2016 IEEE Wireless Communications and Networking Conference (WCNC '16)*, Doha, Qatar, April 2016.

[19] R. Ratasuk, M. A. Uusitalo, N. Mangalvedhe et al., "License-exempt LTE deployment in heterogeneous network," in *Proceedings of the 9th International Symposium on Wireless Communication Systems (ISWCS 12)*, pp. 246–250, Paris, France, August 2012.

[20] A. Bhorkar, C. Ibars, and P. Zong, "Performance analysis of LTE and Wi-Fi in unlicensed band using stochastic geometry," in *Proceedings of the 25th IEEE Annual International Symposium on Personal, Indoor, and Mobile Radio Communication (IEEE PIMRC '14)*, pp. 1310–1314, Washington, Wash, USA, September 2014.

[21] A. Babaei, J. Andreoli-Fang, and B. Hamzeh, "On the impact of LTE-U on Wi-Fi performance," in *Proceedings of the 25th IEEE Annual International Symposium on Personal, Indoor, and Mobile Radio Communication (IEEE PIMRC '14)*, pp. 1621–1625, Washington, Wash, USA, September 2014.

[22] J. Xiao and J. Zheng, "An adaptive channel access mechanism for LTE-U and WiFi coexistence in an unlicensed spectrum," in *Proceedings of the 2016 IEEE International Conference on Communications (ICC '16)*, Kuala Lumpur, Malaysia, May 2016.

[23] F. Liu, E. Erkip, M. C. Beluri, R. Yang, and E. Bala, "Dual-band femtocell traffic balancing over licensed and unlicensed bands," in *Proceedings of the 2012 IEEE International Conference on Communications (ICC '12)*, pp. 6809–6814, Ottawa, Canada, June 2012.

[24] M. G. S. Sriyananda and M. Bennis, "Learning-based small cell traffic balancing over licensed and unlicensed bands," *IEEE Wireless Communications Letters*, vol. 6, no. 5, pp. 694–697, 2017.

[25] Y. Xu, R. Yin, Q. Chen, and G. Yu, "Joint licensed and unlicensed spectrum allocation for unlicensed LTE," in *Proceedings of the 26th IEEE Annual International Symposium on Personal, Indoor, and Mobile Radio Communications (PIMRC '15)*, pp. 1912–1917, Hong Kong, China, September 2015.

[26] Y. Lan, L. Wang, H. Jiang et al., "A field trial of LTE in unlicensed bands with SDL (supplemental downlink) transmission," in *Proceedings of the 2016 IEEE Wireless Communications and Networking Conference (WCNC '16)*, Doha, Qatar, April 2016.

[27] X. Huang, F. Zhu, Y. Zou, and Q. Chen, "Dynamic base station assignment and resource allocation in MIMO CR small-cell networks," in *Proceedings of the 14th International Symposium on Communications and Information Technologies (ISCIT '14)*, pp. 61–65, Incheon, South Korea, September 2014.

[28] X. Huang, L. Chen, Q. Chen, and B. Shen, "Coalition based optimization of resource allocation with malicious user detection in cognitive radio networks," *KSII Transactions on Internet and Information Systems*, vol. 10, no. 10, pp. 4661–4680, 2016.

[29] X. Huang, S. Liu, Y. Li, F. Zhu, and Q. Chen, "Dynamic cell selection and resource allocation in cognitive small cell networks," in *Proceedings of the 27th IEEE Annual International Symposium on Personal, Indoor, and Mobile Radio Communications (PIMRC '16)*, Valencia, Spain, September 2016.

[30] R. A. Waltz, J. L. Morales, J. Nocedal, and D. Orban, "An interior algorithm for nonlinear optimization that combines line search and trust region steps," *Mathematical Programming*, vol. 107, no. 3, pp. 391–408, 2006.

[31] R. H. Byrd, M. E. Hribar, and J. Nocedal, "An interior point algorithm for large-scale nonlinear programming," *SIAM Journal on Optimization*, vol. 9, no. 4, pp. 877–900, 1999.

[32] European Telecommunications Standards Institute, *Radio Frequency (RF) System Scenarios, 3GPP TR 36.942 Version 10.2.0 Release 10, LTE: Evolved Universal Terrestrial Radio Access (E-UTRA)*, European Telecommunications Standards Institute, 2011.

[33] FCC, "Second Report and Order," FCC 08-260, Federal Communications Commission, November, 2008.

Hindawi
Wireless Communications and Mobile Computing
Volume 2017, Article ID 3592792, 9 pages
https://doi.org/10.1155/2017/3592792

Research Article

Cognitive Security of Wireless Communication Systems in the Physical Layer

Mustafa Harun Yılmaz,[1] Ertuğrul Güvenkaya,[2] Haji M. Furqan,[3] Selçuk Köse,[4] and Hüseyin Arslan[3,4]

[1]*Institute for Telecommunication Sciences, National Telecommunications & Information Administration, Boulder, CO 80305, USA*
[2]*Maxlinear Inc., Carlsbad, CA, USA*
[3]*School of Engineering and Natural Sciences, Istanbul Medipol University, Beykoz, 34810 İstanbul, Turkey*
[4]*Department of Electrical Engineering, University of South Florida, Tampa, FL 33620, USA*

Correspondence should be addressed to Mustafa Harun Yılmaz; harunyilmaz62@gmail.com

Received 23 April 2017; Revised 3 October 2017; Accepted 1 November 2017; Published 18 December 2017

Academic Editor: Mohammad Shikh-Bahaei

While the wireless communication systems provide the means of connectivity nearly everywhere and all the time, communication security requires more attention. Even though current efforts provide solutions to specific problems under given circumstances, these methods are neither adaptive nor flexible enough to provide security under the dynamic conditions which make the security breaches an important concern. In this paper, a cognitive security (CS) concept for wireless communication systems in the physical layer is proposed with the aim of providing a comprehensive solution to wireless security problems. The proposed method will enable the comprehensive security to ensure a robust and reliable communication in the existence of adversaries by providing adaptive security solutions in the communication systems by exploiting the physical layer security from different perspective. The adaptiveness relies on the fact that radio adapts its propagation characteristics to satisfy secure communication based on specific conditions which are given as user density, application specific adaptation, and location within CS concept. Thus, instead of providing any type of new security mechanism, it is proposed that radio can take the necessary precautions based on these conditions before the attacks occur. Various access scenarios are investigated to enable the CS while considering these conditions.

1. Introduction

The proliferation of wireless technologies in our daily life leads to an increasing demand for these technologies. While the prevalence of wireless communication systems presents indisputable advantages to the users, due to the open broadcast nature of the wireless signals, the communication exchanges are exposed to the attacks of adversaries. As opposed to its wired counterparts, the enhanced mobility support of the wireless communication systems comes with the handicap of serious security vulnerabilities from the physical layer to the application layer. To protect the wireless signals from malicious attacks, security measures should be provided to the user. In the existing wireless communication systems, security concerns are addressed in the upper layers by means of various encryption techniques. Encryption is achieved in such a way that the message is encrypted with a key generated by using cipher, that is, an encryption algorithm, before the signal is transmitted. The receiver can decrypt the message by using the same key. However, since encryption is a way of protecting the message in the upper layers, it does not prevent the signal from being detected by adversaries in the medium. Additionally, encryption increases the infrastructural overhead and power consumption to enable the authentication, which may not be feasible in some applications such as wireless sensor networks [1]. Data security in wireless domain has to adapt itself to the new wireless communications paradigm by becoming more adaptive and flexible. To this end, implementation of communication security in the physical layer has recently become a field of interest. Existing security threats in the physical layer can be categorized into three groups: eavesdropping,

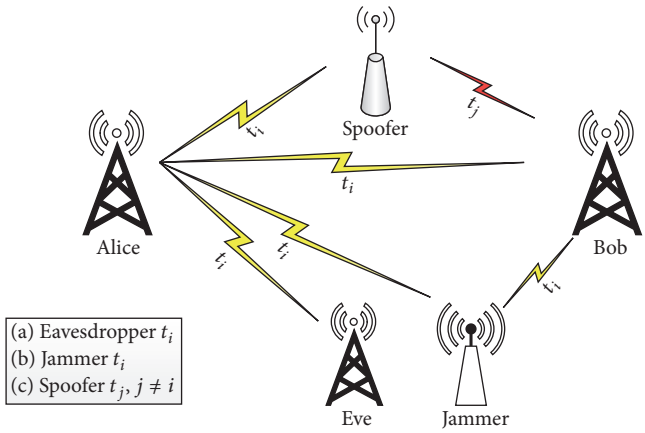

Figure 1: When Alice transmits a message to Bob at time t_i, (a) eavesdropper receives/listens the same message at time t_i, (b) jammer transmits a jamming signal to Bob at time t_i, and (c) spoofer listens to the message at time t_i and then transmits a spoofing message at time t_j where $t_j \neq t_i$.

jamming, and spoofing as depicted in Figure 1. In the physical layer security studies, legitimate transmitter, legitimate receiver, and passive attacker are symbolized, respectively, as Alice, Bob, and Eve. The attacker might be considered as either a jammer or a spoofer if attacker is active.

(1) *Eavesdropping*: when Alice transmits a message to Bob, any receiver can receive the message since the message is propagated through the whole environment. Eavesdropping refers to a situation where Eve can receive the message transmitted by Alice. The message needs to be protected against the eavesdroppers.

(2) *Jamming*: when Alice and Bob are communicating with each other, a jammer transmits a noise type of signal to Bob with the aim of corrupting the communication. When Bob receives both signals at the same time, legitimate signal would be received as meaningless signal. Therefore, the signal would not be decoded. This type of attack is named as jamming. When the attack is held, it needs to be identified by legitimate users, and the signal needs to be protected accordingly.

(3) *Spoofing*: spoofing refers to a situation where the attacker deceives Bob. Spoofing can be carried out in two ways. (a) When Alice stops transmitting the signal, an attacker starts to transmit a deceiving signal to Bob. (b) When Alice transmits the signal, if an attacker transmits deceiving signal with higher power than Alice's signal power, Bob would receive the attacker's signal as legitimate signal while it would consider Alice's signal as interference signal. Similar to the jamming case, this attack needs to be identified and necessary precautions should be taken.

In the literature, studies on physical layer security mainly focus on spread spectrum (SS) techniques and channel and power based solutions. In SS techniques, the energy of the signal is spread over the wider spectrum by means of possessing a wider band. SS techniques are particularly useful against the jamming attacks and eavesdropping. In eavesdropping case, these techniques are used to attain the low probability of interception and detection. Frequency hopping spread spectrum (FHSS) and direct sequence spread spectrum (DSSS) are primary SS techniques used in the literature. FHSS is derived by hopping the signal with a predefined pseudorandom code in the spectrum while in DSSS the energy of the signal is spread over a wide spectrum with a pseudonoise (PN) sequence which keeps the signal power under noise level. As mentioned in [2], these techniques can be utilized to provide security against jamming attacks with certain vulnerabilities. For instance, FHSS technique may be vulnerable against spoofing attacks. To overcome this issue, an antijamming scheme that is based on transmitting a secure identity generated with cryptographic methods is proposed in [3]. Thus, the legitimate transceiver communication can be protected against jamming and spoofing attacks. The drawbacks of DSSS scheme against jammers are investigated in [4]. This drawback is defined in such a way that when PN sequence of jammer is matched with the transmitter's PN sequence, the legitimate receiver can be jammed. To address this drawback, authors propose a watermarked DSSS scheme. In this scheme, an authentication information is embedded to PN sequence to make the system more resistant against jamming attacks.

In channel based solutions, the uniqueness feature of the channel can be utilized to improve security. Since the communication channel between Alice and Bob is different from the channel between Eve and Bob, Alice can perform a secure communication by using its unique channel with Bob. The effects of artificial noise insertion in the presence of Eve are explored in [5]. The primary objective of the artificial noise insertion is to degrade Eve's channel while not affecting Bob's channel. To carry out this aim, Alice adds noise intentionally to the null spaces of Bob's channel. Since Eve does not know the intentional addition of noise, she is not able to detect the signal correctly. Thus, the secure communication would be satisfied even if Eve's channel is not known. Primarily, eavesdropping and spoofing can be prevented with channel based solutions.

In power based solutions, received signal strength (RSS) and directional antenna are used to provide security. RSS is utilized to detect the primary user (PU) emulation attack in [6]. In the cognitive radio network, there are PUs and secondary users (SUs). SUs use the licensed spectrum of PUs. If PU utilizes any bands in its spectrum, SU does not use the same band in order not to cause interference with PU. To determine which bands are utilized by PU, SU can use spectrum sensing algorithm. There might be spoofers in the environment to deceive SUs by masquerading the PU. A verification algorithm to detect the spoofers is proposed in [6] by utilizing the signal characteristics and location of the legitimate transmitter. RSS measurements are performed within a wireless sensor network. All transmitters locations can be estimated by identifying the RSS peaks. In [7], directional antennas are explored against jamming attacks instead of the more conventional omnidirectional

antennas. The connectivity is maintained under jamming attacks with directional antennas. Since there are multiple antennas in Bob, certain antennas can easily be reconfigured towards a direction other than the direction where the jamming signal is coming from. In this case, the transmitter can keep the connectivity with the legitimate receiver with higher data rate when compared to omnidirectional antenna usage case. Wyner introduces the wiretap channels, namely, eavesdropper's channel, in [8]. He aims at rendering the signal meaningless taken by wire-tapper. To achieve this, Wyner utilizes signal-to-noise ratio (SNR) differences observed at Bob and Eve. If Eve's SNR is lower than Bob's SNR, Alice can initiate a secret communication with Bob without any information leakage to Eve via encoding.

While the aforementioned studies provide a security only in the physical layer, the security in cross-layer is investigated in the following studies. The requirements and benefits of cross-layer security are presented for wireless sensor network (WSN) in [9]. As explained in [9], cross-layer design should work collaboratively to detect the adversaries while enabling the efficient power consumption. The cross-layer utilization by means of the intrusion detection is proposed in [10]. It is proved that security which is obtained by exploiting the data coming from different layers such as link and network layers is increased significantly when compared to the single layered security solutions in terms of true positive rates.

Besides the studies focusing on the specific security issue, in a few studies, the physical layer security literature is surveyed. In each of these papers, authors examine the security studies from different perspectives. In [11, 12], and from a bigger picture in [13, 14], authors investigate the security in cognitive networks. While authors in [15] explain the security issues in health care domain, authors in [16] look at these issues in smart grid applications.

2. Motivation

Although existing efforts satisfy the security needs of the users under certain conditions and for specific wireless communications systems, they might fail in others. For instance, since channel based solutions have complete dependency on channel conditions, while these solutions would work when legitimate transceiver is static and has reciprocal channel, these solutions would fail when the legitimate transceiver is either mobile or performs communication based on frequency division duplexing. Alternatively, SS techniques can be employed to protect data against jamming attacks and eavesdropping. When there is a spoofer in the environment, if an additional protection algorithm as given in [3] is not proposed, SS technique would fail. Moreover, using an additional algorithm would increase the complexity of the legitimate transceiver. Another issue with SS techniques is related to PN or hopping sequence sharing. When a legitimate transmitter sends PN or a hopping sequence to a legitimate receiver, if the sequence is not protected, an illegitimate node can capture this secret information. Therefore, illegitimate node can easily eavesdrop, jam, or spoof the legitimate receiver. As explained in Section 1, localization can be performed with power based solutions. In RSS based localization, it is assumed that illegitimate node uses omnidirectional antennas and multiple receivers measure the RSS of this node to be able to perform true localization. If illegitimate node employs the directional antenna, localization would fail [17]. On the other hand, since the location of eavesdropper is unknown, power based solutions cannot provide security against eavesdroppers either.

All of these weaknesses of the existing solutions indicate the necessity that the security threats need to be investigated with more comprehensive solutions in the physical layer. In this study, we propose cognitive security (CS) concept which provides adaptive security solutions in the communication systems by exploiting the physical layer security from different perspective. The adaptiveness relies on the fact that radio adapts its propagation characteristics to satisfy secure communication based on specific conditions. In this paper, the conditions are defined as the user density, application specific adaptation, and location. Please note that, in the existing efforts, security is provided when the legitimate transceiver is under attack(s). However, the security is performed in CS concept before the attack occurs. In other words, CS proposes that the necessary precautions are required to be taken before the attack takes place based on the conditions which are explained in detail in the subsequent sections. Thus, the systems would adjust the propagation parameters of the radio against possible threats. With the given conditions, CS should

(i) Increase the reliability in the wireless communication systems: since transceiver would be able to adjust the security level, increasing the security adaptively will increase the overall reliability of the communication system automatically. Especially, when a receiver is under jamming attack, one of the most important problems is to satisfy reliable communication to guarantee the quality of service requirement. CS would play an important role in this situation.

(ii) Decrease the system complexity: the active attackers need to be detected in current security mechanisms. This requires additional algorithms to be implemented in the systems. Since, in CS concept, detecting the attackers is not necessitated, this would reduce the complexity caused by the usage of the additional algorithms.

Along with these advantages, CS should also

(i) Increase the data rate: the radio resources allocated for providing secure communication can be reduced for the cases which do not necessitate high level of security due to low probability of threat. For instance, if the security is based on the location, let us say, in rural areas, security level is lowered when compared to urban areas. Since some resources which are allocated to provide security would remain empty, these resources will be used for data communication. Thus, the users who live in rural areas would have higher data rates.

(ii) Decrease the energy consumption: it is important to lower the consumed energy in the systems during the communication, for example, in mobile devices. If

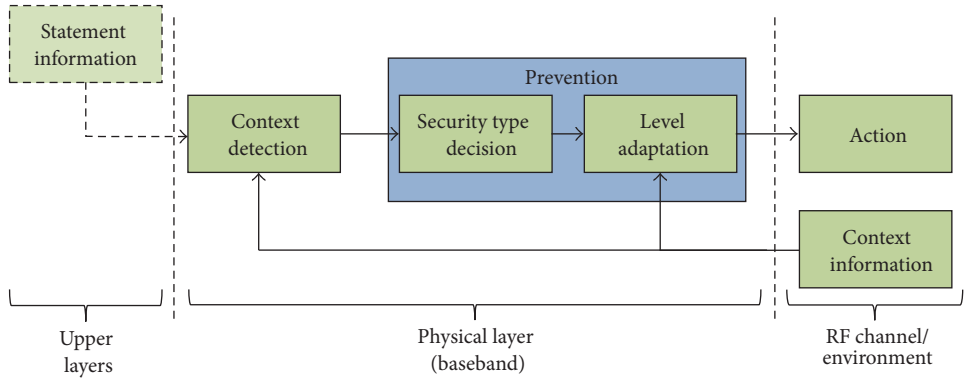

Figure 2: System model for cognitive security.

security level is lowered in uplink, the mobile device would be able to transmit the same amount of data in less duration since the data rate would be higher.

3. Cognitive Security Concepts

The system model for cognitive physical layer security is illustrated in Figure 2. The radio combines the relevant information obtained from the radio channel and environment. Based on the available knowledge, the context is detected. To improve the detection performance, the statement information can be attained from the upper layers. After an associated security mechanism is determined by the radio, the level of the security can be adjusted as a function of the intensity of threat.

In this study, we define three the CS concepts: user density, application specific adaptation, and location.

3.1. User Density. User density refers to a number of users per unit area. If the number of users is high in a given area when compared to a predetermined normal, for example, schools and hospitals, it can be stated that the area has high density in terms of the number of users and named as high user density through the rest of the paper. From the security perspective, high user density is an important parameter, especially for CS concept. As mentioned in Section 1, there are three threat groups in physical layer security studies. The radio can act intelligently to provide secure communication in spite of the fact that these three groups are probable to occur related to the user density. For specific places such as hospitals, office blocks, and airports, security is highly important. Jammers, eavesdroppers, or spoofers are expected to exist in such places as shown in Figure 3. In [18], authors define the probability of eavesdropping (or attacking) in a given area A.

$$P(e) = 1 - e^{-\rho A}, \tag{1}$$

where ρ is the node density. For a given area, when the node density increases, probability of eavesdropping increases as well.

Density is the detectable data by the radio. In a high user dense area, since most of the resources would be occupied by the users, the detection of the density can be achieved by observing the total number of allocated resources at a time. When high density is detected, attackers would aim to affect the communication in between legitimate users, for instance, between a patient and a doctor in the hospital. Implantable medical devices (IMDs) such as defibrillators and peacemakers are implanted within the patient's body and are monitored and controlled by the physician with the help of external unit wirelessly. This wireless nature will make the IMDs vulnerable to attacks which might disrupt the communication by jamming or sending wrong information to the legitimate receiver by spoofing. In both cases, if the patient is in a critical condition and needs an emergent treatment, since the doctor will not be able to know the patient's situation because of jamming or spoofing, s/he will not treat his/her patient. The result might therefore be fatal for the patient. In this case, to be immune to attacks, the radio might increase the security. If the high user density stems from the office block, legitimate users might be eavesdropped on. The aim of the eavesdropper is to capture the company's critical information. Another important issue is that there might be many jammers, eavesdroppers, or spoofers who work collaboratively in high user dense areas. The security can possibly be improved significantly by adaptively adjusting the propagation parameters of the radio.

There might be various reasons for users to gather in a given area such as stadium, hospital, school, or airport. Since it is not possible for a radio to detect the reason of users' gathering, the necessary information can be obtained from the upper layers. For instance, if the users in the high dense area send important documents, this can be detected by the upper layers and this information is provided to radio. Based on this notice, radio can consider that the density stems from the employees who work in an office block. This type of security approach is named as cross-layer security in the literature [9]. As defined in Section 2, one of the key advantages of CS is to increase the data rate. If a holistic approach is not considered, data rate might be decreased unnecessarily in some cases. For instance, assume that the security should be higher in office blocks than the security in stadiums. Since radio does not have the reason of users' gathering, it would increase the security to the same level in all high user dense areas. This may not be desirable for

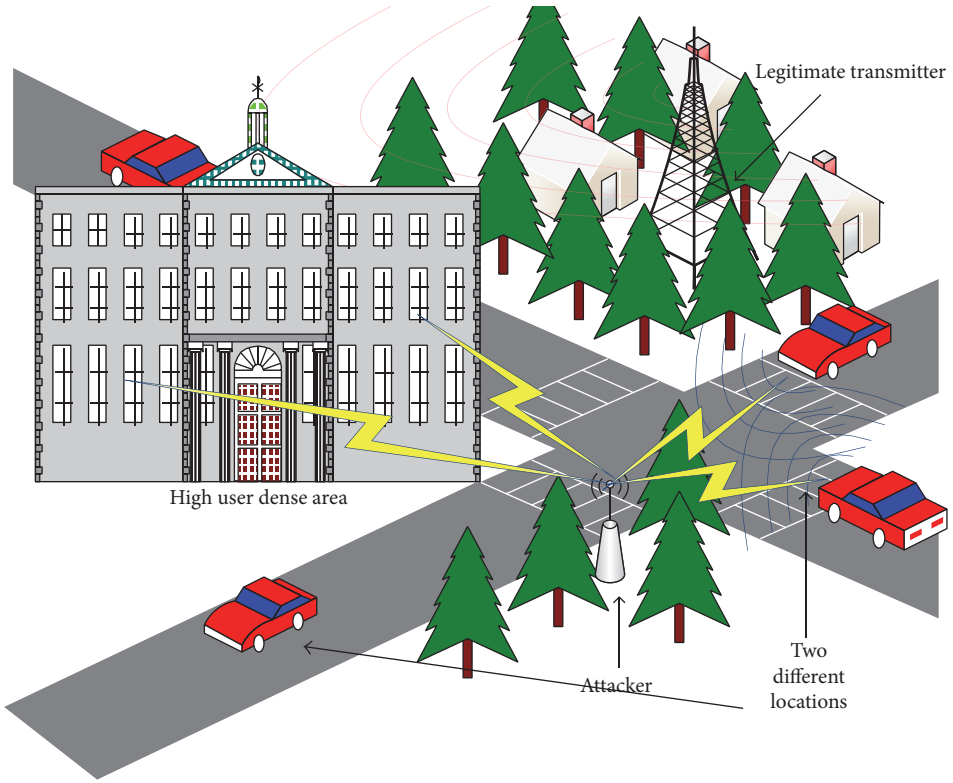

Figure 3: Attackers would appear in the user dense areas. Also, they are more likely to jam or spoof the vehicular communication in the intersections.

every situation. For the same amount of user data, high secure communication might necessitate more resources to be allocated than less secure communication. Therefore, data rate in the relevant dense area would decrease. When the density in question occurs in the stadiums, data rate would become more critical. The security level in the stadium should not be the same as the one in the office blocks. This situation can be considered as the probability of error in the increment level of security.

3.2. Application Specific Adaptation. Application specific refers to different fields such as military, commercial, and health monitoring in which the radio is used. Communication is typically held wirelessly in these fields. To minimize or alleviate the interference, different frequency bands are allocated for each field. These different bands carry significant context information for the radio. This helps the radio to detect the type of application for which the communication is being fulfilled.

Each application has different security requirement. While it is high for military communication, it might be low for commercial applications, such as for cellular communication. Ensuring secure communication requires more resources to be allocated and a higher data rate is vital for commercial sector. Allocating as many resources as in military communication for security reasons to carry out the communication may therefore not be feasible in commercial domain. In any case, communication needs to be provided securely when the transceiver is under attacks. Existing security threats would differ based on time and place where the communication is being held for each application. For instance, when the country is in peace, passive attacks like eavesdropping would be significant for military communication. But, if there is an emergency situation such as a battle, jamming and spoofing are going to be very serious issues as well. In these types of situations, security needs to be adjusted accordingly. The existing algorithms which are proposed to protect the data from eavesdroppers may not provide the security in jamming or spoofing scenarios as mentioned in Section 2. This indicates that securing the communication against each type of attacks necessitates different solutions. In any emergency situation, military may need to reach out to the public across the country or may need additional resources for the communication. To meet this demand, military has to utilize certain ubiquitous structures such as cellular base stations and broadcasting antennas. Although security level might be lower in cellular communication when compared to military, when the emergency situations occur, radio should be able to detect it and adapt itself to new situations. Since the cellular or broadcasting structure is not suitable to implement the same security methods, the radio should provide more secure communication via the physical layer security mechanisms. Herein, military would protect its communication against jamming or spoofing attacks. If

the security level depends on the application, it needs to be adaptively managed.

Another important application is the Internet of things (IoT) for future wireless networks. Various types of technologies such as implantable medical devices (IMDs), WSN, and autonomous vehicles will share the bands in IoT. These different technologies may require different level of security. For instance, while it is critical to provide high security for IMD, it may need less security in smart home applications such as controlling the refrigerator over the Internet. Therefore, CS will play an important role in 5G and beyond networks in terms of providing and adjusting necessary security and data rate needs for each application.

3.3. Location. Specific location or social environment where the communication is fulfilled is an important parameter for CS concept. For some devices such as unmanned aerial vehicles (UAVs), the location information is required to find their geographical position. Therefore, it is important to provide security against attacks based on the location information. It can be said that there is a high correlation between the type of the security threats and the location. For instance, for vehicle-to-vehicle (V2V) communication, location determines the type of the communication between vehicles. When two vehicles go back-to-back on the road, the communication is performed to maintain a minimum distance between vehicles, namely, space cushion, through the sensors at all times to not cause an accident. Alternatively, when two vehicles encounter an intersection where there is a significant decision-making process, the type of the communication would be different. One issue is the order of the vehicles to cross the intersection [19]. While this example highlights the importance of the location in terms of the type of the V2V communication, this location information is also critical to satisfy the secure communication between vehicles. The two vehicles at the intersection point need to talk to each other while simultaneously monitoring the measurement of the sensors to detect any possible rear vehicle. This may lead to some security gaps to attack the vehicles that are at the intersection point as depicted in Figure 3. In this situation, there are two possible security issues: jamming and spoofing. An attacker may destroy the communication of the vehicles or may send the same message to two vehicles such as the priority of who would pass first. Both situations would eventually cause an accident. The security level can be significantly increased if the radio is able to detect the location. Thus, the accident may be precluded.

In terms of social environment, three types of environments can be considered: rural, suburban, and urban areas. The main difference between the environment types is the population density. At this point, it is important to emphasize that the social environment should not be confused with user density in terms of the detectability. As mentioned above, user density definition covers a small area such as stadiums and schools, and it can be within urban, suburban, and rural areas. However, environment covers the whole urban, suburban, or rural area by definition.

In wireless communication, environment information is important in terms of the capacity. For instance, to increase the capacity, various deployment strategies of the base stations (BSs) are applied. While the BSs whose coverage area is as high as 1-2 km might be sufficient to serve for the users in rural areas, the small BSs whose coverage area is around 10–200 m would need to be deployed in urban areas to meet the users' demands. To provide a secure communication, environment is a significant parameter. Based on the environment type, security need would differ, especially in the public safety context. The crime rates are much higher in urban areas. For example, 39 crimes are recorded per 1,000 residents in rural areas while 79 crimes are reported in urban areas in England [20]. To decrease the crime rate, governments need to take necessary preventions. When a crime or an emergency situation occurs, each unit of the system, for example, mobile devices and networks, should work coordinately and securely so that the relevant government agent can act promptly. If the system is under jamming or spoofing attacks, the communication might be disrupted. Therefore, a high security level should be provided for each unit. Since, most of the time, this is the case for the urban areas, radio should adaptively increase the security based on the environmental information for the wireless systems. In conclusion, the type of environment also determines the level of security rather than just the security itself.

Figure 4 shows the relation between security needs and type of environment in terms of probability of attacks. This figure is drawn, that is, not based on simulation, to only help readers to visualize this relation. The probability of attack increases in the urban areas when compared to rural areas. It is also visualized that the increasing probability of attack increases the usage of resources for security reasons, which also leads to decreasing data rate.

Another importance of the location information is related to the devices which have dependency on accurate geographical position such as UAVs. While UAVs can be controlled from a ground station, they can also have preinstalled location and mission information and perform duty automatically. In both cases, UAVs necessitate location information obtained from global positioning system (GPS) satellites. Attackers would intend to disrupt the communication between UAV and GPS satellite.

Please note that UAVs are used for different purposes in different areas. While they are used for policing in public safety, they are also utilized in scientific researches, for disaster relief, and in armed attacks. Each type of usage may require the security in different levels in terms of localization. While the low level of security might be enough to provide communication in disastrous relief cases with the aim of obtaining high data rate, high level of security would be necessary in armed attacks. On the other hand, when the country is in battle, UAVs used for other purposes such as for commercial usage can also be utilized to defend the country against the enemies. Since the enemies' aim would be to disrupt or spoof the communication between UAVs and GPS satellites, UAVs would need to increase the security accordingly to not be harmed or controlled by the enemies.

As highlighted above, the aim in this study is to take the necessary precautions based on some conditions; any type of

Table 1: Advantages of cognitive security concept against security threats.

Security threats	Explanation of cognitive security conditions	Benefits
Eavesdropping	(i) Increase the secrecy rate (versus information rate) in scenarios of high user dense areas such as office blocks and airports or locations such as urban areas or specific applications such as military and public safety (ii) Relax the secrecy constraints, that is, increase the information rate, for conditions such as rural areas, WiFi, and cellular communication	Data rate Latency Energy consumption
Jamming	The level of security against jamming, for example, processing gain in spread spectrum, is adaptively increased in locations such as intersections of roads or specific applications such as military and public safety	Reliability Complexity Latency
Spoofing	Enable the spoofing detection mechanism when the condition exists, and disable the algorithm, or use a simpler method, in high user dense areas such as office blocks, stadiums, or locations such as intersections of roads and location dependent UAV devices, or specific applications such as military and in vivo communication	Complexity Reliability

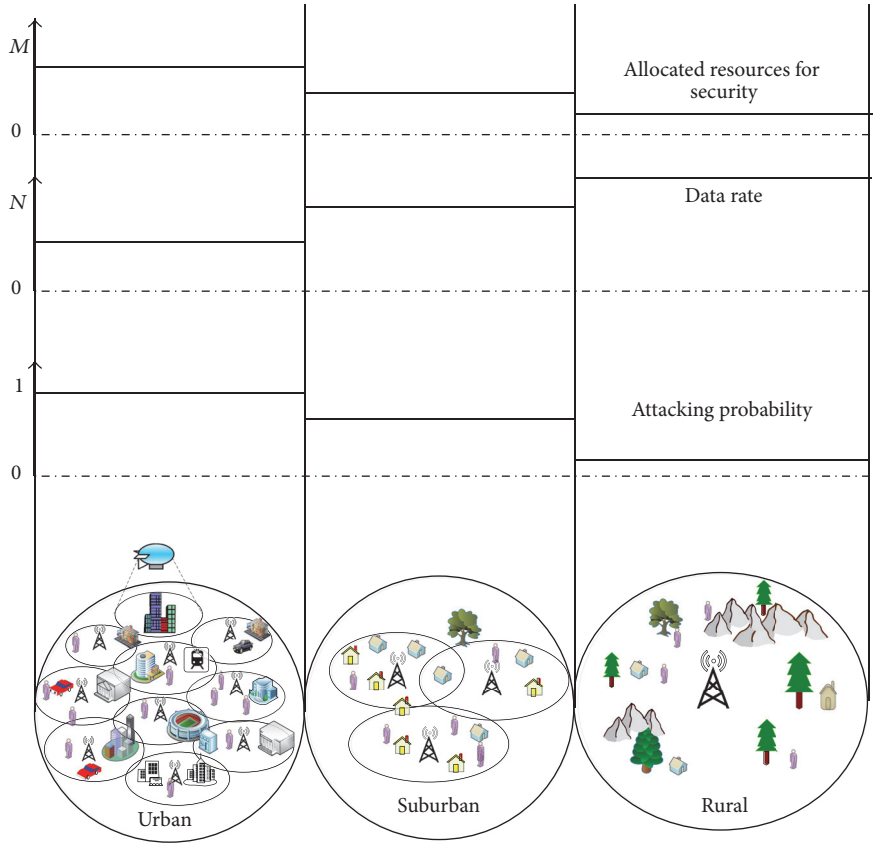

Figure 4: Based on the environment information, security needs can change. While the probability of attack might be higher in urban areas, it might be low in rural areas. The increased probability of attack increases also the resource usage to provide higher security, which also leads to decreased data rate.

new security mechanism is therefore not proposed within CS concept. Instead, three different conditions are given to help radio to determine if the security is a need or not. In Table 1, the benefits of the CS concept related to security threats are enlisted. After the security need occurs, any current security solution can be utilized. At this point, it is worth mentioning that the CS should not be confused with context-aware security concept. In context-aware security, the information is mainly obtained by different sensors. Based on the these information, the system in upper layers tries to detect if there is an attack. If so, then, the necessary security algorithm is placed. In other words, the focus in context-aware security is

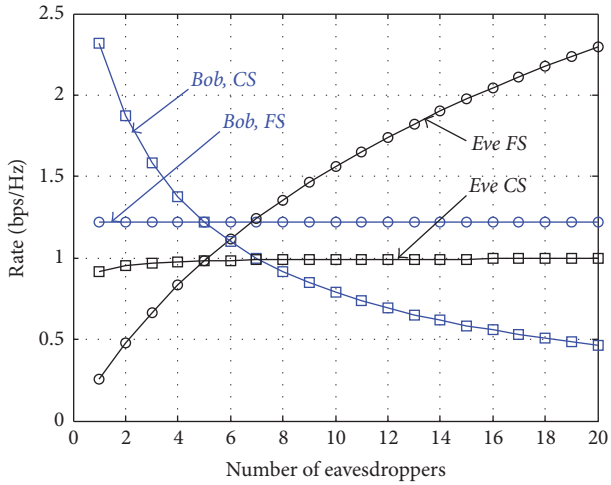

Figure 5: When the number of eavesdroppers increases in a given area, while the rate of Bob remains constant in the FS case, it is decreasing in CS. However, in terms of the security, CS provides higher security than FS case.

on providing the necessary security when it is a need based on the context information like temperature, speed, and so on [21] as in conventional approaches in the security studies [13, 14]. In CS, the security need is determined based on the conditions regardless of the attack that occurs.

In Figure 5, we compare the CS with fixed security (FS), in which the security level is the same for any conditions, for the user density case in terms of rate versus the number of eavesdropper. The rate is computed as Rate $= \sum_i \log_2(1 + \mathrm{SNR}_i)$, where i is the antenna index. As given in (1), when the user density increases in a given area, the probability of eavesdropping also increases. Based on (1), we realize this increment as the increasing number of eavesdroppers in the figure. We assume that Alice transmits the signal to Bob from multiple antennas and there are multiple eavesdroppers working collaboratively. We assume that the transmitter utilizes multiple antennas with artificial noise to provide security during communication with Bob. Invoking that the signal transmitted by multiple antennas can be considered as multidimensional signal, one of these dimensions is allocated for the data transmission to Bob while the remaining ones are used for the artificial noise transmission. In FS case, we assume that the number of transmit antennas of Alice is fixed. In this case, when the number of eavesdroppers increases, Eve's rate will also increase. Since only fixed number of antennas is used to send artificial noise signal, the desired security will be achieved only for the cases where the number of eavesdroppers is less than the number of dimensions allocated for the artificial noise at the transmitter. Therefore, the sum rate of the eavesdroppers will increase by increasing the number of collaborating malicious nodes. For this case, the rate of Bob will remain constant. In CS case, the number of transmit dimensions for the artificial noise of Alice changes with the number of eavesdroppers in the environment. While the security level of eavesdropper stays the same because of having constant rate, Alice's rate decreases. It is because the total transmit power of Alice is fixed and shared between the data and artificial noise signals.

4. Conclusion and Open Issues

Providing security in wireless communication is a critical task. In this paper, we focused on the security in physical layer where we proposed CS concept. Radio can adapt its security level in CS by considering three different conditions which are defined as user density, application specific adaptation, and location. These conditions come along with certain challenges which can be listed as follows.

4.1. How to Detect If the Condition Exists? To make the security adaptive, ensuring the detectability of context information is critical. While some of the context information such as user density is easy to detect via available spectrum sensing techniques [22], for some of them such as application specific, it is a hard task. As explained in Section 3.2, when the country is in battle and the military needs to use the cellular stations and frequencies for the communication, radio should have the capability to increase the security. Here, the question arises as to how the radio realizes that condition. If there is a need to obtain some parameters from the upper layers to detect the context information, how should radio collaborate with those layers? Collaboration between the layers is also a subject of cross-layer techniques [9].

4.2. How to Identify the Correct Statement about the Context? As mentioned in Section 3.1, detailed knowledge might be needed to adapt the security level after detecting the existence of context information. For instance, the reason of users' gathering can be an entertainment event which might not necessitate a high security level while it can be required in business environments. How one can differentiate the statement of the context emerges as a hot topic.

4.3. What Type of Security Mechanism Can Be Used and How Many Resources Should Radio Allocate? There are many studies to secure the communication in physical layer most of which focus on specific circumstances. Especially, after detecting the context information and identifying the correct statement, the third step is: "Other than current efforts, what type of security mechanisms should be performed depending on the information captured from the environment and upper layers?" Will this new method provide higher security than the existing efforts? For which context will it be a remedy? Regardless of whether a new method is proposed or any existing solution is used, how is the security level adjusted? For instance, based on the security threat, the waveform can be determined in the physical layer. If there is a jamming attack, spread spectrum waveform can be utilized. In this case, the security level can be considered as the processing gain, that is, the amount of spreading. As a final note, the adaptation ability of a specific technique to change the security needs should also be considered. For instance, transmit power can be a limiting factor for some users which might restrict the flexibility of the security level in artificial noise insertion based techniques. Alternatively, in SS, total

available bandwidth needs to be considered while performing the adaptation.

In this study, we provided different conditions which necessitate CS. However, it is highlighted that various new context information can be integrated into CS concept by taking the dynamic nature of the wireless communication systems.

Conflicts of Interest

The authors declare that there are no conflicts of interest regarding the publication of this paper.

Acknowledgments

This paper is partially supported by the Scientific and Technological Research Council of Turkey (TUBITAK) under Grant no. 114E244.

References

[1] Y. Chen, W. Trappe, and R. P. Martin, "Detecting and localizing wireless spoofing attacks," in *Proceedings of the 2007 4th Annual IEEE Communications Society Conference on Sensor, Mesh and Ad Hoc Communications and Networks, SECON*, pp. 193–202, San Diego, Calif, USA, June 2007.

[2] Y.-S. Shiu, S. Y. Chang, H.-C. Wu, S. C.-H. Huang, and H.-H. Chen, "Physical layer security in wireless networks: a tutorial," *IEEE Wireless Communications Magazine*, vol. 18, no. 2, pp. 66–74, 2011.

[3] L. Zhang, H. Wang, and T. Li, "Anti-jamming message-driven frequency hopping. Part I. System design," *IEEE Transactions on Wireless Communications*, vol. 12, no. 1, pp. 70–79, 2013.

[4] X. Li, C. Yu, M. Hizlan, W.-T. Kim, and S. Park, "Physical layer watermarking of direct sequence spread spectrum signals," in *Proceedings of the 2013 IEEE Military Communications Conference, MILCOM 2013*, pp. 476–481, San Diego, Calif, USA, November 2013.

[5] R. Negi and S. Goel, "Secret communication using artificial noise," in *Proceedings of the 62nd Vehicular Technology Conference, VTC 2005*, pp. 1906–1910, Dallas, Tex, USA, September 2005.

[6] R. Chen, J.-M. Park, and J. H. Reed, "Defense against primary user emulation attacks in cognitive radio networks," *IEEE Journal on Selected Areas in Communications*, vol. 26, no. 1, pp. 25–37, 2008.

[7] G. Noubir, "On Connectivity in Ad Hoc Networks under Jamming Using Directional Antennas and Mobility," in *Wired/Wireless Internet Communications*, vol. 2957 of *Lecture Notes in Computer Science*, pp. 186–200, Springer Berlin Heidelberg, Berlin, Germany, 2004.

[8] A. D. Wyner, "The wire-tap channel," *Bell Labs Technical Journal*, vol. 54, no. 8, pp. 1355–1387, 1975.

[9] M. Xiao, X. Wang, and G. Yang, "Cross-layer design for the security of wireless sensor networks," in *Proceedings of the 6th World Congress on Intelligent Control and Automation, WCICA 2006*, pp. 104–108, China, June 2006.

[10] G. Thamilarasu and R. Sridhar, "Exploring cross-layer techniques for security: Challenges and opportunities in wireless networks," in *Proceedings of the Military Communications Conference, MILCOM 2007*, Orlando, Fla, USA, October 2007.

[11] Z. Shu, Y. Qian, and S. Ci, "On physical layer security for cognitive radio networks," *IEEE Network*, vol. 27, no. 3, pp. 28–33, 2013.

[12] J. L. Burbank, "Security in cognitive radio networks: The required evolution in approaches to wireless network security," in *Proceedings of the 3rd International Conference on Cognitive Radio Oriented Wireless Networks and Communications, CrownCom 2008*, Singapore, May 2008.

[13] S. Parvin, F. K. Hussain, O. K. Hussain, S. Han, B. Tian, and E. Chang, "Cognitive radio network security: A survey," *Journal of Network and Computer Applications*, vol. 35, no. 6, pp. 1691–1708, 2012.

[14] G. Baldini, T. Sturman, A. R. Biswas, R. Leschhorn, G. Gódor, and M. Street, "Security aspects in software defined radio and cognitive radio networks: a survey and a way ahead," *IEEE Communications Surveys & Tutorials*, vol. 14, no. 2, pp. 355–379, 2012.

[15] P. Kumar and H.-J. Lee, "Security issues in healthcare applications using wireless medical sensor networks: a survey," *Sensors*, vol. 12, no. 1, pp. 55–91, 2012.

[16] E.-K. Lee, M. Gerla, and S. Y. Oh, "Physical layer security in wireless smart grid," *IEEE Communications Magazine*, vol. 50, no. 8, pp. 46–52, 2012.

[17] T. Wang and Y. Yang, "Analysis on perfect location spoofing attacks using beamforming," in *Proceedings of the 32nd IEEE Conference on Computer Communications, IEEE INFOCOM 2013*, pp. 2778–2786, Italy, April 2013.

[18] H.-N. Dai, Q. Wang, D. Li, and R. C.-W. Wong, "On eavesdropping attacks in wireless sensor networks with directional antennas," *International Journal of Distributed Sensor Networks*, vol. 2013, Article ID 760834, 13 pages, 2013.

[19] V. Milanés, J. Pérez, E. Onieva, and C. González, "Controller for Urban intersections based on wireless communications and fuzzy logic," *IEEE Transactions on Intelligent Transportation Systems*, vol. 11, no. 1, pp. 243–248, 2010.

[20] T. Pateman, "Rural and urban areas: comparing lives using rural/urban classifications," *Regional Trends*, vol. 43, no. 1, pp. 11–86, 2011.

[21] K. Wan and V. Alagar, "Context-aware security solutions for cyber-physical systems," *Mobile Networks and Applications*, vol. 19, no. 2, pp. 212–226, 2014.

[22] T. Yücek and H. Arslan, "A survey of spectrum sensing algorithms for cognitive radio applications," *IEEE Communications Surveys & Tutorials*, vol. 11, no. 1, pp. 116–130, 2009.

Hindawi
Wireless Communications and Mobile Computing
Volume 2017, Article ID 5017653, 8 pages
https://doi.org/10.1155/2017/5017653

Research Article

Distributed Schemes for Crowdsourcing-Based Sensing Task Assignment in Cognitive Radio Networks

Linbo Zhai,[1,2] Hua Wang,[2] and Chengcheng Liu[1]

[1]*Shandong Provincial Key Laboratory for Novel Distributed Computer Software Technology, Shandong Normal University, Jinan, China*
[2]*School of Computer Science and Technology, Shandong University, Jinan, China*

Correspondence should be addressed to Linbo Zhai; zhai@mail.sdu.edu.cn

Received 28 April 2017; Revised 24 September 2017; Accepted 29 November 2017; Published 14 December 2017

Academic Editor: Mohammad Shikh-Bahaei

Spectrum sensing is an important issue in cognitive radio networks. The unlicensed users can access the licensed wireless spectrum only when the licensed wireless spectrum is sensed to be idle. Since mobile terminals such as smartphones and tablets are popular among people, spectrum sensing can be assigned to these mobile intelligent terminals, which is called crowdsourcing method. Based on the crowdsourcing method, this paper studies the distributed scheme to assign spectrum sensing task to mobile terminals such as smartphones and tablets. Considering the fact that mobile terminals' positions may influence the sensing results, a precise sensing effect function is designed for the crowdsourcing-based sensing task assignment. We aim to maximize the sensing effect function and cast this optimization problem to address crowdsensing task assignment in cognitive radio networks. This problem is difficult to be solved because the complexity of this problem increases exponentially with the growth in mobile terminals. To assign crowdsensing task, we propose four distributed algorithms with different transition probabilities and use a Markov chain to analyze the approximation gap of our proposed schemes. Simulation results evaluate the average performance of our proposed algorithms and validate the algorithm's convergence.

1. Introduction

According to Cisco's report, the wireless traffic has increased sharply in the past few years and the global mobile data traffic grew by 63% in 2016 [1]. The high growth rate of wireless traffic leads to crowd wireless spectrum. This upward trend of mobile traffic, which is attributed to the rapid proliferation of mobile devices (e.g., smartphones and tablets), will lead to a looming shortage of wireless spectrum [2]. Nevertheless, a recent study reveals that much of the licensed spectrum, under current policy in the fixed spectrum assignment, is in fact poorly utilized [3]. To improve wireless spectrum utilization, cognitive radio has recently emerged as a solution [4]. When the licensed wireless spectrum is sensed to be idle, cognitive radio allows unlicensed users to access the idle licensed wireless spectrum opportunistically. Therefore, wireless spectrum sensing is the premise for unlicensed users to use the wireless spectrum.

Nowadays, mobile terminals, including smartphones and tablets, are very popular. These mobile terminals are intelligent and they can sense the wireless spectrum. Therefore, spectrum sensing tasks can be assigned to mobile terminals, which is called crowdsourcing, a new sensing method empowering ordinary users to carry out sensing with their mobile devices and aggregating the sensing data [5].

In this paper, based on the crowdsourcing method, we propose distributed algorithms to assign mobile terminals the spectrum sensing task. Mobile terminals in different positions may have different sensing results about the same channel since shadowing, multipath fading, and other issues may influence the sensing results. Considering the impact of mobile terminals' positions, we propose a precise sensing effect function of the crowdsourcing-based sensing task assignment. We aim to maximize the sensing effect function and cast this optimization problem to address crowdsensing task assignment in cognitive radio networks. Because the

complexity of this problem increases exponentially with the growth in mobile terminals, this problem is difficult to be solved. To assign crowdsensing task, we propose four distributed algorithms with different transition probabilities and use a Markov chain to analyze the approximation gap of our proposed schemes. As the proposed algorithms are distributed, it is convenient for each mobile terminal to carry out algorithms independently. Based on the details of our proposed algorithms, the complexity is low. Therefore, it is comfortable for mobile terminals to implement the distributed algorithms.

In this paper, we study crowdsourcing-based sensing task assignment. The main contributions of the paper are summarized as follows:

(i) Considering the impact of mobile terminals' positions, we propose a precise objective function for the crowdsensing task assignment.

(ii) It is difficult to assign crowdsensing task for the reason that the complexity of this problem increases exponentially with the growth in mobile terminals. Therefore, we design four distributed algorithms with different transition probabilities to solve this problem in cognitive radio networks.

(iii) Using a Markov chain, we analyze the approximation gap of our proposed schemes.

(iv) Simulation results validate the algorithm's convergence and show that our proposed algorithms achieve the optimal sensing effect.

The rest of the paper is organized as follows. In Section 2, related literatures are introduced. In Section 3, we formulate the system model of crowdsensing task assignment. In Section 4, we propose four distributed algorithms to solve the sensing task assignment and use a Markov chain to analyze the approximation gap of our schemes. In Section 5, the proposed algorithm is evaluated with simulation results. Finally, conclusions are shown in Section 6.

2. Related Work

Whether licensed users utilize the wireless spectrum or not decides the spectrum state. Therefore, to search for the idle spectrum, it is necessary to model licensed users' activity [6]. Then, spectrum sensing is carried out. A single user, experiencing shadowing, multipath fading, and other issues, may acquire a wrong sensing result. To improve the sensing accuracy, cooperative spectrum sensing has been proposed by multiple users [7].

There are some related works about cooperative spectrum sensing. In wideband cooperative sensing, users, by exchanging their compressed sensing results, estimate the spectrum states cooperatively [8, 9]. In [10], the cooperative spectrum sensing that is assigned to multiple users, namely, crowdsourcing-based method, is proposed to address the security issue of false data launched by malicious mobile users. The studies only relate to single-channel system, while in multichannel networks, the assignment of channel sensing is studied to maximize the quality of monitoring [11–14]. These literatures propose a simplistic objective function which is a weighted sum of some binary variables. And there is no budget constraint in these literatures. In [15], the authors, considering a limited budget, propose the sensing task assignment by selecting a subset of mobile users and solve the problem by greedy algorithm and Linear Program rounding algorithm.

In all aforementioned literatures, centralized algorithms are implemented to assign spectrum sensing. However, the system employing a centralized algorithm is not robust when the central node goes down. Moreover, the centralized system is not flexible in users joining or leaving the system [16]. To tackle the faults of centralized algorithms, the problem of spatial spectrum sensing is studied in a distributed way to make full use of spatial spectrum opportunities [17]. Using stochastic geometry, the performance of spatial spectrum sensing is analyzed. In [18], the authors propose a game-theoretic distributed power control mechanism based on channel sensing results of users in cognitive wireless sensor network. Tiny operating system (TinyOS), widely used in sensing system, is considered to be the most robust and energy-efficient system. In [19], the authors provide a review of TinyOS at its design paradigm, scheduling algorithms, programming model, and other features. Sensing nodes with TinyOS are more flexible in different sensing applications.

Compared to the spectrum sensing in recent studies, the paper solves sensing task assignment in distributed ways with the two major differences: (i) an objective function, considering different sensing outcomes in various subregions, is introduced to represent sensing effect; (ii) aiming to achieve higher sensing effect, four distributed algorithms, with different transition probabilities, are designed to tackle the problem of sensing task assignment.

3. System Model of Crowdsensing Task Assignment

In this section, we describe the system model of crowdsensing task assignment. Since shadowing, multipath fading, and other issues may influence the sensing results, mobile terminals in different positions may have different sensing results about the same channel. Considering the impact of mobile terminals' positions, we propose a precise sensing effect function of the crowdsourcing-based sensing task assignment.

Let N denote the number of channels and let M denote the number of mobile terminals in the system. We assume that a mobile terminal can only choose one channel to sense from all N channels. A channel-assignment configuration f is a vector indicating the channel choice of each mobile terminal; that is, $f = \{f_1, f_2, \ldots, f_M\}$, where $f_i \in \{1, 2, \ldots, N\}$ denotes the chosen channel of mobile terminal i. We define F as the set of all feasible f's. Given a channel-assignment configuration f, we design the sensing effect as follows.

Some issues may influence the sensing results of mobile terminals. In a region, mobile terminals may experience different shadowing and multipath fading in the sensing process when they are at different positions of this region. Therefore, the sensing results of these terminals are different even if they sense the same channel. Considering the impact of positions, we can divide a region into several subregions.

Mobile terminals in these subregions obtain different sensing results which capture the spatial diversity. It is assumed that there are m subregions. For the mobile terminals in a subregion h, each terminal chooses a channel to sense. If a channel i is sensed by at least a mobile terminal, we use ${z^i}_h = 1$ to denote this case. If no mobile terminals sense the channel i, we use ${z^i}_h = 0$ to denote this case. As the channel i may be sensed in multiple subregions, we use y^i to denote the number of sensing subregions. Then we can obtain $y^i = \sum_{h=1}^{m} z_h^i$. The sensing effect can be represented by y^i. When y^i equals a larger value, the sensing result is more effective. Therefore, if y^i equals m, the maximized sensing effect is reached. If y^i equals zero, the sensing effect is also zero. When y^i is small, we can imagine that the growth rate of sensing effect is higher as y^i increases. On the contrary, when y^i is large, the growth rate of sensing effect is slower as y^i increases.

Therefore, given a channel-assignment configuration f, we design the sensing effect function of channel i as follows:

$$U_f(i) = \left(\frac{y^i}{m}\right)^{1/m}, \quad i = 1, 2, \ldots, N. \tag{1}$$

According to (1), we can see that the sensing effect function increases as y^i increases from zero to m. When y^i is small, the sensing effect function increases faster with the growth of y^i. When y^i is large, the sensing effect function increases more slowly with the growth of y^i.

Figure 1 depicts an instance of crowdsensing task assignment with any one channel-assignment configuration $f \in F$. It is assumed that there are three channels in the system. In the sensing region, we assume that there are four terrain types. Mobile terminals in different terrain types may have different sensing results about the same channel. Therefore, the sensing region can be divided into four subregions. Obviously, the sensing region may be divided into more subregions when there are more terrain types. Due to the influence of terrain types, mobile terminals in different subregions may obtain different sensing results when they sense the same channel. According to the channel-assignment configuration f, each mobile terminal is assigned a channel to sense.

Let $V_f = \sum_{i=1}^{N} U_f(i)$ denote the sensing effect function of all channels with channel-assignment configuration f. To obtain optimized sensing effect of the system, we aim to maximize the sensing effect function of all channels by choosing the optimal channel-assignment configuration f from F. Therefore, the objective function can be expressed as

$$\max_{f \in F} \quad V_f. \tag{2}$$

4. Distributed Algorithms

In the system, the size of feasible set F is very large even for a fewer mobile terminals, since $|F| = N^M$, where N denotes the number of channels and M denotes the number of mobile terminals. Therefore, the maximization problem in (2) is hard to be solved. In this section, we design four distributed algorithms to address crowdsensing task assignment. Then we use a Markov chain to analyze the approximation gap of our distributed algorithms. Each mobile terminal broadcasts its sensing result representing the channel status to other terminals with one bit result (0 denoting the idle state and 1 denoting the busy state). Therefore, the signaling overhead is small and can be overlooked.

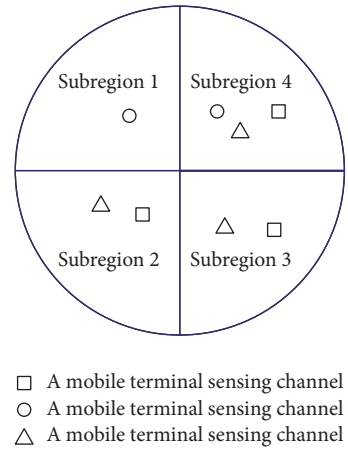

Figure 1: An instance of crowdsensing task assignment.

4.1. Distributed Algorithms. Initially, each mobile terminal chooses a channel to sense randomly. Using an additional report, each mobile terminal broadcasts the chosen channel and its position to other mobile terminals. When all mobile terminals have received other terminals' chosen channels and positions, each terminal can obtain the current channel-assignment configuration f and calculate V_f independently. Then each mobile terminal generates a random number following exponential distribution [20], and its mean equals E which is predefined.

After mobile terminals generate their random numbers independently, they count down their random numbers one by one. When the countdown of a mobile terminal expires, this mobile terminal (named mobile terminal j) chooses one of its not-in-sensing channels randomly. Then mobile terminal j may switch to the chosen channel with the probability p_{fg} or stay at the current channel with the probability $1 - p_{fg}$, where g denotes a new channel configuration if mobile terminal j switches to the chosen channel to sense.

If mobile terminal j stays at its current channel, there is still the channel-assignment configuration f. On the contrary, if mobile terminal j switches to the chosen channel to sense, a new channel-assignment configuration g appears. When mobile terminal j switches to the chosen channel to sense, it generates a random number following exponential distribution and broadcasts the new channel-assignment configuration g to other mobile terminals. After other terminals receive the channel-assignment configuration g, they can calculate the new sensing effect function V_g and continue their current countdown processes. When the countdown process of a mobile terminal ends, the terminal can calculate the transition probability based on new V_g.

Input E, β
(1) Each mobile terminal chooses a channel to sense randomly.
(2) Mobile terminal j broadcasts its chosen channel and position to other mobile terminals.
(3) When terminal j receives all other terminals' choice and positions, it calculate V_f independently.
(4) Terminal j generates a timer following exponential distribution with mean equaling E.
(5) Terminal j begins to count down.
(6) When the timer expires, terminal j chooses one of its not-in-sensing channels randomly. Terminal j switches to this channel with p_{fg} or stay at the current channel with $1 - p_{fg}$.
(7) If terminal j switches, it broadcasts g to other mobile terminals.
(8) Other terminals calculate V_g under the new channel-configuration g.
(9) Then the terminal j repeats step (4)–(9).

Algorithm 1: Wait-and-Selection algorithms for terminal j.

In this implementation, the transition probability p_{fg} is so important that it will influence the sensing effect of the system. We design p_{fg} by four different algorithms as follows.

Algorithm 1. In this algorithm, the transition probability p_{fg} is designed as

$$p_{fg} = \frac{1}{\exp\left(\beta V_f\right)}, \tag{3}$$

where β is a positive constant which is predefined. This algorithm is easy to achieve as p_{fg} only depends on the sensing effect function V_f under current channel-assignment configuration f. And p_{fg} is independent of sensing effect under the targeting channel-assignment configuration g. Therefore, mobile terminal j switches to the chosen channel with the transition probability determined by the current channel-assignment configuration f.

Algorithm 2. In this algorithm, the transition probability p_{fg} is designed as

$$p_{fg} = \frac{\min\left\{\exp\left(\beta V_f\right), \exp\left(\beta V_g\right)\right\}}{\exp\left(\beta V_f\right)}. \tag{4}$$

When the sensing effect function V_g under targeting channel-assignment configuration g is larger than V_f under current channel-assignment configuration f, the transition probability equals 1. This means that the mobile terminal must switch to the chosen channel. When V_g is smaller than V_f, the transition probability can be obtained based on (4).

Algorithm 3. In this algorithm, the transition probability p_{fg} is designed as

$$p_{fg} = \frac{\exp\left(\beta V_g\right)}{\exp\left(\beta V_f\right) + \exp\left(\beta V_g\right)}. \tag{5}$$

When V_g is larger than V_f, the transition probability is more than 50%. This means that the mobile terminal is more likely to switch to the chosen channel. When V_g is smaller than V_f, the transition probability is less than 50%. This means that the mobile terminal is more likely to stay at the current channel.

Algorithm 4. In this algorithm, the transition probability p_{fg} is designed as

$$p_{ff'} = \frac{\exp\left(\beta V_g\right)}{\max\left\{\exp\left(\beta V_f\right), \exp\left(\beta V_g\right)\right\}}. \tag{6}$$

When V_g is larger than V_f, the transition probability equals 1. This means that the mobile terminal must switch to the chosen channel. When V_g is smaller than V_f, the transition probability is calculated based on (6).

In Algorithms 2–4, the transition probability p_{fg} depends on both the current channel-configuration f and the targeting channel-assignment configuration g. Therefore, the algorithms employing Algorithms 2–4 are more complicated than that employing Algorithm 1.

We name this implementation with four different transition probabilities as Wait-and-Selection (WS) algorithms.

Each mobile terminal carries out the Wait-and-Selection (WS) algorithms independently. The distributed algorithms are described as in Algorithm 1.

4.2. Analysis of Approximation Gap. We define the approximation gap as the difference between the maximum sensing effect in our algorithms and that in theory. A Markov chain is used to describe the transition among channel-assignment configurations in the system. Based on the balance equation, the probability of each state in the Markov chain can be obtained. Then we can use the state probabilities to calculate the approximation gap. The details are described as follows.

According to the "Wait-and-Selection" algorithms, each channel-assignment configuration f corresponds to one state. Thus, there are finite states of the designed Markov chain. The number of states equals $|F|$, with F representing

the set of all feasible f's. Each channel-assignment configuration can be reachable from any adjacent state based on one-step transition.

Let N denote the number of channels and let M denote the number of mobile terminals in the system. According to the WS algorithms, each mobile terminal counts down following exponential distribution which is memoryless. Since each mobile terminal counts down with the rate $1/E$ under the current state f, the rate by which the process has the opportunity to leave state f is M/E.

After count-down expiration, a mobile terminal chooses one of its not-in-sensing channels randomly with the probability $1/(N-1)$. Then the mobile terminal may switch to the chosen channel with transition probability p_{fg} designed by four algorithms in (3)–(6). Therefore, the transition probability from state f to state g after count-down expiration is $p_{fg}/(N-1)$.

Then, we can obtain the transition rate q_{fg} from state f to state g as follows:

$$q_{fg} = \frac{Mp_{fg}}{E(N-1)}. \tag{7}$$

Let p_f^* be the stationary distribution of state f. Since the detailed balance equation must be satisfied, we obtain

$$\begin{aligned} p_f^* q_{fg} &= p_g^* q_{gf} \\ \sum_{f\in F} p_f^* &= 1. \end{aligned} \tag{8}$$

From (8), we can obtain the stationary distribution p_f^* of state f. For each transition probability of four algorithms, the stationary distribution p_f^* of state f is the same as others.

$$p_f^* = \frac{\exp\left(\beta V_f\right)}{\sum_{g\in F}\exp\left(\beta V_g\right)}, \quad f \in F. \tag{9}$$

The stationary distribution p_f^* also denotes the percentage of the duration that the system is under the channel-assignment configuration f. Obviously, it represents the optimal solution of the problem which is expressed as follows:

$$\begin{aligned} \max_{p_f\geq 0} \quad & \sum_{f\in F} p_f V_f - \frac{1}{\beta}\sum_{f\in F} p_f \log p_f, \\ \text{s.t.} \quad & \sum_{f\in F} p_f = 1, \end{aligned} \tag{10}$$

where β is a constant.

With the stationary distribution p_f^* obtained in (9), the optimal value in (10) is

$$\gamma = \frac{1}{\beta}\log\left(\sum_{f\in F}\exp\left(\beta V_f\right)\right). \tag{11}$$

Table 1: The approximation gap of sensing effect with $\beta = 10$.

Algorithm	M				
	20	22	24	26	28
Algorithm 1	0.17	0.14	0.093	0.068	0.065
Algorithm 2	0.1	0.089	0.066	0.05	0.044
Algorithm 3	0.099	0.087	0.068	0.048	0.045
Algorithm 4	0.1	0.087	0.067	0.049	0.056

The aforementioned analysis illustrates that our distributed algorithm realizes the optimal value of the problem in (10). From (11), we can obtain

$$\begin{aligned} \gamma = \frac{1}{\beta}\log\Bigg(&\exp\left(\beta\max_{f\in F} V_f\right) \\ &\cdot \sum_{f\in F}\exp\beta\left(V_f - \max_{f\in F} V_f\right)\Bigg) \leq \frac{1}{\beta} \\ &\cdot \log\left(\exp\left(\beta\max_{f\in F} V_f\right)|F|\right) = \max_{f\in F} V_f + \frac{1}{\beta}\log|F|, \end{aligned} \tag{12}$$

where $|F|$ describes the size of channel-assignment set F.

From (12), we can obtain the approximation gap of our proposed algorithms as follows:

$$\left|\gamma - \max_{f\in F} V_f\right| \leq \frac{1}{\beta}\log|F|. \tag{13}$$

Therefore, the upper bound of approximation gap is

$$\frac{1}{\beta}\log|F|. \tag{14}$$

Based on formulation (14), the approximation gap is close to zero when β approaches to infinity. This illustrates that our distributed algorithms approach the optimal value of the maximization problem in (2) with a large value of β. On the other hand, the approximation gap ratio is $(1/\beta)\log|F|/\max_{f\in F} V_f$. When $\max_{f\in F} V_f$ is much larger than $(1/\beta)\log|F|$, β has less impact on the results of our distributed algorithms. Under this condition, our distributed algorithms are not sensitive to β and approach the optimal value of the maximization problem in (2) even if β is not large.

5. Simulations

In this section, our proposed algorithms are evaluated by simulations. The average solution is derived by running the algorithm 1000 times. The simulation parameters are described as follows. The sensing region is a circular region with a 100-meter radius. And the sensing region is equally divided into four subregions. Mobile terminals are located in the subregions randomly.

Let N denote the number of channels and let M denote the number of mobile terminals. There are three channels in the system. Then $N = 3$. E is set to be 3. In Tables 1 and 2, we set $\beta = 10$ and 20, respectively. It is easy to see

Table 2: The approximation gap of sensing effect with $\beta = 20$.

Algorithm	M				
	20	22	24	26	28
Algorithm 1	0.15	0.114	0.092	0.069	0.067
Algorithm 2	0.073	0.073	0.035	0.037	0.032
Algorithm 3	0.074	0.072	0.035	0.035	0.031
Algorithm 4	0.074	0.071	0.035	0.038	0.031

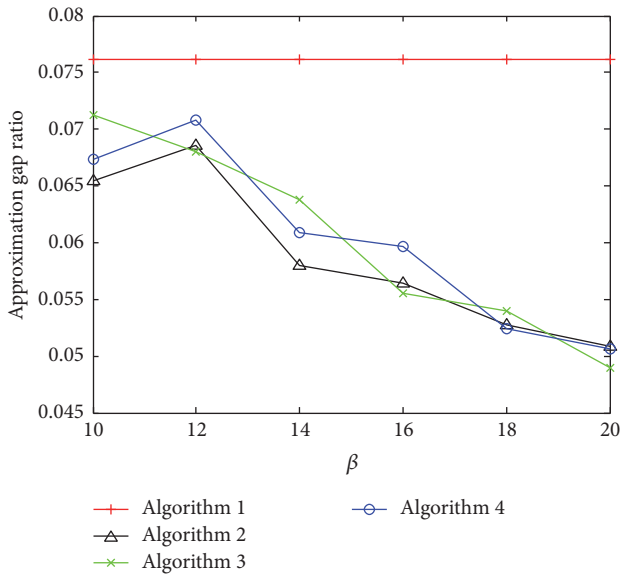

Figure 2: The approximation gap ratio varies with β ($N = 3$; $M = 12$).

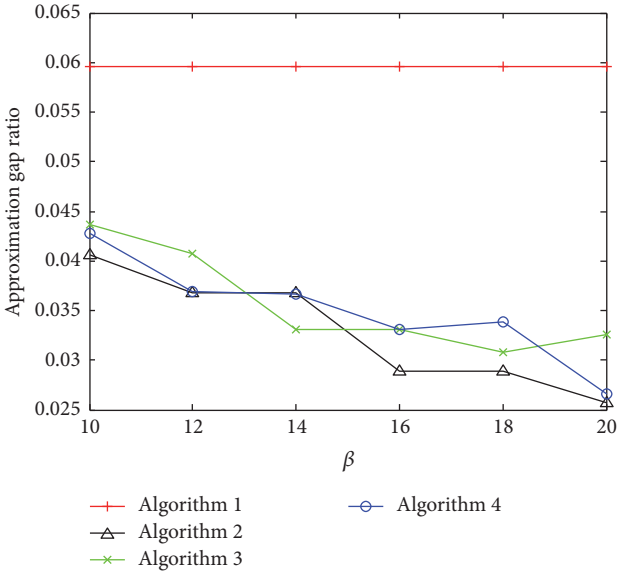

Figure 3: The approximation gap ratio varies with β ($N = 5$; $M = 30$).

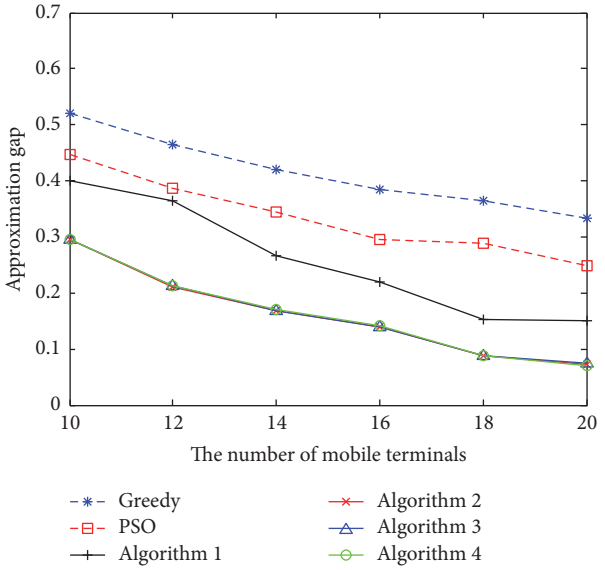

Figure 4: Our algorithm compared with centralized algorithms.

that the optimal channel-assignment configuration can be realized when each channel is sensed in all four subregions. According to formulation (1), the optimal sensing effect of a channel is 1. Therefore, we can obtain that the optimal sensing effect of the system is 3 when there are three channels in the system. As M varies from 20 to 28 and β changes, Tables 1 and 2 show the approximation gap of the sensing effect following our Wait-and-Selection algorithms. As shown in Tables 1 and 2, we can see that the approximation gap of our proposed algorithms employing four transition probabilities decreases as the number of mobile terminals increases. As there are more mobile terminals, more subregions will be sensed. Therefore, the approximation gap decreases as M increases, and its magnitude is less than the gap's upper bound $(1/\beta)\log|F|$, where $|F|$ equals N^M. We also see that the approximation gap is smaller when β is larger. This means that our distributed algorithms approach the optimal sensing effect with a large value of β. In addition, the approximation gap of Algorithm 1 is more than the other three algorithms. This implies that the algorithms employing Algorithms 2–4 approach the optimal sensing effect at the cost of increased complexity.

Figures 2 and 3 depict the impact of β on the real gap ratio of our four algorithms when $E = 3$. In Figure 2, the number of mobile terminals equals 12, and the number of channels equals 3. In Figure 3, the number of mobile terminals equals 30, and the number of channels equals 5. As shown in Figures 2 and 3, the gap ratio of Algorithms 2–4 decreases as β increases, while the gap ratio of Algorithm 1 does not change as β increases. For Algorithm 1, the transition rate q_{fg} is so little that mobile terminals almost do not switch to other channels. Therefore, the sensing effect will not change and the gap ratio is stable. For Algorithms 2–4, this means that the larger β is, the more accurate our distributed algorithms are. Moreover, we can see that the gap ratio of Figure 3 is lower than that of Figure 2. That means β has less impact on our distributed algorithms when there are more channels.

When there are three channels in the system ($\beta = 20$), Figure 4 depicts the gap of our algorithms and other

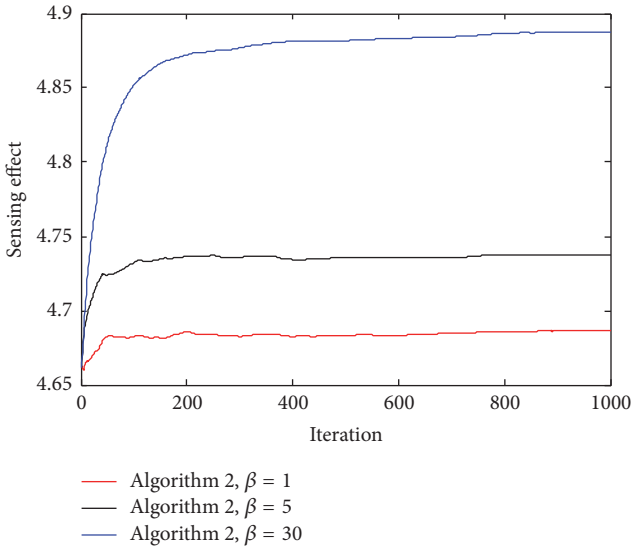

Figure 5: The impact of β for Algorithm 2.

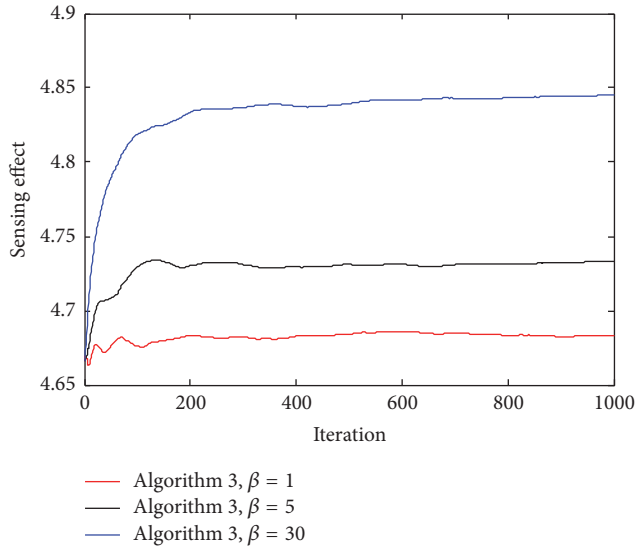

Figure 6: The impact of β for Algorithm 3.

centralized algorithms such as the greedy algorithm in [15] and the particle swarm optimization (PSO) algorithm which is good at optimization problem [21]. As shown in Figure 4, the approximation gap of our algorithms is lower than centralized algorithms. And our algorithms' gap decreases as the number of mobile terminals increases. That means our distributed algorithms have better performance than centralized algorithms. The distributed algorithms employing Algorithms 2–4 have similar performance which is better than the algorithm employing Algorithm 1. This implies that Algorithms 2–4 make mobile terminals switch to channels to obtain higher sensing effect.

Figure 5 depicts the impact of β on the sensing effect of the system and the convergence time for the distributed algorithm employing Algorithm 2. There are five channels and 30 mobile terminals in the system. Therefore, the optimal sensing effect is five. As shown in Figure 5, the sensing effect is close to the optimal value and the convergence time is long when $\beta = 30$. On the other hand, the sensing effect is far from the optimal value and the convergence time is short when $\beta = 1$. Therefore, the proposed algorithm employing Algorithm 2 approaches the optimal value and the convergence time increases as β increases.

Figures 6 and 7 depict the impact of β for Algorithms 3 and 4, respectively. There are also five channels and 30 mobile terminals in the system. Therefore, the optimal sensing effect is five. As shown in Figures 6 and 7, the sensing effects of Algorithms 3 and 4 increase as β increases. The larger β is, the higher the sensing effect is. And we also observe that convergence time is longer when β is larger.

Through contrasting Figures 5, 6, and 7, we can observe that the sensing effect of Algorithm 2 is similar to that of Algorithm 4. And the sensing effect of Algorithm 3 is less than those of Algorithms 2 and 4. The reason is that Algorithms 2 and 4 make the channel-assignment configuration f move to g with a higher probability if the new configuration g corresponds to higher sensing effect.

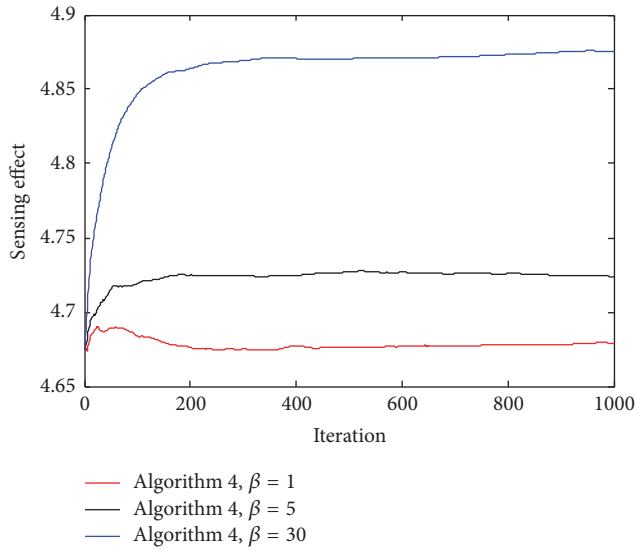

Figure 7: The impact of β for Algorithm 4.

6. Conclusion

Spectrum sensing can be assigned to mobile intelligent terminals, which is called crowdsourcing method. This paper studies crowdsensing task assignment to maximize sensing effect. Considering the fact that mobile terminals' positions may influence the sensing results, we design a precise sensing effect function for the crowdsourcing-based sensing task assignment and aim to maximize sensing effect and cast this optimization problem to address crowdsensing task assignment in cognitive radio networks. To tackle the impact of interference and multipath, we design the objective function considering the sensing results influenced by different locations. When users locate at various areas, the sensing process may be affected differently. Thus, the sensing outcomes may be different. To decrease the impact

of different locations, the objective function of this paper, representing the sensing effect, is designed based on the number of locations sensed by users. The larger the number is, the higher the sensing effect is. Therefore, maximizing the objective function means considering the impact of interference and multipath. Compared to aforementioned literatures implementing centralized algorithms, distributed algorithms are proposed with different transition probabilities to obtain bounded close-to-optimal solutions. Simulation results show that our distributed algorithms approach the optimal sensing effect and validate the algorithm's convergence. In the future, some related issues such as multipath should be studied in the cooperative spectrum sensing.

Conflicts of Interest

The authors declare that there are no conflicts of interest regarding the publication of this paper.

Acknowledgments

This research is supported in part by the Natural Science Foundation of Shandong Province, China (no. BS2015DX003), and in part by Key Research and Development Program of Shandong Province, China (nos. 2017GGX10142 and 2017GGX10122).

References

[1] Cisco, "Cisco visual networking index: Global mobile data traffic forecast update," Tech. Rep. 2016-2021, Tech., Cisco visual networking index, Global mobile data traffic forecast update, 2017.

[2] Federal Communications Commission (FCC), "Mobile broadband: The benefits of additional spectrum," Tech. Rep., 2010.

[3] The New America Foundation and Shared Spectrum Company, Dupont circle spectrum utilization during peak hours, http://newamerica.net/DownloadDocs/pdfs/DocFile1831.pdf.

[4] J. Mitola and G. Maguire, "Cognitive Radio: Making Software Radios More Personal," *IEEE Personal Communications*, vol. 4, pp. 13–18, 1999.

[5] B. Guo, Z. Wang, Z. Yu et al., "Mobile crowd sensing and computing: the review of an emerging human-powered sensing paradigm," *ACM Computing Surveys*, vol. 48, no. 1, article 7, 2015.

[6] Y. Saleem and M. H. Rehmani, "Primary radio user activity models for cognitive radio networks: a survey," *Journal of Network and Computer Applications*, vol. 43, pp. 1–16, 2014.

[7] T. Yucek and H. Arslan, "A survey of spectrum sensing algorithms for cognitive radio applications," *IEEE communications surveys tutorials*, vol. 11, no. 1, pp. 116–130, 2009.

[8] F. Zeng, C. Li, and Z. Tian, "Distributed compressive spectrum sensing in cooperative multihop cognitive networks," *IEEE Journal on Selected Topics in Signal Processing*, vol. 5, no. 1, pp. 37–48, 2010.

[9] F. Zeng, Z. Tian, and C. Li, "Distributed compressive wideband spectrum sensing in cooperative multi-hop cognitive networks," in *Proceedings of the 2010 IEEE International Conference on Communications, ICC 2010*, May 2010.

[10] R. Zhang, J. Zhang, Y. Zhang, and C. Zhang, "Secure crowdsourcing-based cooperative pectrum sensing," in *Proceedings of the 32nd IEEE Conference on Computer Communications, IEEE INFOCOM 2013*, pp. 2526–2534, April 2013.

[11] P. Arora, N. Xia, and R. Zheng, "A Gibbs sampler approach for optimal distributed monitoring of multi-channel wireless networks," in *Proceedings of the 54th Annual IEEE Global Telecommunications Conference: "Energizing Global Communications", GLOBECOM 2011*, December 2011.

[12] D.-H. Shin and S. Bagchi, "An optimization framework for monitoring multi-channel multi-radio wireless mesh networks," *Ad Hoc Networks*, vol. 11, no. 3, pp. 926–943, 2013.

[13] P. Arora, C. Szepesvári, and R. Zheng, "Sequential learning for optimal monitoring of multi-channel wireless networks," in *Proceedings of the IEEE INFOCOM 2011*, pp. 1152–1160, April 2011.

[14] D.-H. Shin, S. Bagchi, and C.-C. Wang, "Distributed online channel assignment toward optimal monitoring in multi-channel wireless networks," in *Proceedings of the IEEE Conference on Computer Communications, INFOCOM 2012*, pp. 2626–2630, March 2012.

[15] D.-H. Shin, S. He, and J. Zhang, "Joint sensing task and subband allocation for large-scale spectrum profiling," in *Proceedings of the 34th IEEE Annual Conference on Computer Communications and Networks, IEEE INFOCOM 2015*, pp. 433–441, 2015.

[16] M. Chen, S. C. Liew, Z. Shao, and C. Kai, "Markov approximation for combinatorial network optimization," *Institute of Electrical and Electronics Engineers Transactions on Information Theory*, vol. 59, no. 10, pp. 6301–6327, 2013.

[17] H. Chen, L. Liu, T. Novlan, J. D. Matyjas, B. L. Ng, and J. Zhang, "Spatial Spectrum Sensing-Based Device-to-Device Cellular Networks," *IEEE Transactions on Wireless Communications*, vol. 15, no. 11, pp. 7299–7313, 2016.

[18] J. Zhu, D. Jiang, S. Ba, and Y. Zhang, "A game-theoretic power control mechanism based on hidden Markov model in cognitive wireless sensor network with imperfect information," *Neurocomputing*, vol. 220, pp. 76–83, 2017.

[19] M. Amjad, M. Sharif, M. K. Afzal, and S. W. Kim, "TinyOS-new trends, comparative views, and supported sensing applications: a review," *IEEE Sensors Journal*, vol. 16, no. 9, pp. 2865–2889, 2016.

[20] M. Chen, S. C. Liew, Z. Shao, and C. Kai, "Markov approximation for combinatorial network optimization," in *Proceedings of the IEEE INFOCOM 2010*, March 2010.

[21] J. Kennedy and R. Eberhart, "Particle swarm optimization," in *Proceedings of the IEEE International Conference on Neural Networks*, pp. 1942–1948, Perth, Australia, December 1995.

Hindawi
Wireless Communications and Mobile Computing
Volume 2017, Article ID 8491920, 14 pages
https://doi.org/10.1155/2017/8491920

Research Article

Cooperative Full-Duplex Physical and MAC Layer Design in Asynchronous Cognitive Networks

Teddy Febrianto, Jiancao Hou, and Mohammad Shikh-Bahaei

Centre for Telecommunications Research, King's College London, London WC2R 2LS, UK

Correspondence should be addressed to Teddy Febrianto; teddy.febrianto@kcl.ac.uk

Received 26 May 2017; Revised 29 August 2017; Accepted 17 September 2017; Published 19 November 2017

Academic Editor: Gonzalo Vazquez-Vilar

In asynchronous cognitive networks (CNs), where there is no synchronization between primary users (PUs) and secondary users (SUs), spectrum sensing becomes a challenging task. By combining cooperative spectrum sensing and full-duplex (FD) communications in asynchronous CNs, this paper demonstrates improvements in terms of the average throughput of both PUs and SUs for particular transmission schemes. The average throughputs are derived for SUs and PUs under different FD schemes, levels of residual self-interference, and number of cooperative SUs. In particular, we consider two types of FD schemes, namely, FD transmit-sense-reception (FDr) and FD transmit-sense (FDs). FDr allows SUs to transmit and receive data simultaneously, whereas, in FDs, the SUs continuously sense the channel during the transmission time. This paper shows the respective trade-offs and obtains the optimal scheme based on cooperative FD spectrum sensing. In addition, SUs' average throughput is analyzed under different primary channel utilization and multichannel sensing schemes. Finally, new FD MAC protocol design is proposed and analyzed for FD cooperative spectrum sensing. We found optimum parameters for our proposed MAC protocol to achieve higher average throughput in certain applications.

1. Introduction

Cognitive networks (CNs), which can dramatically improve spectrum efficiency using dynamic spectrum access (DSA) technology, is a promising solution for the spectrum scarcity problem [1–3]. CNs allow the cognitive devices or secondary users (SUs) to use licensed or primary users' (PUs) frequency spectrum in an opportunistic way while guaranteeing the quality of both systems.

The majority of research works in this area have studied these problems in synchronous conditions, where PUs and SUs are time slotted and synchronized. However, in realistic scenarios, SUs have no information about the PUs' signals, which results in operations in asynchronous mode. Jiang et al. have studied some key issues for asynchronous CNs in [4].

Asynchronous cooperative spectrum sensing has been proposed in [5, 6] which shows improvement in the average throughput of SUs. In-band full-duplex (FD) communication [7] is also a promising technology that can improve the performance of CNs. FD spectrum sensing has been proposed in [8] which allows SUs sense and transmit data at the same time.

In shared-spectrum full-duplex networking, it is common for the FD transceivers to operate in the transmit-sense mode, that is, to transmit and sense simultaneously and in the same frequency band [9, 10]. In this mode no data is received during the data transmission period, in contrast with standard noncognitive full-duplex scenarios. It has been shown that operating in transmit-sense mode can reduce the outage probability of the primary network significantly, compared to the conventional listen-before-talk scheme (i.e., compared to the cognitive scenario where half-duplex transmission is performed following a short sensing period) [11].

An alternative approach to full-duplex networking in CNs is to combine sensing with data transmission and reception [12, 13]. Exploiting full-duplex communication capability of the transceivers, data transmission takes place simultaneously with data reception in this scheme, as it does with standard full-duplex networks. However, to allow spectrum

sharing with the primary network, the reception process is divided in time so that sensing and data receiving can take place in different time slots, while data transmission continues over the entire time period, that is, using time division duplex (TDD) in reception.

The advantage of transmit-sense mode approach is that it allows continuous sensing which can, in turn, improve the probability of detecting returning primary users. This improvement in the likelihood of detection is also a result of more advanced learning algorithms that can be implemented in continuous sensing. This is in contrast with data transmit-sense-reception mode, where sensing takes place in short periods of time; that is, data reception and sensing are scheduled according to a time-division-duplex scheme. Intermittent sensing in this mode does not allow the employment of advanced and reliable learning algorithms, which implies higher missed detection probability, compared to the transmit-sense mode. On the other hand, operation in transmit-sense-reception mode improves the secondary users' throughput at the cost of deteriorating primary network's performance.

The authors in [12, 13] have introduced adaptive full-duplex transmit-sense (FDs) and full-duplex transmit-receive-sense (FDr) to improve the performance of the spectrum-sharing mechanism. These two works use energy-based sensing and waveform-based sensing, respectively. However, both of these works have not considered cooperative spectrum sensing in order to further improve the spectrum sensing accuracy. On the other hand, the effect on the primary network can be alleviated by deploying cooperative sensing. Cooperation among the secondary users in sensing the licensed channel can improve the quality of detecting the activity of primary users in the licensed spectrum. By combining cooperative sensing and full-duplex communication features, full-duplex cooperative spectrum sensing mechanism is analyzed to improve the average throughput of SUs, while guaranteeing PUs' quality and throughput. This solution has been proposed in [14] only for time-slotted PUs and in [15] for cooperative acknowledgement. The recent work in [16] has analyzed SUs' performance in non-time-slotted case, without looking into the imposed effect on PUs.

Motived by the above observation, the contributions of this paper can be summarized as follows. The throughput of both secondary and primary users is derived under FDr and FDs schemes as functions of residual self-interference (SI) and the number of cooperating users in spectrum sensing. Furthermore, the results are extended for different primary channel utilization. Unlike our previous work in [17], in this paper, we introduce the full-duplex cooperative multichannel based FDr and FDs sensing schemes and also find the minimum number of cooperating secondary users required in FDr scheme so that the achievable throughput for the primary users is very close to that in the FDs scheme. In the literature, the full-duplex cooperative multichannel scenarios have also been considered [8, 18, 19]. However, these works assume SUs perform the standard p-persistent carrier sense multiple access (CSMA) mechanism for contention resolution on the selected channel. Such distributed mechanism can effectively avoid the data crash and improve the spectrum efficiency of the network. On the other hand, by comparing with the cooperative multichannel allocation mechanism which will be considered in this paper, the distributed version has to be limited to a "small" network. Based on the cooperative SUs design, in this paper, we also propose a MAC layer protocol design and analyze the average throughputs of SUs and PUs when utilizing TV white space as primary channels. The results show that, by increasing the number of sensed channels, the average throughput of proposed FD schemes may not always be improved, especially for FDr scheme. This is because the duration of sensing is considered as nontransmitting time, which reduce the time for data transmission.

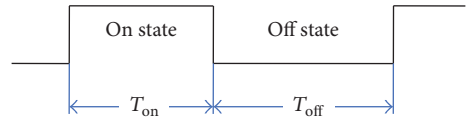

Figure 1: On-off process channel model.

The rest of this paper is organized as follows. The system model and throughput analysis are presented in Section 2. Spectrum sensing and self-interference effect are analyzed in Section 3. Formulation of secondary and primary average throughput for the cooperative full-duplex sensing scenario is in Sections 4 and 5, respectively. The analysis for the average throughput optimization and its corresponding numerical results are provided in Section 6. A new MAC protocol design is proposed and evaluated in Section 7. Finally, conclusions are drawn in Section 8.

2. System Model

As discussed in abstract and introduction sections, the asynchronous cognitive networks are defined that only the primary and secondary networks are not synchronized, but within the secondary network, the secondary users will be assumed to be synchronized. Moreover, the primary users in this case may or may not be synchronized. In addition, we also assume that SUs always have packets to "receive" as [9, 20], and this assumption is meaningful if the number of SUs is directly linked to the traffic demand in MAC protocol design.

2.1. Primary Users. One pair of PUs is considered to communicate in half-duplex (HD) mode over W spectrum bands, where the bands are not overlapped and with the same spectrum utilization as β. PUs' channel is modeled as an on-off process as [21], which is shown in Figure 1. The channel is considered in on state when it is occupied by PUs. On the other hand, off state means there is an available spectrum that can be exploited by SUs. The length of the on state (T_{on}) and off state (T_{off}) follows the exponential distribution with averages of ρ_{on} and ρ_{off}, respectively. In this case, the primary channel utilization β can be calculated as

$$\beta = \frac{\rho_{on}}{\rho_{off} + \rho_{on}}. \quad (1)$$

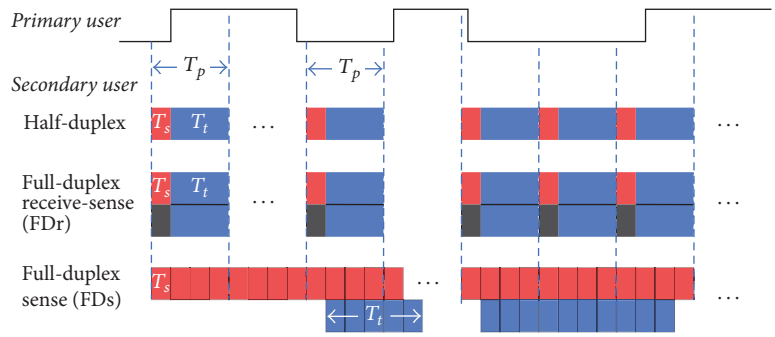

FIGURE 2: Secondary users transmission, reception, and sensing schemes.

2.2. Secondary Users. We consider that there are M SUs that cooperate in sensing the PUs' spectrum bands. Among these M cooperating SUs, there is one coordinator node which decides whether the primary channel is available for SUs. The coordinator node will collect the sensed information from M collaborating SUs [5] and use it for "soft decision" [22]. If, during the SUs' transmission, the coordinator node realizes the PU's return to the channel, it would immediately inform the active SUs to stop opportunistic transmission in the primary band. Spectrum allocation by the coordinator is not studied in this paper, and the spectrum allocation scheme will be considered to be independent of the asynchronous spectrum sensing process.

As shown in Figure 2, we consider two full-duplex sensing mechanisms for SUs to use the available primary users' channels opportunistically. In addition, we also include the half-duplex (HD) mechanisms for comparison. Specifically, for the HD communication sensing process, SUs' frame is divided into two intervals, that is, sensing (T_s) and transmitting (T_t), with sampling rate of ω_s. Energy-based sensing is applied for the sensing process of SUs. $T_p = T_s + T_t$ is defined as sensing period. In the second scheme, SUs use full-duplex communication to sense, transmit, and receive data within the same frame time T_p. This scheme is referred to as full-duplex transmit-receive-sense (FDr), and it allows SUs to receive data during the data transmitting process. The third scheme is full-duplex transmit-sense (FDs), where SUs sense the primary channel continuously during data transmission.

2.3. Average Throughputs. We assume that each SU can sense $v(\leq W)$ channels over T_p seconds, where each channel is sensed for T_{so} seconds. In this case, we have

$$T_s = V \cdot T_{so}. \tag{2}$$

In addition, L is defined as the average number of sensed idle channels by M SUs, which can be derived as [6]

$$L = \sum_{v=0}^{W} v \cdot P_v(v), \tag{3}$$

where $P_v(v)$ is the probability that v idle channels can be sensed by M SUs, and by considering (1), we have [6]

$$P_v(v) = (Lv)\,\beta^{L-v}(1-\beta)^v. \tag{4}$$

Therefore, SU's average throughput with v sensible channels can be expressed as

$$\tau_{s,\text{scheme}}^{(v)} = \frac{L \cdot \tau_{s,\text{scheme}}}{W}, \tag{5}$$

where $\tau_{s,\text{scheme}}$ is SU's average throughput per channel for a specific sensing scheme, for example, HD, FDr or FDs. On the other hand, PU's average throughput (i.e., $\tau_{p,\text{scheme}}^{(v)}$) with multiple channels will have the same behaviour as for the single channel case (i.e., $\tau_{p,\text{scheme}}$) since all the channels are independently distributed. From following sections, we will mathematically derive the average throughputs per channel for both SU and PU in detail.

3. Spectrum Sensing and Self Interference Effect

The two fundamental measures to be evaluated in spectrum sensing are the detection probability (P_d) and the false alarm probability (P_f). P_d is the probability that SUs can detect a busy channel when PUs do use the channel. P_f is the probability that SUs falsely detect a busy channel whereas there is actually no PU activities.

Residual self-interference (SI) in full-duplex communication affects the detection probability and the probability of false alarms in sensing the activity of primary users. An energy detection technique is widely deployed for detecting the primary users' activity in the shared spectrum. In full-duplex sensing, that is, simultaneous data transmission and spectrum sensing in the same frequency band, the energy of the residual SI, as a result of imperfect SI cancellation, may be mistaken for primary users' signal. This, in turn, will increase the false alarm probability and reduce the secondary users' throughput. Waveform-based sensing is an alternative sensing method that can alleviate this problem in full-duplex scenarios. In this approach sensing the primary signals is carried out by correlating the received samples with known pattern samples.

Another alternative to energy detection is cyclostationary feature detection, which is based on the estimation of the Fourier spectrum cyclic density and can detect weak signals from primary users by only exploiting the cyclostationarity property of communication signals. However, this approach

is rather complex for implementation. A different approach in detecting primary users' signals is based on tracking the primary users by employing smart antennas and avoiding spatial interference with their signals through transmit beamforming. Cooperative sensing can improve the probability of detecting primary signals, at the cost of higher computation and networking complexities. Using full-duplex radios, transmission and reception of data can be implemented simultaneously for further increase in the secondary user throughput. In this paper, cooperative energy-detection-based sensing is considered in the analysis.

Hypotheses H_0 and H_1 correspond to the cases where primary channel is in the off state and on state, respectively. Under the H_0 and H_1 conditions, the SUs' received signals at time instant n ($r_m[n]$) are, respectively, given by

$$\begin{aligned} H_0&: r_m[n] = x_m[n] + u_m[n], \\ H_1&: r_m[n] = x_m[n] + s_m[n] + u_m[n], \end{aligned} \tag{6}$$

where n refers to the nth sample and subscript m denotes the mth SU. x_m is the self-interference of mth SU and s_m is the signal transmitted by PU and received at the mth SU. The background noise which is assumed as circular symmetric complex Gaussian is denoted by u_m. The mean of u_m is zero, and the variance is σ^2.

The overall energy statistic of primary channel received at the coordinator SU (R) is given by [5]

$$R = \frac{1}{M\omega_s T_s} \sum_{m=1}^{M} \sum_{n=1}^{\omega_s T_s} |r_m[n]|^2. \tag{7}$$

In addition, P_d and P_f are given by [8]

$$\begin{aligned} P_d &= \Pr[R \geq \varepsilon_{\text{th}} \mid H_1] \\ &= Q\left(\frac{\varepsilon_{\text{th}}/\sigma^2 - ((U-a)/U)\,\kappa \text{SNR}_{s,p} - 1}{\sqrt{((U-a)/U^2)\left(\kappa \text{SNR}_{s,p} + 1\right)^2 + a/U^2}} \right), \\ P_f &= \Pr[R \geq \varepsilon_{\text{th}} \mid H_0] \\ &= Q\left(\frac{\varepsilon_{\text{th}}/\sigma^2 - (d/U)\,\kappa \text{SNR}_{s,p} - 1}{\sqrt{(d/U^2)\left(\kappa \text{SNR}_{s,p} + 1\right)^2 + (U-d)/U^2}} \right), \end{aligned} \tag{8}$$

where ε_{th} is the energy detection threshold, U is the number of primary samples during the sensing period, a is the number of samples during off state before primary's return to an active (ON) state, and d is the number of samples during in which the primary is at on state before becoming inactive. $\text{SNR}_{x,y}$ is the signal-to-noise ratio at receiver x due to the signal transmitted by transmitter y. $x, y \in \{p, s\}$, where p and s, respectively, refer to a primary and secondary user. κ ($0 < \kappa \leq 1$) represents the self-interference mitigation coefficient [8, 23]. If κ is high, this means that self-interference is mitigated well. On the other hand, low values of κ imply that self interference at the receiver is high. $Q(\cdot)$ is the complementary distribution function of standard Gaussian, which is defined by

$$Q(x) = \frac{1}{\sqrt{2\pi}} \int_x^{\infty} e^{(-t^2/2)} dt. \tag{9}$$

Consider multichannel sensing scenarios, where PUs may change their states (i.e., on or off) during SUs' sensing period. In this case, there are four possible cases when we calculate P_d and P_f in order to obtain the average throughputs.

Case 1. PU is not active during the SUs' sensing period. In this case, P_f which is used for SUs' achievable throughput calculation can be expressed as

$$P_f = Q\left(\left(\frac{\varepsilon_{\text{th}}}{\sigma^2} - 1 \right) \sqrt{M\omega_s T_s} \right), \tag{10}$$

where this equation is derived by setting $d = 0$ and $U = M\omega_s T_s$.

Case 2. PU is always active during the SUs' sensing period. In this case, P_d which is used for PU's achievable throughput calculation can be expressed as

$$P_d = Q\left(\left(\frac{\varepsilon_{\text{th}}}{\sigma^2} - \kappa \text{SNR}_{s,p} - 1 \right) \sqrt{\frac{M\omega_s T_s}{\left(\kappa \text{SNR}_{s,p} + 1\right)^2}} \right), \tag{11}$$

where, here, we set up $a = 0$ and $U = M\omega_s T_s$.

Case 3. PU is firstly active until the d-th sample and then not active for the rest. In this case, P_d, which is used to calculate the PU's achievable throughput, is derived from (11). For calculating the SUs' throughput, apart from P_f in (10), they still need to take the following P_f into account, which is given by

$$P_f = Q\left(\frac{\varepsilon_{\text{th}}/\sigma^2 - ((d - \lfloor d/U \rfloor)/U)\,\kappa \text{SNR}_{s,p} - 1}{\sqrt{((d - \lfloor d/U \rfloor)/U^2)\left(\kappa \text{SNR}_{s,p} + 1\right)^2 + (U - d + \lfloor d/U \rfloor)/U^2}} \right), \tag{12}$$

where $U = M\omega_s T_s$ and $\lfloor a \rfloor$ represents the maximum integer that is smaller than a.

Case 4. PU is firstly not active until the a-th sample and then active for the rest. In this case, P_f which is used to

calculate the SUs' average throughput is derived from (10). For calculating the PU's average throughput, apart from P_d in (11), they also need to take the following P_d into account, which is given by

$$P_d = Q\left(\frac{\varepsilon_{\text{th}}/\sigma^2 - ((U - a + \lfloor a/U \rfloor)/U)\,\kappa \text{SNR}_{s,p} - 1}{\sqrt{((U - a + \lfloor a/U \rfloor)/U^2)\left(\kappa \text{SNR}_{s,p} + 1\right)^2 + (a - \lfloor a/U \rfloor)/U^2}}\right), \tag{13}$$

where $U = M\omega_s T_s$.

4. Secondary Users' Average Throughput Analysis

4.1. SUs' Achievable Data Rate. During the off state, the maximum achievable data rate ($D_{s,0}$) for SUs under the effect of background noise and residual SI is

$$D_{s,0} = \log_2\left(1 + \frac{\text{SNR}_{s,s}}{1 + (1 - \kappa)\,\text{SNR}_{s,s}}\right). \tag{14}$$

If the coordinator falsely detects that there is no primary activity in the on state, the achievable data rate ($D_{s,1}$) for SUs is

$$D_{s,1} = \log_2\left(1 + \frac{\text{SNR}_{s,s}}{1 + \text{SNR}_{s,p} + (1 - \kappa)\,\text{SNR}_{s,s}}\right). \tag{15}$$

In this paper, the effect of multiuser interference is assumed to be controlled and cancelled effectively, using physical layer and MAC layer techniques, for example, through adaptive beamforming as in [24], adaptive rate/power control and scheduling mechanisms as in [25, 26].

4.2. SUs' Average Throughput in Half-Duplex Mode. In order to compare our proposed full-duplex based sensing protocols to the existing protocols, in this subsection, we first introduce the SUs' average throughput in conventional half-duplex mode. As illustrated in Figure 3(a), there are four different states that should be considered to formulate the half-duplex (HD) SUs' average throughput ($\tau_{s,\text{HD}}$). As derived in [5], assuming asynchronicity between SUs and PUs, $\tau_{s,\text{HD}}$ can be expressed as

$$\tau_{s,\text{HD}} = \sum_{i=00}^{11} P\left[S_{i,\text{HD}}\right] C_{i,\text{HD}}, \tag{16}$$

where $P[S_{i,\text{HD}}], \forall i$ are defined as probability of event $S_{i,\text{HD}}$ occurred in HD scheme, and following the assumed ON/OFF distributions, they can be expressed as

$$P\left[S_{00,\text{HD}}\right] = \frac{\rho_{\text{off}}}{\rho_{\text{off}} + \rho_{\text{on}}} e^{-T_p/\rho_{\text{off}}}, \tag{17}$$

$$P\left[S_{01,\text{HD}}\right] = \frac{\rho_{\text{off}}}{\rho_{\text{off}} + \rho_{\text{on}}}\left(1 - e^{-T_p/\rho_{\text{off}}}\right), \tag{18}$$

$$P\left[S_{10,\text{HD}}\right] = \frac{\rho_{\text{on}}}{\rho_{\text{off}} + \rho_{\text{on}}}\left(1 - e^{-T_p/\rho_{\text{on}}}\right), \tag{19}$$

$$P\left[S_{11,\text{HD}}\right] = \frac{\rho_{\text{on}}}{\rho_{\text{off}} + \rho_{\text{on}}} e^{-T_p/\rho_{\text{on}}}. \tag{20}$$

In addition, $C_{i,\text{HD}}$ is data rate for $S_{i,\text{HD}}$ event for HD scheme, which can be found in [5].

4.3. SUs' Average Throughput in Full-Duplex Transmit-Sense-Reception Mode. Following the similar approach as in the HD scheme under the same four different cases, the average throughput for FDr scheme ($\tau_{s,\text{FDr}}$) can be obtained as

$$\tau_{s,\text{FDr}} = \sum_{i=00}^{11} P\left[S_{i,\text{FDr}}\right] C_{i,\text{FDr}}, \tag{21}$$

where $P[S_{i,\text{FDr}}], \forall i$, are defined as probability of event $S_{i,\text{FDr}}$ occurring in FDr scheme, and $C_{i,\text{FDr}}$ is the achievable throughput for $S_{i,\text{FDr}}$ event for FDr scheme. In this case, as illustrated in Figure 3(b), we have

$$P\left[S_{i,\text{FDr}}\right] = P\left[S_{i,\text{HD}}\right], \quad \forall i. \tag{22}$$

For an ideal single channel point-to-point communication, the achievable throughput in FDr is twice as high as that in HD scheme. However, due to the SI effect (when $0 \le \kappa < 1$) on $D_{s,0}$, $D_{s,1}$, and P_d, the achievable throughput will be lower

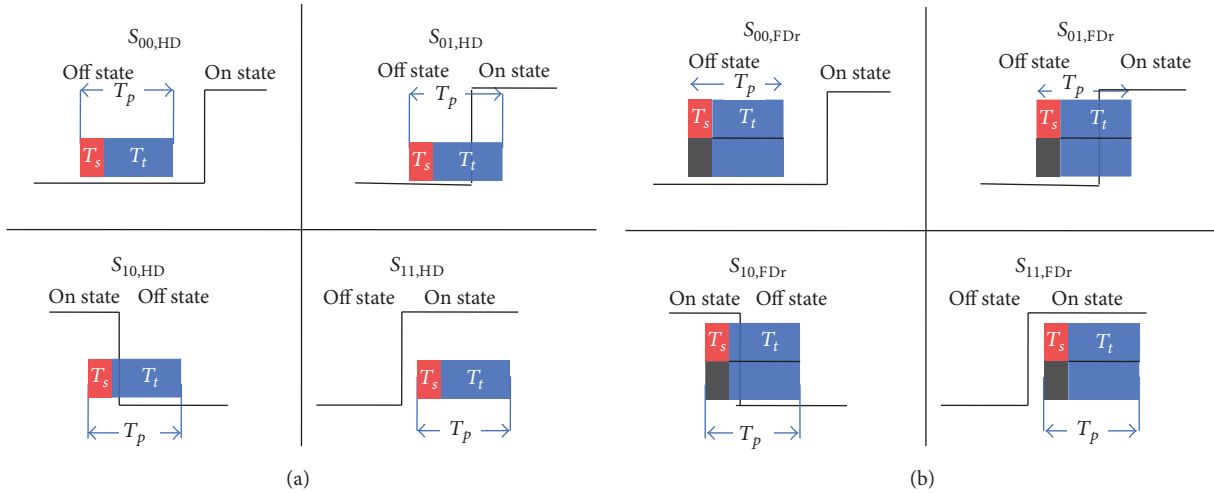

Figure 3: Four possible states in (a) HD and (b) FDr scenario.

than in the perfect SI cancellation case ($\kappa = 1$). $C_{i,\mathrm{FDr}}$ can be calculated as

$$C_{00,\mathrm{FDr}} = 2\overline{P_f}\frac{T_p - T_s}{T_p}D_{s,0}$$

$$C_{01,\mathrm{FDr}} = \frac{2}{T_p}\frac{\left(D_{s,0}\overline{P_f} - D_{s,1}\overline{P_d}\right)\left(\rho_{\mathrm{off}} - \left(T_p + \rho_{\mathrm{off}}\right)e^{-T_p/\rho_{\mathrm{off}}}\right)}{1 - e^{-T_p/\rho_{\mathrm{off}}}} + \frac{2}{T_p}\left(\overline{P_d}D_{s,1}T_p - \overline{P_f}D_{s,0}T_s\right)$$

$$C_{10,\mathrm{FDr}} = \frac{2}{T_p}\frac{\left(D_{s,1}\overline{P_d} - D_{s,0}\overline{P_f}\right)\left(\rho_{\mathrm{on}} - \left(T_p + \rho_{\mathrm{on}}\right)e^{-T_p/\rho_{\mathrm{on}}}\right)}{1 - e^{-T_p/\rho_{\mathrm{on}}}} + \frac{2}{T_p}\left(\overline{P_f}D_{s,0}T_p - \overline{P_d}D_{s,1}T_s\right)$$

$$C_{11,\mathrm{FDr}} = 2\overline{P_d}\frac{T_p - T_s}{T_p}D_{s,1}, \tag{23}$$

where $\overline{P_d} = 1 - P_d$ and $\overline{P_f} = 1 - P_f$.

4.4. SUs' Average Throughput in Full-Duplex Transmit-Sense Mode. In contrast with HD and FDr schemes, in FDs, the transmission time during a frame is not constant. SUs continuously sense the channel and can immediately start or stop transmission based on the sensing result. Hence, only two states are studied for average throughput calculation as shown in Figure 4. The probabilities of the events $S_{00,\mathrm{FDs}}$ and $S_{11,\mathrm{FDs}}$ are defined as the probability of being in off and on state, respectively, and they can be expressed as

$$P\left[S_{00,\mathrm{FDs}}\right] = \frac{\rho_{\mathrm{off}}}{\rho_{\mathrm{off}} + \rho_{\mathrm{on}}}$$
$$P\left[S_{11,\mathrm{FDs}}\right] = \frac{\rho_{\mathrm{on}}}{\rho_{\mathrm{off}} + \rho_{\mathrm{on}}}. \tag{24}$$

Average data rate during $S_{00,\mathrm{FDs}}$ and $S_{11,\mathrm{FDs}}$ can be calculated by

$$C_{00,\mathrm{FDs}} = \overline{P_f}D_{s,0} \tag{25}$$

$$C_{11,\mathrm{FDs}} = \overline{P_d}D_{s,1}. \tag{26}$$

Therefore, SUs' average throughput ($\tau_{s,\mathrm{FDs}}$) for FDs scheme is

$$\tau_{s,\mathrm{FDs}} = \sum_{i=00}^{11} P\left[S_{i,\mathrm{FDs}}\right]C_{i,\mathrm{FDs}}. \tag{27}$$

5. Primary Users' Average Throughput Analysis

5.1. PUs' Achievable Data Rate. The PUs' achievable data rate without interference ($D_{p,0}$) from SU is

$$D_{p,0} = \log_2\left(1 + \mathrm{SNR}_{p,p}\right). \tag{28}$$

The PUs' achievable data rate with interference ($D_{p,1}$) from SU due to miss-detection can be calculated as

$$D_{p,1} = \log_2\left(1 + \frac{\mathrm{SNR}_{p,p}}{1 + \mathrm{SNR}_{p,s}}\right). \tag{29}$$

5.2. PUs' Average Throughput When Secondary Is in Half-Duplex or Full-Duplex Transmit-Sense-Reception Modes. The PUs' average throughput can be calculated by modeling the

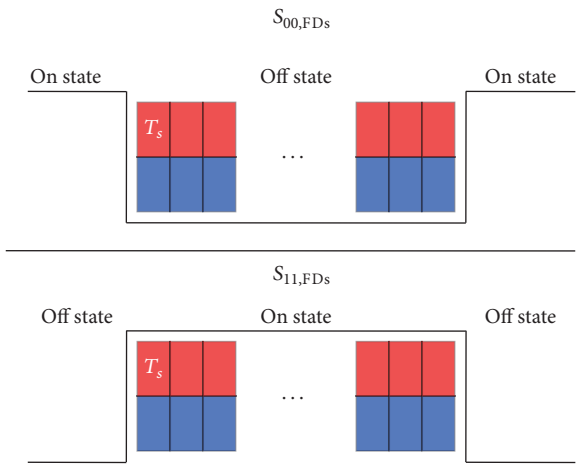

Figure 4: Two possible conditions in FDs scenario.

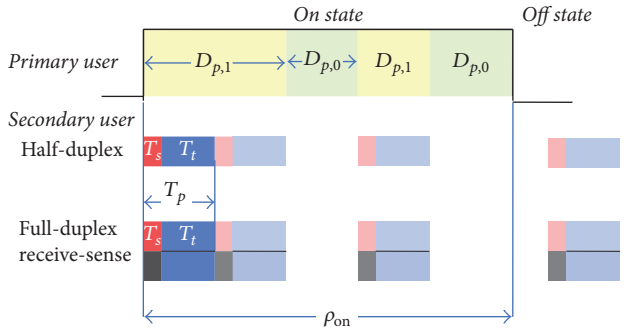

Figure 5: Illustration of PU's average throughput when SU uses HD or FDr schemes.

on state event as a time-slotted frame of size T_p, as shown in Figure 5. The average number of slots (b_{Tp}) is defined as ratio of the primary user on sate (ρ_{on}) to sensing period (T_p). Furthermore, the event where SUs transmit during the on state can be modeled as binomial distribution with the probability of occurrence given by $1 - P_d$. $P[S_{j,p}]$ is defined as probability that j frames of SUs are transmitted during ρ_{on} of PU when SUs use HD or FDr scheme, which can be expressed as

$$P\left[S_{j,p}\right] = \binom{b_{T_p}}{j} \overline{P_d}^{j} P_d^{(b_{T_p}-j)}, \tag{30}$$

where

$$b_{Tp} = \left[\frac{\rho_{\mathrm{on}}}{T_p}\right], \tag{31}$$

and $[\cdot]$ is rounded to nearest integer number operator. The average data rate ($C_{j,p}$) when j frames of SUs are transmitted during ρ_{on} of PU can be calculated as

$$C_{j,p} = \left(j \cdot D_{p,1} \cdot \frac{\rho_{\mathrm{on}}}{\rho_{\mathrm{off}} + \rho_{\mathrm{on}}} \cdot \frac{T_p}{\rho_{\mathrm{on}}}\right)$$

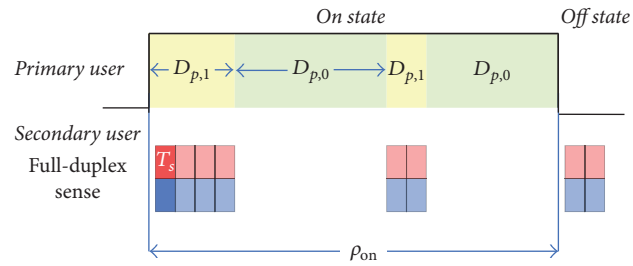

Figure 6: Illustration of PU's average throughput when SU uses FDs scheme.

$$+\left(D_{p,0} \cdot \frac{\rho_{\mathrm{on}}}{\rho_{\mathrm{off}} + \rho_{\mathrm{on}}} \cdot \frac{\rho_{\mathrm{on}} - jT_p}{\rho_{\mathrm{on}}}\right)$$

$$= \frac{\rho_{\mathrm{on}} D_{p,0} - jT_p\left(D_{p,0} - D_{p,1}\right)}{\rho_{\mathrm{off}} + \rho_{\mathrm{on}}}. \tag{32}$$

Finally, the PUs' average throughput for HD ($\tau_{p,\mathrm{HD}}$) and FDr ($\tau_{p,\mathrm{FDr}}$) cases can be formulated as

$$\tau_{p,\mathrm{HD}} = \tau_{p,\mathrm{FDr}} = \sum_{j=0}^{b_{Tp}} P\left[S_{j,p}\right] C_{j,p}. \tag{33}$$

5.3. PU's Average Throughput When Secondary User Is in Full-Duplex Transmit-Sense Mode. In the same fashion as in Section 5.2, PUs' average throughput when SUs use FDs scheme can be calculated as shown in Figure 6. Instead of dividing by T_p, ρ_{on} is divided by T_s to estimate the number of slots, b_{Ts}. $P[S_{l,p\mathrm{FDs}}]$ is defined as probability that l frames of SUs are transmitted during ρ_{on} of PU when SUs use FDs scheme, which can be expressed as

$$P\left[S_{l,p\mathrm{FDs}}\right] = \binom{b_{T_s}}{l} \overline{P_d}^{l} P_d^{(b_{Ts}-l)}, \tag{34}$$

where

$$b_{Ts} = \left[\frac{\rho_{\mathrm{on}}}{T_s}\right]. \tag{35}$$

The average data rate ($C_{l,p\mathrm{FDs}}$) when l frames of SU are transmitted during ρ_{on} of PU can be calculated as

$$C_{l,p\mathrm{FDs}} = \left(l \cdot D_{p,1} \cdot \frac{\rho_{\mathrm{on}}}{\rho_{\mathrm{off}} + \rho_{\mathrm{on}}} \cdot \frac{T_s}{\rho_{\mathrm{on}}}\right)$$

$$+\left(D_{p,0} \cdot \frac{\rho_{\mathrm{on}}}{\rho_{\mathrm{off}} + \rho_{\mathrm{on}}} \cdot \frac{\rho_{\mathrm{on}} - lT_s}{\rho_{\mathrm{on}}}\right) \tag{36}$$

$$= \frac{\rho_{\mathrm{on}} D_{p,0} - lT_s\left(D_{p,0} - D_{p,1}\right)}{\rho_{\mathrm{off}} + \rho_{\mathrm{on}}}.$$

The PU's average throughput when SUs use FDs scheme ($\tau_{p,\mathrm{FDs}}$) can be calculated as

$$\tau_{p,\mathrm{FDs}} = \sum_{l=0}^{b_{Ts}} P\left[S_{l,p\mathrm{FDs}}\right] C_{l,p\mathrm{FDs}}. \tag{37}$$

Table 1: Proposed MAC simulation parameters.

Parameter	Value	Description
T_p	32 ms	Sensing period
κ	0.99	Self-interference mitigation coefficient
W	11 [28]	Number of primary user's channels
$\varepsilon_{\text{th}}/\sigma^2$	1.03 [5]	Received signal power-to-noise ratio threshold
$\text{SNR}_{s,s}$	10 dB [5]	Average signal-to-noise ratio received by secondary user from secondary signal
$\text{SNR}_{s,p}$	−10 dB [5]	Average signal-to-noise ratio received by secondary user from primary signal
$\text{SNR}_{p,p}$	10 dB	Average signal-to-noise ratio received by primary user from primary signal
$\text{SNR}_{p,s}$	−10 dB	Average signal-to-noise ratio received by primary user from secondary signal
ω_s	100 kHz [5]	Sampling rate
ρ_{off}	640 ms	Average length of off state for primary user
ρ_{on}	160 ms	Average length of on state for primary user

6. Analysis for Physical Layer Method and Numerical Results

Based on the above derived average throughputs for both secondary and primary users per channel, the generalised average throughput for multichannel case can be formulated by inserting (14), (19), and (25) into (5), respectively, for secondary users. As discussed in Section 2, for the primary users, the average throughput for multichannel case is equal to the ones for single channel case, which are given by (31) and (35). Then, the optimization problems which aim to maximize the secondary users average throughput can be expressed as

$$\begin{aligned} \max_{m,v,T_s} \quad & \tau_{s,\text{scheme}}^{(v)} = \frac{L \cdot \tau_{s,\text{scheme}}}{W}, \\ \text{s.t.} \quad & \tau_{p,\text{scheme}}^{(v)} \geq \overline{R}_{p,\text{scheme}} \\ & \text{SNR}_{x,y} \leq \overline{\text{SNR}}_{x,y}, \quad \forall x, y, \end{aligned} \tag{38}$$

where $m(\leq M)$ is number of active secondary users, $\overline{R}_{p,\text{scheme}}$ is primary user's minimum rate constraint, and $\overline{\text{SNR}}_{x,y}$ is the SNR upper limit for (x, y) link. In order to obtain the optimal solution of problem (36), we can implement the first-order derivation of the objective function with respect to either m, v, or T_s and then set the derived equation to zero if there is unique root. Alternatively, numerical results can be implemented to help to find the optimal solution. In the following subsections, numerical results are provided for both primary and secondary users, and the parameters used in the numerical results are shown in Table 1, which are in line with those in [5] for fair comparison.

6.1. Secondary Users' Average Throughput. In Figure 7, SUs' average throughput is presented versus number of cooperating SUs (M) for different schemes and κ values. It shows that FDr scheme achieves higher average throughput for SUs compared to FDs and HD. This is due to the longer transmitting time (T_t) in FDr compared to the other schemes.

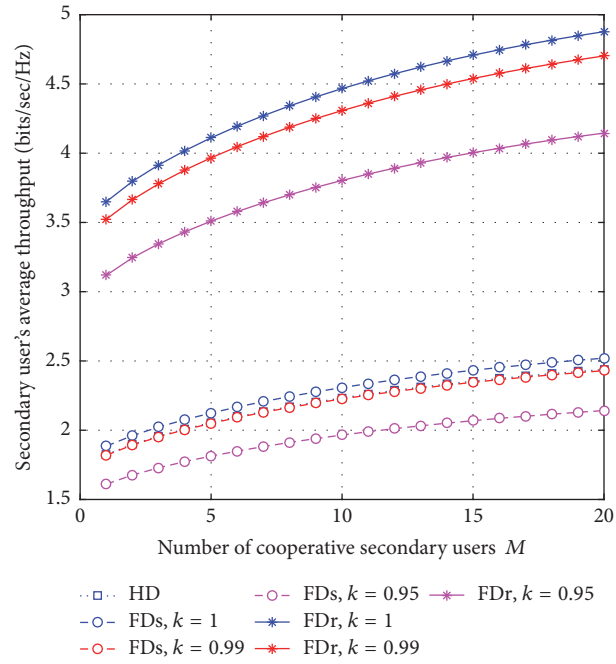

Figure 7: SU's average throughput versus M for different schemes and different value of κ.

The SU's average throughput of different schemes monotonically increases with the number of cooperating SUs, M. As expected, it shows that cooperative sensing offers better performance compared to the noncooperative case ($M = 1$). This figure also demonstrates the effect of κ on the SUs' average throughput for FDr and FDs schemes, noting that in HD scheme SI is zero ($\kappa = 1$). By decreasing κ, the average throughput for both FDs and FDr deteriorates slightly.

6.2. Primary Users' Average Throughput. Figure 8 shows the average throughput of PU versus the number of SUs (M) for different schemes and κ values. Although for the SUs' average throughput, FDr outperforms FDs and HD, for the PUs' average throughput FDr gives the worse performance, especially

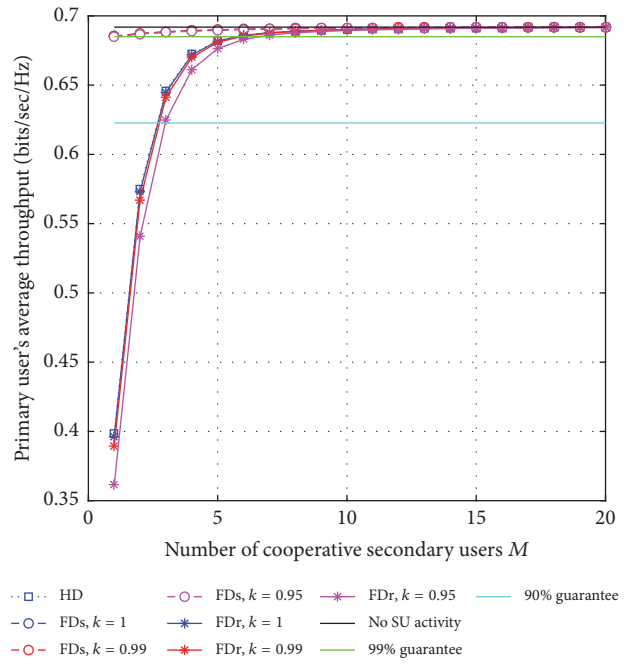

FIGURE 8: PU's average throughput versus M for different schemes and κ.

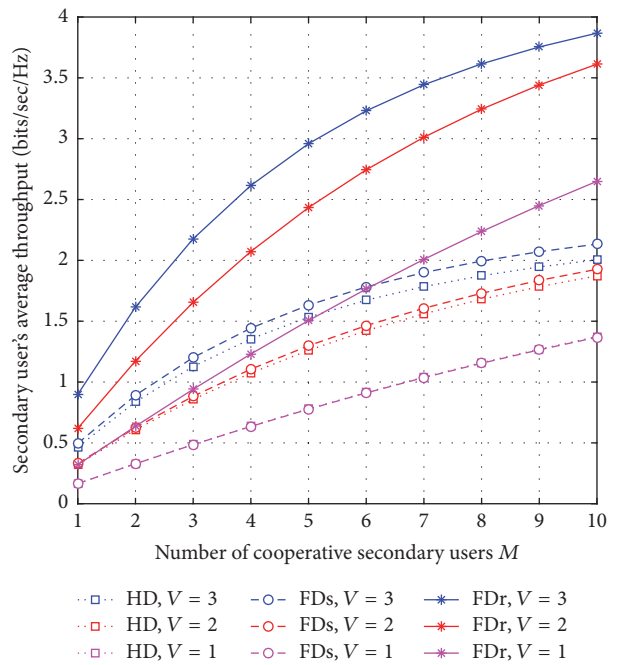

FIGURE 9: SU's average throughput versus M for different schemes and values for V and with $\kappa = 0.99$, $W = 11$, $T_{so} = 1$ ms, and $\beta = 0.2$.

for lower M. Indeed, it shows an average throughput trade-off between SUs and PUs. FDs gives similar average throughput performance as no SUs active case even the number of cooperative SUs is equal to one. This is because secondary users incorporate continuous sensing, and cooperation in this case does not provide much performance improvement for primary users. Furthermore, it can reduce transmitting time of the SU, T_t during on state. As a result, PUs can transmit in the absence of SUs for most of the time during the on state.

According to this figure, the average throughput of PU increases with M especially when SUs employ FDr or HD schemes. It shows that the use of cooperative sensing outperforms noncooperative sensing from both PU and SU points of view. The graphs also reveal that κ plays an important role in PU's performance. In FDr case, a significant gain in PU's average throughput is achieved for higher values of κ. The reason is that the higher κ would increase the P_d, which is in turn closely related to the average throughput of the PUs. When P_d increases, the average throughput of PUs will increase. As seen from the figure, the PUs' average throughput for HD case is the same as for FDr when κ is equal to one.

6.3. Multi-Channel Sensing Results. In Figure 9, SUs' average throughput in multichannel sensing case is presented versus number of cooperating SUs (M) for different schemes, with $\kappa = 0.99$, $W = 11$, $T_{so} = 1$ ms, and $\beta = 0.2$. What is shown here is that an increasing number of channels, V, sensed by SUs will increase the average throughput. This is due to the fact that increasing V will increase the sensing time T_s, so that the probability that SUs detect idle channels is increased as well. In addition, according to this figure, FDr still outperforms HD and FDs schemes for the multichannel sensing case. When M increases, average throughput will also increase. By increasing M, the false alarm probability will be reduced, while the number of sensed idle channels will increase. This is consistent with our previous results (Figure 7). It is worthwhile to note that, for multichannel sensing case, the sensing time T_s increases as the number of multichannels increase. In this case, with a fixed T_p, the detection probability P_d will increase and b_{T_s} in (33) will decrease, so that the primary users' average throughput will be affected.

7. Proposed MAC Protocol Design

7.1. Deployment Architecture. Our MAC design is based on a limited infrastructure support architecture in cognitive vehicular networks [27]. Road side units (RSU), as defined in IEEE 802.11p standard, are placed on the road. These play the role of coordinator nodes in the cooperative cognitive radio network, taking care of spectrum selection and access. On the other hand, vehicular nodes act as secondary users (SUs). Figure 10 illustrates the network architecture for our proposed MAC.

7.2. Proposed MAC Framework. Our MAC framework is developed based on a slotted time MAC structure illustrated in Figure 11. There is one control channel (CCC) and W primary licensed channels, within T_p time duration. Moreover, the proposed MAC protocol is divided into four phases.

The first phase is sensing phase (SP). Each SU which has packets to send senses V channels from W licensed channels during this phase. Energy detection technique is

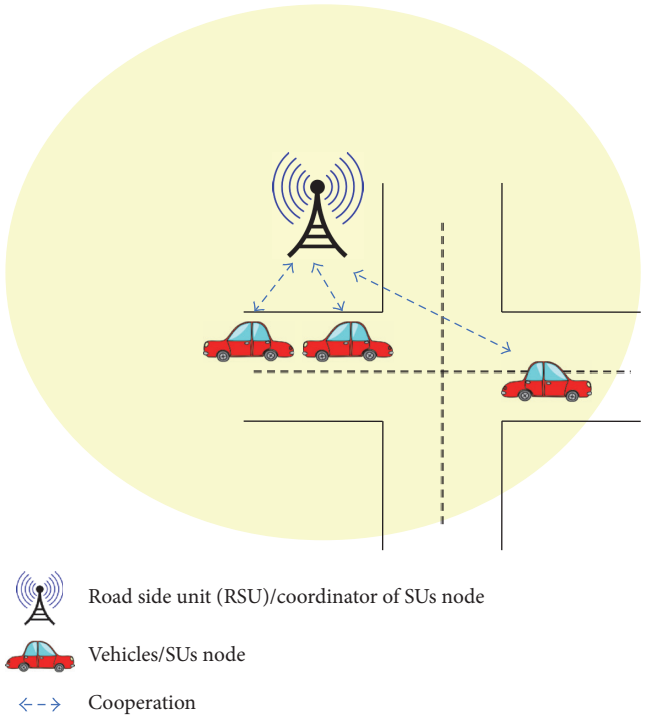

Figure 10: MAC deployment topology.

used to detect PU's activity. Furthermore, SUs listen to CCC for broadcast information.

The second phase is reporting and contending phase (RCP). In this phase, the SU informs the coordinator about the sensing result and its intention to use licensed channels. The CCC frame is split into M_x minislots. Each SU selects one minislot based on the broadcast information received during the SP phase.

The third phase is the broadcast phase (BP). After receiving the sensing result information, the coordinator performs spectrum decision, access and SU management. Spectrum decision is performed by selecting idle channels based on overall energy statistic calculation as in [5]. Furthermore, L identified available licensed channels are allocated among M_c SUs. If $L < M_c$, only the first of L SUs can use one channel per user. The remaining SUs will be allocated in the next time slot. If $L > M_c$, then each SU may be eligible for $\lfloor L/M_c \rfloor$ channels. $\lfloor \cdot \rfloor$ is rounded down to nearest integer operator. In relation to management of SUs, the coordinator removes inactive SUs and adds new SUs into its list of M_c SUs. In addition, broadcast is also used for acknowledging arrival of new SUs.

Broadcast messages contain the following information:

(1) Number of current SUs in the cooperative network (M_c): this information is required for the new SU to join the cooperative network. The new SU selects a random minislot number from $M_c + 1$ to M_x.

(2) Available licensed channels for specific SUs: transmission mode, FDr or FDs, according to Figure 11 is decided by the coordinator based on M_c values. M_{th} is defined as a threshold which allows each SU to use FDr mode based on PU's performance guarantee. Coordinator selects FDs transmission mode by default. However, If $M_c > M_{\text{th}}$ and both the coordinator and the SU have packets to send, then FDr can be selected.

(3) Synchronization information for all SUs in the cooperative network.

The last phase is data transmission phase (DTP). If an SU uses FDr mode, then data and acknowledgement can be transmitted in both uplink and downlink directions. FDs mode allows SU to send data in uplink or downlink direction and sense at the same time. During the DTP phase, if the SU detects primary user activity, it will stop transmitting the current data or acknowledgement.

7.3. Proposed MAC Protocol Average Throughput. In this section, the proposed MAC is evaluated using average throughput as performance metric.

7.3.1. Proposed MAC's Average Throughput Using Full-Duplex Transmit-Sense-Reception Mode. Average throughput can be calculated using the same method as in Section 4.3. However, average throughput calculation in the proposed MAC requires preparation time (T_{pr}), which consists of sensing time (T_s), reporting time (T_r), and broadcasting time (T_b). Figure 12 shows the frame structure of the proposed MAC.

$$T_{\text{pr,FDr}} = T_s + T_r + T_b = V \cdot T_{\text{so}} + M_x \cdot T_{\text{ro}} + T_b. \tag{39}$$

The average throughput for the proposed MAC ($\tau_{s,\text{MFDr}}$) can be calculated as

$$\tau_{s,\text{MFDr}}^{(V,M_x)} = \frac{L \cdot \sum_{i=00}^{11} P\left[S_{i,\text{FDr}}\right] C_{i,\text{MFDr}}}{W}, \tag{40}$$

where

$$C_{00,\text{MFDr}} = 2\overline{P_f}\frac{T_p - T_{\text{pr,FDr}}}{T_p} D_{s,0}$$

$$C_{01,\text{MFDr}} = \frac{2}{T_p\left(1 - e^{-T_p/\rho_{\text{off}}}\right)} D_{s,0}\overline{P_f} - \frac{2D_{s,1}\overline{P_d}\left(\rho_{\text{off}} - \left(T_p + \rho_{\text{off}}\right)e^{-T_p/\rho_{\text{off}}}\right)}{T_p\left(1 - e^{-T_p/\rho_{\text{off}}}\right)}$$

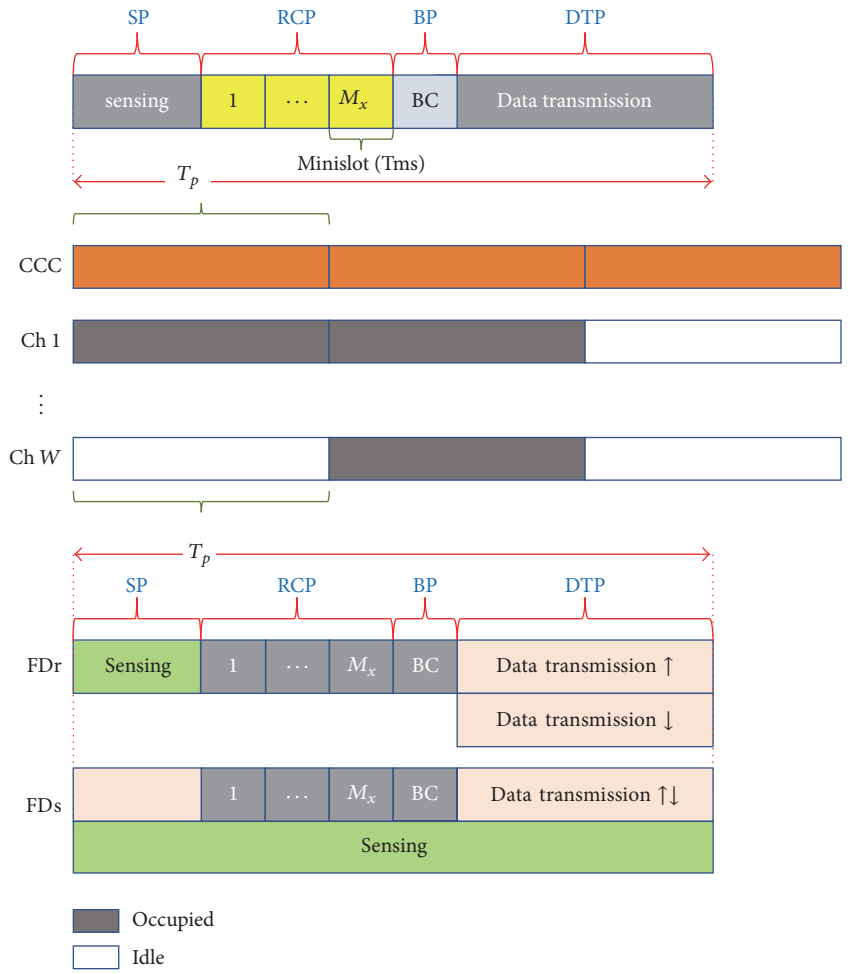

Figure 11: Proposed MAC framework.

$$+\frac{2}{T_p}\left(\overline{P_d}D_{s,1}T_p-\overline{P_f}D_{s,0}T_{\mathrm{pr,FDr}}\right)$$

$$C_{10,\mathrm{MFDr}}=\frac{2}{T_p}\frac{D_{s,1}\overline{P_d}-D_{s,0}\overline{P_f}\left(\rho_{\mathrm{on}}-\left(T_p+\rho_{\mathrm{on}}\right)e^{-T_p/\rho_{\mathrm{on}}}\right)}{1-e^{-T_p/\rho_{\mathrm{on}}}}+\frac{2}{T_p}\left(\overline{P_f}D_{s,0}T_p-\overline{P_d}D_{s,1}T_{\mathrm{pr,FDr}}\right)$$

$$C_{11,\mathrm{MFDr}}=2\overline{P_d}\frac{T_p-T_{\mathrm{pr,FDr}}}{T_p}D_{s,1}. \tag{41}$$

$C_{i,\mathrm{MFDr}}$ is the achievable throughput of the proposed MAC for $S_{i,\mathrm{FDr}}$ event in the FDr scheme.

7.3.2. Proposed MAC's Average Throughput Using the Full-Duplex Transmit-Sense Mode. In FDs scheme, T_{pr} only consists of reporting (T_s) and broadcasting time (T_b), because sensing time (T_s) is in parallel with transmission time (T_t).

$$T_{\mathrm{pr,FDs}}=T_r+T_b=M_x\cdot T_{\mathrm{ro}}+T_b. \tag{42}$$

Following the same method as in Section 4.4, the average throughput for the proposed MAC can be calculated as

$$\tau_{s,\mathrm{MFDs}}^{(V,M_x)}=\frac{L\cdot\sum_{i=00}^{11}P\left[S_{i,\mathrm{FDs}}\right]C_{i,\mathrm{MFDs}}}{W}, \tag{43}$$

where $C_{i,\mathrm{MFDs}}$ is the achievable throughput of our proposed MAC for $S_{i,\mathrm{FDs}}$ event for FDs scheme

$$C_{00,\mathrm{MFDs}}=\frac{\overline{P_f}D_{s,0}\left(T_p-T_{\mathrm{pr,FDs}}\right)}{T_p},\qquad C_{11,\mathrm{MFDs}}=\frac{\overline{P_d}D_{s,1}\left(T_p-T_{\mathrm{pr,FDs}}\right)}{T_p}. \tag{44}$$

7.4. Proposed MAC Protocol Numerical Results and Analysis. Tables 1 and 2 summarize the parameters for evaluation of our proposed MAC protocol. In order to perform an evaluation based on the realistic scenario (i.e., utilizing TV white space channels), the number of primary channels (W) is established based on system B TV channels in Western Europe and many other countries in Africa, Asia, and the Pacific [28]. It is

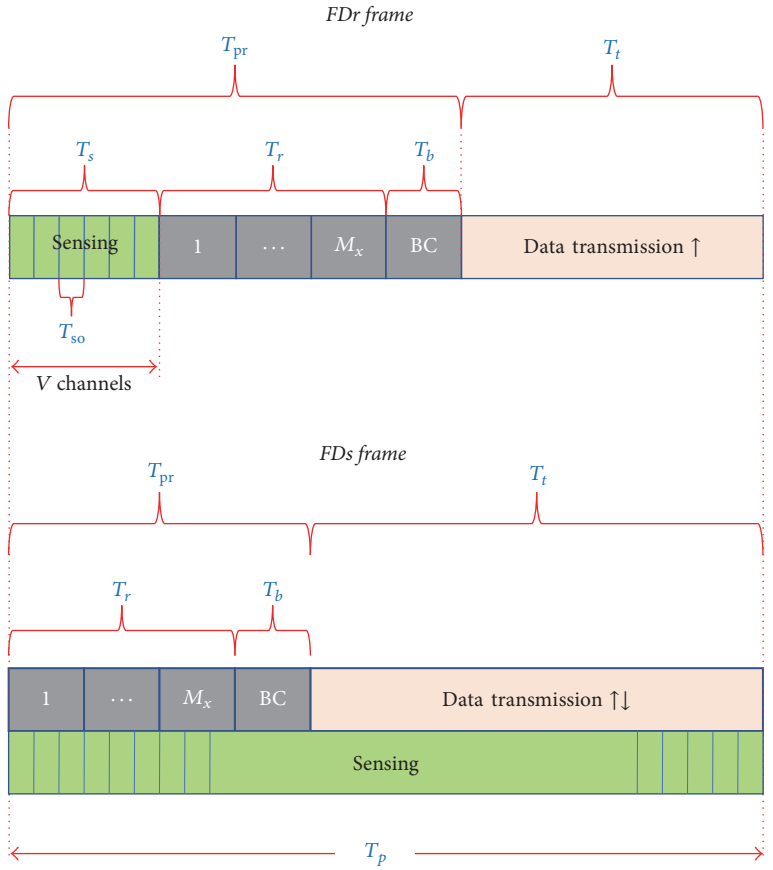

Figure 12: Proposed MAC frame structure.

Table 2: Proposed MAC simulation parameters.

Parameter	Value	Description
T_p	32 ms	Sensing period
T_{so}	1 ms	Sensing time of each channel
T_{ro}	0.5 ms	Reporting time for one minislot
T_b	2 ms	Broadcasting time

assumed the cooperative networks are saturated when the number of cooperative users (M) is equal to the maximum number of minislot (M_x).

Figure 13 demonstrates average throughput of the proposed MAC for various number of channels sensed by SU (V) and different number of minislots (M_x). It shows FDr scheme has a higher average throughput compared to FDs scheme. In both schemes, increasing M_x improves average throughput until the optimum value of M_x. It deteriorates slightly after reaching the optimum value. Here, M_x can be linked with the number of cooperative users which have been activated. Specifically, M_x increases throughput by improving the number of SUs (M) that perform cooperative spectrum sensing. Furthermore, cooperative spectrum sensing improves the average throughput. At the same time, minislots consume

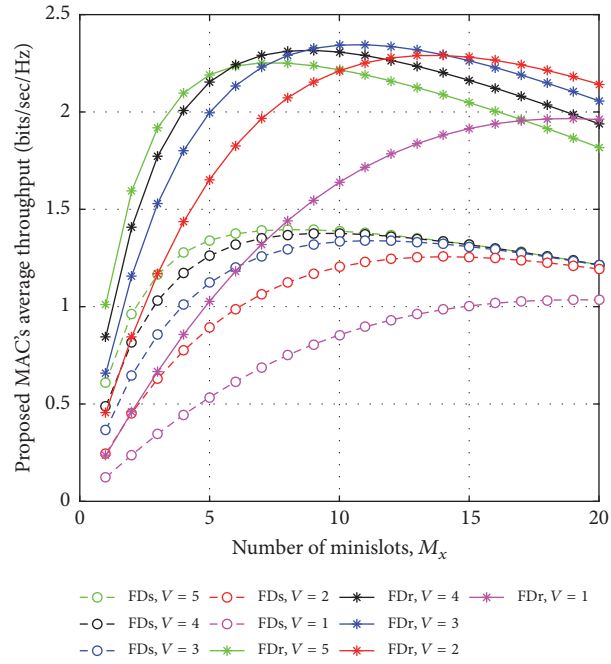

Figure 13: Proposed MAC's average throughput versus M_x for different schemes and value for V.

allocated time in a framework which cannot be used for data transmission. As a result, increasing M_x shortens the transmission time in one frame. In general, when throughput gain from cooperative spectrum sensing cannot compensate for throughput loss due to allocated minislot in a frame, it reduces the average throughput.

The number of sensed channels (V) has a different effect for FDr and FDs schemes. In FDs scheme, increasing the value of V slightly improves the average throughput. This is due to the fact that increasing V will increase the probability that SUs detect idle channels. Different from FDs scheme which only has throughput gain, in FDr scheme, there is throughput loss due to sensing time. Sensing time is considered as nontransmitting time, which reduces data transmission time. As a result, an increment of V will decrease slightly the average throughput. When throughput gain cannot compensate for throughput loss, increasing V deteriorates the average throughput.

Based on the numerical results, the optimum values for V and M_x are shown to be 3 and 11, respectively. It produces the maximum average throughput of 2.3436 bits/sec/Hz when operating in FDr mode and 1.3387 bits/sec/Hz in FDs mode. In other words, the stated parameter values can be implemented for optimum proposed MAC protocol in the cooperative cognitive network, while utilizing system B TV channels. It is worthwhile to note that our proposed cooperative full-duplex spectrum sensing technique needs to set up a coordinator to allocate the spectrum resource to the SUs. Such scheme is quite different with the distributed user contention based resource allocation (e.g., see [9]). In this case, fair comparison between these schemes is difficult to obtain. In addition, like the work in [9], the author proposed the frame fragmentation during the data transmission phase in order to protect the PUs. Such design makes the data transmission model quite different from ours. On the other hand, we compare our proposed full-duplex scenarios with the conventional half-duplex scheme in order to show the performance improvement.

8. Conclusion

Performance trade-offs for FDr, FDs, and HD schemes are found by analyzing the average throughput of both PUs and SUs under multichannel spectrum sharing and considering the effect of residual self-interference. The FDr scheme can offer similar achievable PU throughput as in FDs by incorporating a sufficient number of cooperating SUs for full-duplex cooperative sensing. In addition, it is shown that the result is consistent for different primary channel utilization and parameters setup. Furthermore, the proposed MAC protocol based on numerical results is designed and evaluated. The optimum parameter sets for proposed MAC are found to be implemented in particular cognitive networks in the future (e.g., the cognitive vehicular network by utilizing system B TV channels).

Conflicts of Interest

The authors declare that they have no conflicts of interest.

Acknowledgments

This work was partially supported by the Engineering and Physical Science Research Council (EPSRC) through the SENSE Grant EP/P003486/1.

References

[1] J. Mitola III and G. Q. Maguire Jr., "Cognitive radio: making software radios more personal," *IEEE Personal Communications*, vol. 6, no. 4, pp. 13–18, 1999.

[2] S. Haykin, "Cognitive radio: brain-empowered wireless communications," *IEEE Journal on Selected Areas in Communications*, vol. 23, no. 2, pp. 201–220, 2005.

[3] A. Shadmand, K. Nehra, and M. Shikh-Bahaei, "Cross-layer design in dynamic spectrum sharing systems," *EURASIP Journal on Wireless Communications and Networking*, vol. 2010, article 458472, 2010.

[4] C. Jiang, N. C. Beaulieu, L. Zhang, Y. Ren, M. Peng, and H.-H. Chen, "Cognitive radio networks with asynchronous spectrum sensing and access," *IEEE Network*, vol. 29, no. 3, pp. 88–95, 2015.

[5] C. Jiang, N. C. Beaulieu, and C. Jiang, "A novel asynchronous cooperative spectrum sensing scheme," in *Proceedings of the 2013 IEEE International Conference on Communications, ICC 2013*, pp. 2606–2611, Hungary, June 2013.

[6] C. Jiang, C. Jiang, and N. C. Beaulieu, "A contention-based wideband DSA algorithm with asynchronous cooperative spectrum sensing," in *Proceedings of the 2013 IEEE Global Communications Conference, GLOBECOM 2013*, pp. 1069–1074, USA, December 2013.

[7] A. Sabharwal, P. Schniter, D. Guo, D. W. Bliss, S. Rangarajan, and R. Wichman, "In-band full-duplex wireless: challenges and opportunities," *IEEE Journal on Selected Areas in Communications*, vol. 32, no. 9, pp. 1637–1652, 2014.

[8] W. Cheng, X. Zhang, and H. Zhang, "Full-duplex spectrum-sensing and MAC-protocol for multichannel nontime-slotted cognitive radio networks," *IEEE Journal on Selected Areas in Communications*, vol. 33, no. 5, pp. 820–831, 2015.

[9] L. T. Tan and L. B. Le, "Distributed MAC Protocol Design for Full-Duplex Cognitive Radio Networks," in *Proceedings of the GLOBECOM 2015 - 2015 IEEE Global Communications Conference*, pp. 1–6, San Diego, CA, USA, December 2015.

[10] Y. Liao, T. Wang, L. Song, and Z. Han, "Listen-and-Talk: Protocol Design and Analysis for Full-Duplex Cognitive Radio Networks," *IEEE Transactions on Vehicular Technology*, vol. 66, no. 1, pp. 656–667, 2017.

[11] W. Afifi and M. Krunz, "Incorporating Self-Interference Suppression for Full-duplex Operation in Opportunistic Spectrum Access Systems," *IEEE Transactions on Wireless Communications*, vol. 14, no. 4, pp. 2180–2191, 2015.

[12] L. T. Tan and L. B. Le, "Design and optimal configuration of full-duplex MAC protocol for cognitive radio networks considering self-interference," *IEEE Access*, vol. 3, pp. 2715–2729, 2015.

[13] W. Afifi and M. Krunz, "Adaptive transmission-reception-sensing strategy for cognitive radios with full-duplex capabilities," in *Proceedings of the 2014 IEEE International Symposium on Dynamic Spectrum Access Networks, DYSPAN 2014*, pp. 149–160, USA, April 2014.

[14] Y. Liao, T. Wang, L. Song, and B. Jiao, "Cooperative spectrum sensing for full-duplex cognitive radio networks," in *Proceedings*

of the 2014 IEEE International Conference on Communication Systems, IEEE ICCS 2014, pp. 56–60, China, November 2014.

[15] V. Towhidlou and M. Shikh-Bahaei, "Cooperative ARQ in full duplex cognitive radio networks," in *Proceedings of the 27th IEEE Annual International Symposium on Personal, Indoor, and Mobile Radio Communications, PIMRC 2016*, Spain, September 2016.

[16] S. Ha, W. Lee, J. Kang, and J. Kang, "Cooperative spectrum sensing in non-time-slotted full duplex cognitive radio networks," in *Proceedings of the 13th IEEE Annual Consumer Communications and Networking Conference, CCNC 2016*, pp. 820–823, usa, January 2016.

[17] T. Febrianto and M. Shikh-Bahaei, "Optimal full-duplex cooperative spectrum sensing in asynchronous cognitive networks," in *Proceedings of the 3rd IEEE Asia Pacific Conference on Wireless and Mobile, APWiMob 2016*, pp. 1–6, Indonesia, September 2016.

[18] L. T. Tan and L. B. Le, "Multi-channel MAC protocol for full-duplex cognitive radio networks with optimized access control and load balancing," in *Proceedings of the 2016 IEEE International Conference on Communications, ICC 2016*, Malaysia, May 2016.

[19] T.-N. Hoan, V.-V. Hiep, and I.-S. Koo, "Multichannel-sensing scheduling and transmission-energy optimizing in cognitive radio networks with energy harvesting," *Sensors*, vol. 16, no. 4, article no. 461, 2016.

[20] G. Bianchi, "Performance analysis of the IEEE 802.11 distributed coordination function," *IEEE Journal on Selected Areas in Communications*, vol. 18, no. 3, pp. 535–547, 2000.

[21] C. Jiang, Y. Chen, and K. J. R. Liu, "A renewal-theoretical framework for dynamic spectrum access with unknown primary behavior," in *Proceedings of the 2012 IEEE Global Communications Conference, GLOBECOM 2012*, pp. 1422–1427, USA, December 2012.

[22] K. J. R. Liu and B. Wang, "Cognitive radio networking and security: A Game-Theoretic view," *Cognitive Radio Networking and Security: A Game-Theoretic View*, pp. 1–601, 2010.

[23] W. Cheng, X. Zhang, and H. Zhang, "Optimal dynamic power control for full-duplex bidirectional-channel based wireless networks," in *Proceedings of the 32nd IEEE Conference on Computer Communications, IEEE INFOCOM 2013*, pp. 3120–3128, Italy, April 2013.

[24] J. Hou, N. Yi, and Y. Ma, "Joint space-frequency user scheduling for MIMO random beamforming with limited feedback," *IEEE Transactions on Communications*, vol. 63, no. 6, pp. 2224–2236, 2015.

[25] A. Shadmand and M. Shikh-Bahaei, "Multi-user time-frequency downlink scheduling and resource allocation for LTE cellular systems," in *Proceedings of the IEEE Wireless Communications and Networking Conference 2010, WCNC 2010*, Australia, April 2010.

[26] A. Kobravi and M. Shikh-Bahaei, "Cross-layer adaptive ARQ and modulation tradeoffs," in *Proceedings of the 18th Annual IEEE International Symposium on Personal, Indoor and Mobile Radio Communications, PIMRC'07*, Greece, September 2007.

[27] S. Basagni, M. Conti, S. Giordano, and I. Stojmenovic, "Mobile Ad Hoc Networking: Cutting Edge Directions: Second Edition," *Mobile Ad Hoc Networking: Cutting Edge Directions: Second Edition*, 2013.

[28] IEEE Standard for Information Technology-Telecommunications and Information Exchange between System Wireless Regional Area Networks (WRAN)-Specific Requirements-Part 22: Cognitive Wireless RAN Medium Access Control (MAC) and Physical Layer (PHY) Specifications: Policies and Procedures for Operation in the TV bands, IEEE Standard 802.22 https://standards.ieee.org/about/get/802/802.22.html, 2011.

Hindawi
Wireless Communications and Mobile Computing
Volume 2017, Article ID 3984529, 8 pages
https://doi.org/10.1155/2017/3984529

Research Article

Fast Cooperative Energy Detection under Accuracy Constraints in Cognitive Radio Networks

Shengliang Peng,[1,2] Weibin Zheng,[1] Renyang Gao,[1] and Kejun Lei[3]

[1]*Xiamen Mobile and Multimedia Communications Key Laboratory, Huaqiao University, Xiamen 361021, China*
[2]*Department of Electrical and Computer Engineering, Stevens Institute of Technology, Hoboken, NJ 07030, USA*
[3]*College of Information Science and Engineering, Jishou University, Jishou 416000, China*

Correspondence should be addressed to Shengliang Peng; peng.shengliang@gmail.com

Received 26 May 2017; Accepted 8 August 2017; Published 13 September 2017

Academic Editor: Mohammad Shikh-Bahaei

Cooperative energy detection (CED) is a key technique to identify the spectrum holes in cognitive radio networks. Previous study on this technique mainly aims at improving the detection accuracy, while paying little attention to the performance of detection time. This paper concentrates on the issue of fast CED, which is achieved by minimizing its detection time subject to the constraints on detection accuracy. Firstly, the prevalent counting rule based CED algorithm is optimized. Taking the special cases of counting rule (AND rule and OR rule), for example, we show that detection time can be minimized by selecting an optimal number of secondary users. Moreover, we prove that OR rule is superior to AND rule in detection time, and thus OR rule based CED is faster than AND rule based CED. Then, a sequential test (ST) based CED algorithm is proposed to exploit the benefit of ST and detect primary user even faster. After analyzing its detection time, we illustrate that ST based CED is able to spend the minimal detection time in satisfying the accuracy constraints by choosing an optimal sample number. Simulation results are provided to verify the effectiveness of both fast algorithms discussed in this paper.

1. Introduction

The significant achievement in wireless technologies has inspired masses of wireless services, which not only facilitate human life but also bring about considerable requirements on spectrum resource, causing the so-called "spectrum scarcity" problem. Cognitive radio (CR) is one of the promising techniques to alleviate this problem by allowing secondary users (SUs) to recycle the "spectrum holes" on the spectrum band that has been licensed to primary user (PU) for exclusive use. In order to identify the spectrum holes, SUs should detect whether PU is using the licensed band [1].

Several classical methods, such as energy detection, match filter detection, and cyclostationary feature detection, have been proposed for PU detection [2]. Among them, energy detection is preferable because of its simplicity, low computational complexity, and small amount of requirement on prior information about PU's signal. However, this method works badly when the signal-to-noise ratio (SNR) is low [3]. To combat the performance degradation at low SNR region, literatures [4, 5] suggest multiple SUs in a CR network cooperate and introduce the cooperative energy detection (CED). CED is usually implemented according to two successive stages: firstly in the sensing stage, each SU individually performs energy detection and outputs its sensing result; then in the fusing stage, a fusion center (FC) collects and fuses multiple SUs' sensing results to make a final decision. The sensing results can be either raw information SUs have observed [6–8] or local decisions SUs have made based on the observations [9, 10], leading to CED with soft and hard combination [11], respectively. Since the latter consumes less dedicated reporting channel resource, it increasingly becomes the dominant choice [6, 10, 12].

Previous research on CED mainly concentrates on designing proper cooperation mechanism to achieve better detection accuracy. However, accuracy is not the only performance metric. Once PU stops using licensed band, SUs ought to immediately reuse it to increase the throughput; once PU begins occupying the band, SUs should vacate it as soon as possible to avoid causing interference [13, 14].

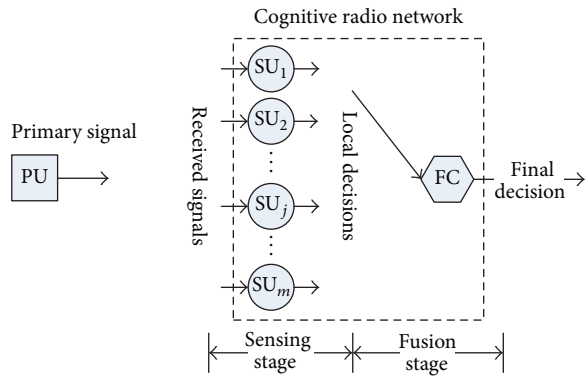

Figure 1: Cooperative primary user detection in CR network.

In other words, the capability of detecting PU speedily is also of vital importance. Unfortunately, there is a trade-off between detection speed and detection accuracy, and the improvement in the former usually leads to the degradation in the latter [13, 15].

Although CED is a popular method that has attracted great attention, its detection accuracy and detection speed are usually discussed separately. This paper jointly considers these two performance metrics based on some well-proved tools in CED and achieves fast CED via minimizing the detection time subject to the detection accuracy constraints. Fast counting rule based CED algorithm is discussed. Sequential test (ST) is applied to complete PU detection even faster. The remainder of this paper is organized as follows. Section 2 describes the CED scenario and the detection time model. Section 3 investigates the problem of minimizing detection time for counting rule based CED algorithm. Section 4 introduces the ST based CED algorithm and maximizes its detection speed. Simulation results are provided in Section 5. Section 6 concludes this paper.

2. Scenario Description and Detection Time Model

A CR network composed by one FC and m SUs is considered in this paper. SUs implement CED with hard combination to cooperatively detect PU with the help of FC. Detailedly, the whole detection procedure comprises two stages, namely, the sensing stage and the fusion stage, as shown in Figure 1.

In the sensing stage, each SU measures the energy of its received signal, based on which a local decision is made. Assume n samples are used to calculate energy, and the sampling interval is T. Note that calculation delay is usually negligible due to powerful computational hardware, so the time required by sensing stage can be expressed as $T_s = nT$. Then in the fusion stage, FC collects multiple SUs' local decisions through a dedicated control channel [6, 10, 12] and combines them to make the final decision. In order to avoid consuming too much spectrum resource, multiple SUs usually access the control channel in time division multiple access mode, and their local decisions need to be collected one by one not in parallel. Assume all m SUs' local decisions are collected, and the time of collecting each SU's local decision is R times of T. Since combination delay is also insignificant, the time required by fusion stage is given by $T_f = mRT$. Consequently, the detection time of CED can be modeled as [16]

$$T_d = T_s + T_f = nT + mRT. \tag{1}$$

This paper focuses on the detection time illustrated above and aims at minimizing it under the constraints of detection accuracy to achieve fast CED. The accuracy of final decision is usually evaluated in terms of global false alarm probability Q_f and global missed detection probability Q_m; thus the optimization problem can be depicted as

$$\begin{aligned} \min_{\text{w.r.t. } m \text{ or } n} \quad & T_d = nT + mRT, \\ \text{s.t.} \quad & Q_f = \alpha, \\ & Q_m = \beta, \end{aligned} \tag{2}$$

where α and β represent the desired false alarm and missed probabilities, respectively.

3. Fast Counting Rule Based CED

As shown in Figure 1, this paper discusses CED with hard combination. One suboptimal solution to hard combination is the counting rule (also referred to as the voting rule or K-out-of-N rule) [4, 11, 12]. This section investigates the fast counting rule based CED algorithm.

3.1. Algorithm Description. According to counting rule based CED, each SU conducts energy detection in the sensing stage. The received energy of the jth SU is given by

$$v_j = \begin{cases} \sum_{i=1}^{n} \left| n_j(i) \right|^2, & H_0, \\ \sum_{i=1}^{n} \left| s_j(i) + n_j(i) \right|^2, & H_1, \end{cases} \tag{3}$$

where $n_j(i)$ and $s_j(i)$ denote the additive noise and the received signal of the jth SU at the ith sample, respectively, and H_0 and H_1 denote the hypotheses of PU using and not using the licensed band, respectively.

Comparing v_j with a threshold λ, the jth SU can make its local decision D_j as follows:

$$\begin{aligned} v_j < \lambda \quad & \text{Accept } H_0 \text{ and } D_j = 0, \\ v_j \geq \lambda \quad & \text{Accept } H_1 \text{ and } D_j = 1. \end{aligned} \tag{4}$$

Without loss of generality, assuming that $n_j(k)$ is white and Gaussian with zero mean and unit variance and that the total energy of primary signal within each observation

block remains constant, v_j approximately follows Gaussian distribution according to the central limit theorem [6, 13]:

$$v_j \sim \begin{cases} \mathcal{N}(n, 2n), & H_0, \\ \mathcal{N}\left(n(1+\gamma), 2n(1+2\gamma)\right), & H_1, \end{cases} \tag{5}$$

where γ is the received SNR of SU.

Based on (5), the false alarm and missed detection probabilities of SU's local decision yield to

$$\begin{aligned} P_f &= Q\left(\frac{\lambda - n}{\sqrt{2n}}\right), \\ P_m &= 1 - Q\left(\frac{\lambda - n(1+\gamma)}{\sqrt{2n(1+2\gamma)}}\right), \end{aligned} \tag{6}$$

where $Q(x) = \int_x^\infty (1/\sqrt{2\pi}) e^{-(t^2/2)} dt$ is the Q function.

In the fusion stage, FC implements counting rule to make the final decision. More specifically, FC accepts H_1 if and only if at least k $(1 \le k \le m)$ SUs accept H_1; otherwise, it accepts H_0:

$$\begin{aligned} \sum_{j=1}^{m} D_j \ge k \quad &\text{Accept } H_1, \\ \sum_{j=1}^{m} D_j < k \quad &\text{Accept } H_0. \end{aligned} \tag{7}$$

So the global false alarm and missed detection probabilities of the final decision can be deduced as

$$\begin{aligned} Q_f &= \sum_{j=k}^{m} \binom{m}{j} P_f^j \cdot \left(1 - P_f\right)^{m-j}, \\ Q_m &= \sum_{j=0}^{k-1} \binom{m}{j} \left(1 - P_m\right)^j \cdot P_m^{m-j}. \end{aligned} \tag{8}$$

Note that, in realistic applications, it is unnecessary for FC to firstly collect all m SUs' local decisions and then count how many of them accept H_1. Once the jth $(\min\{k, m-k+1\} \le j \le m)$ SU's decision has been collected, we may count the number of SUs accepting H_1 in $\{D_1, D_2, \ldots, D_j\}$:

$$N_j = \sum_{q=1}^{j} D_q = N_{j-1} + D_j, \tag{9}$$

where $N_0 \triangleq 0$.

If N_j is equal to or greater than k, FC could stop collecting more local decisions and make the final decision of accepting H_1 directly. If N_j is equal to or smaller than $j - m + k + 1$, FC could also stop collecting and accept H_0 because the number of SUs accepting H_1 is certainly below k even though the remaining SUs all accept H_1. Otherwise, FC continues collecting the next SU's local decision D_{j+1} and calculating N_{j+1}:

$$\begin{aligned} N_j \ge k \quad &\text{Stop collecting, accept } H_1, \\ N_j \le j - m + k - 1 \quad &\text{Stop collecting, accept } H_0, \\ \text{Otherwise} \quad &\text{Continue collecting } D_{j+1}. \end{aligned} \tag{10}$$

Consequently, in counting rule based CED, how many SUs' local decisions will be collected and fused to make the final decision not fixed. It is a random variable denoted by $\widehat{m}$, where $\widehat{m} \in [\min\{k, m-k+1\}, m]$.

When FC finally accepts H_1 under the hypothesis H_0, $\widehat{m} = l$ indicates that the number of SUs accepting H_1 reaches k after the lth SU's local decision of accepting H_1 is taken into consideration. The corresponding probability is given by

$$\Pr\left(\widehat{m} = l, H_1 \mid H_0\right) = P_f \cdot \binom{l-1}{k-1} {P_f}^{k-1} \left(1 - P_f\right)^{l-k}. \tag{11}$$

When FC finally accepts H_0 under the hypothesis H_0, $\widehat{m} = l$ indicates that the number of SUs accepting H_0 reaches $m - k + 1$ (namely, N_l reaches $l - m + k - 1$) after the lth SU's local decision of accepting H_0 is taken into consideration. Its probability is

$$\begin{aligned} &\Pr\left(\widehat{m} = l, H_0 \mid H_0\right) \\ &\quad = \left(1 - P_f\right) \cdot \binom{l-1}{m-k} \left(1 - P_f\right)^{m-k} {P_f}^{l-(m-k+1)}. \end{aligned} \tag{12}$$

Similarly, we obtain

$$\begin{aligned} &\Pr\left(\widehat{m} = l, H_1 \mid H_1\right) \\ &\quad = \left(1 - P_m\right) \cdot \binom{l-1}{k-1} \left(1 - P_m\right)^{k-1} {P_m}^{l-k}, \\ &\Pr\left(\widehat{m} = l, H_0 \mid H_1\right) \\ &\quad = P_m \cdot \binom{l-1}{m-k} {P_m}^{m-k} \left(1 - P_m\right)^{l-(m-k+1)}. \end{aligned} \tag{13}$$

Therefore, the mean of $\widehat{m}$ can be expressed as

$$\begin{aligned} &E\{\widehat{m}\} \\ &= P_0 \left[\Pr\left(\widehat{m} = l, H_0 \mid H_0\right) + \Pr\left(\widehat{m} = l, H_1 \mid H_0\right)\right] \\ &\quad + P_1 \left[\Pr\left(\widehat{m} = l, H_0 \mid H_1\right) + \Pr\left(\widehat{m} = l, H_1 \mid H_1\right)\right], \end{aligned} \tag{14}$$

where P_0 and P_1 are the prior probabilities of H_0 and H_1, respectively.

Since $\widehat{m}$ is a random variable, $\widehat{T}_d = nT + \widehat{m}RT$ is also a random variable. As a result, the optimization problem described in (2) should be rewritten as

$$\begin{aligned} \min_{\text{w.r.t. } m \text{ or } n} \quad & E\left\{\widehat{T}_d\right\} = nT + E\left\{\widehat{m}\right\} RT \\ \text{s.t.} \quad & Q_f = \alpha, \\ & Q_m = \beta. \end{aligned} \tag{15}$$

In the rest of this paper, we will discuss (15) instead of (2).

3.2. $k = m$ (AND Rule). Considering the counting rule with parameter k $(1 \le k \le m)$, this subsection deals with a special case of $k = m$ for simplicity. In this case, FC accepts H_1 if and only if all SUs accept H_1, and the counting rule turns to be the "AND rule" [2].

Substituting $k = m$ into (8), the constraints on detection accuracy can be reexpressed as

$$\begin{aligned} Q_f &= {P_f}^m = \alpha, \\ Q_m &= 1 - \left(1 - P_m\right)^m = \beta. \end{aligned} \tag{16}$$

In addition, using the results of (6) to deduce n and λ, we get

$$n = \frac{2}{\gamma^2}\left[Q^{-1}\left(\sqrt[m]{\alpha}\right) - \sqrt{1+2\gamma}Q^{-1}\left(\sqrt[m]{1-\beta}\right)\right]^2, \tag{17}$$

$$\begin{aligned} \lambda = \frac{2}{\gamma^2}\Bigg\{ & (1+\gamma)\left[Q^{-1}\left(\sqrt[m]{\alpha}\right)\right]^2 \\ & - (2+\gamma)\sqrt{1+2\gamma}Q^{-1}\left(\sqrt[m]{\alpha}\right)Q^{-1}\left(\sqrt[m]{1-\beta}\right) \\ & + (1+2\gamma)\left[Q^{-1}\left(\sqrt[m]{1-\beta}\right)\right]^2\Bigg\}. \end{aligned} \tag{18}$$

It should be pointed out that, given a number of SUs m, accuracy constraints can be satisfied if the sample number n and the threshold λ are chosen according to (17) and (18).

Substituting $k = m$ and (16) into (14), the mean of $\widehat{m}$ yields to

$$E\left\{\widehat{m}\right\} = P_0\frac{1-\alpha}{1-\sqrt[m]{\alpha}} + P_1\frac{\beta}{1-\sqrt[m]{1-\beta}}. \tag{19}$$

Finally, the mean of detection time for AND rule based CED is given by

$$\begin{aligned} E\left\{\widehat{T}_d\right\} = {} & \frac{2T}{\gamma^2}\left[Q^{-1}\left(\sqrt[m]{\alpha}\right) - \sqrt{1+2\gamma}Q^{-1}\left(\sqrt[m]{1-\beta}\right)\right]^2 \\ & + RT\left(P_0\frac{1-\alpha}{1-\sqrt[m]{\alpha}} + P_1\frac{\beta}{1-\sqrt[m]{1-\beta}}\right). \end{aligned} \tag{20}$$

Note that both α and β are usually small, and thus the left part of $E\{\widehat{T}_d\}$ decreases as m increases, while its right part increases as m increases. Intuitively, neither too many nor too few SUs should be used. There exists an optimal number of SUs with which the average detection time can be minimized. Since m is a natural number, its optimal value m_{opt} can be easily obtained via numerical search according to (20). Substituting m_{opt} into (17) and (18), the optimal values for the sample number and the threshold, namely, n_{opt} and λ_{opt}, can be derived as well. In practical scenarios, if implementing AND rule based CED according to the parameters m_{opt}, n_{opt}, and λ_{opt}, we will not only guarantee the desired detection accuracy but also minimize the detection time. In other words, the expected fast PU detection is achieved.

3.3. $k = 1$ (OR Rule). Besides $k = m$, another special case for the counting rule with parameter k $(1 \le k \le m)$ is $k = 1$; that is, FC accepts H_1 if any one of m SUs accepts H_1, resulting in the so-called "OR rule" [2].

Substituting $k = 1$ into (8) and (14), we obtain

$$\begin{aligned} Q_f &= 1 - \left(1 - P_f\right)^m = \alpha, \\ Q_m &= {P_m}^m = \beta, \\ E\left\{\widehat{m}\right\} &= P_0\frac{\alpha}{1-\sqrt[m]{1-\alpha}} + P_1\frac{1-\beta}{1-\sqrt[m]{\beta}}. \end{aligned} \tag{21}$$

Using the equations above, the sample number n, the threshold λ, and the average detection time $E\{\widehat{T}_d\}$ of OR rule based CED are given by

$$n = \frac{2}{\gamma^2}\left[-Q^{-1}\left(\sqrt[m]{1-\alpha}\right) + \sqrt{1+2\gamma}Q^{-1}\left(\sqrt[m]{\beta}\right)\right]^2, \tag{22}$$

$$\begin{aligned} \lambda = \frac{2}{\gamma^2}\Bigg\{ & (1+\gamma)\left[Q^{-1}\left(\sqrt[m]{1-\alpha}\right)\right]^2 \\ & - (2+\gamma)\sqrt{1+2\gamma}Q^{-1}\left(\sqrt[m]{1-\alpha}\right)Q^{-1}\left(\sqrt[m]{\beta}\right) \\ & + (1+2\gamma)\left[Q^{-1}\left(\sqrt[m]{\beta}\right)\right]^2\Bigg\}, \end{aligned} \tag{23}$$

$$\begin{aligned} E\left\{\widehat{T}_d\right\} = {} & \frac{2T}{\gamma^2}\left[-Q^{-1}\left(\sqrt[m]{1-\alpha}\right)\right. \\ & \left. + \sqrt{1+2\gamma}Q^{-1}\left(\sqrt[m]{\beta}\right)\right]^2 + RT\left(P_0\frac{\alpha}{1-\sqrt[m]{1-\alpha}}\right. \\ & \left. + P_1\frac{1-\beta}{1-\sqrt[m]{\beta}}\right). \end{aligned} \tag{24}$$

Similarly, the optimal value for the number of SUs to minimize $E\{\widehat{T}_d\}$, namely, m_{opt}, can be obtained via numerical search according to (24). n_{opt} and λ_{opt} can be derived from (22) and (23), respectively. With these parameters, fast OR rule based CED will be achieved in terms of minimizing average detection time subject to desired detection accuracy.

Moreover, in order to compare two special cases of $k = m$ and $k = 1$, we define the average detection time difference as

$$\Delta T_d = E\left\{\widehat{T}_d \mid k = 1\right\} - E\left\{\widehat{T}_d \mid k = m\right\}. \tag{25}$$

Without loss of generality, considering $P_0 = P_1$ and $\alpha = \beta < 1/2$, it is easy to deduce

$$\Delta T_{KM} = \frac{4T}{\gamma}\left\{\left[Q^{-1}\left(\sqrt[m]{\alpha}\right)\right]^2 - \left[Q^{-1}\left(\sqrt[m]{1-\alpha}\right)\right]^2\right\} < 0. \quad (26)$$

Therefore, given the same number of SUs and the same accuracy constraints, OR rule consumes less detection time compared with AND rule. In other words, it is faster than AND rule.

4. Fast ST Based CED

4.1. Algorithm Description. Invented by Wald, ST is superior in consuming less observations to control both false alarm and missed detection errors compared with other traditional test methods [15, 17]. In this section, FC implements ST to fuse multiple SUs' local decisions, resulting in the ST based CED.

The sensing stage of ST based CED is identical with that of counting rule based CED. In the fusion stage, FC collects multiple SUs' local decisions one by one and fuses them to make the final decision according to ST instead of counting rule. When the jth local decision D_j is obtained, its log-likelihood ratio LD_j and cumulative log-likelihood ratio SD_j can be derived as

$$\begin{aligned} LD_j &= \log\left(\frac{\Pr\left(D_j \mid H_1\right)}{\Pr\left(D_j \mid H_0\right)}\right) \\ &= \begin{cases} \log\left(\dfrac{P_m}{1-P_f}\right) & D_j = 0 \\ \log\left(\dfrac{1-P_m}{P_f}\right) & D_j = 1, \end{cases} \\ SD_j &= \sum_{q=1}^{j} LD_q = SD_{j-1} + LD_j, \end{aligned} \quad (27)$$

where $SD_0 \triangleq 0$.

Comparing SD_j with two thresholds λ_L and λ_H ($\lambda_L < \lambda_H$), whether making the final decision or continuing collecting the next SU's local decision is determined as follows:

$$\begin{aligned} &SD_j \geq \lambda_H \quad \text{Accept } H_1, \\ &SD_j \leq \lambda_L \quad \text{Accept } H_0, \\ &\lambda_L < SD_j < \lambda_H \quad \text{Continue collecting } D_{j+1}, \end{aligned} \quad (28)$$

where both λ_L and λ_H depend on the desired detection accuracy α and β. According to the propositions in [17], these thresholds are given by $\lambda_L = \log(\beta/(1-\alpha))$, $\lambda_H = \log((1-\beta)/\alpha)$ ($\alpha < 1/2, \beta < 1/2$).

4.2. Detection Time Optimization. Inherited from the feature of ST, ST based CED is able to stop collecting once the collected local decisions are sufficient enough to guarantee the desired accuracy. It has two distinctive characteristics: (1) accuracy requirements are autonomously satisfied via ST as shown in (28), so there is no need to care about its detection accuracy any more. (2) How many SUs' local decisions will be collected and fused before making the final decision is not fixed. Similarly, denote this random variable by $\widehat{m}$. The means of $\widehat{m}$ under both hypotheses are given by [17]

$$\begin{aligned} &E\{\widehat{m} \mid H_0\} \\ &\approx \frac{(1-\alpha)\log\left(\beta/(1-\alpha)\right) + \alpha\log\left((1-\beta)/\alpha\right)}{E\left\{LD_j \mid H_0\right\}} \\ &= \frac{(1-\alpha)\log\left(\beta/(1-\alpha)\right) + \alpha\log\left((1-\beta)/\alpha\right)}{\left(1-P_f\right)\log\left(P_m/\left(1-P_f\right)\right) + P_f\log\left(\left(1-P_m\right)/P_f\right)}, \\ &E\{\widehat{m} \mid H_1\} \\ &\approx \frac{\beta\log\left(\beta/(1-\alpha)\right) + (1-\beta)\log\left((1-\beta)/\alpha\right)}{E\left\{LD_j \mid H_1\right\}} \\ &= \frac{\beta\log\left(\beta/(1-\alpha)\right) + (1-\beta)\log\left((1-\beta)/\alpha\right)}{P_m\log\left(P_m/\left(1-P_f\right)\right) + \left(1-P_m\right)\log\left(\left(1-P_m\right)/P_f\right)}. \end{aligned} \quad (29)$$

Then the average detection time of ST based CED yields to

$$E\left\{\widehat{T}_d\right\} = nT + \left(P_0 E\{\widehat{m} \mid H_0\} + P_1 E\{\widehat{m} \mid H_1\}\right) RT. \quad (30)$$

As shown in (30), $E\{\widehat{T}_d\}$ depends on the variables n, P_f, and P_m. Because of (6), $E\{\widehat{T}_d\}$ is eventually determined by the parameters n and λ. Conducting two-dimensional numerical search based on (30), a pair of optimal values for n and λ can be obtained to minimize $E\{\widehat{T}_d\}$ and achieve fast ST based CED.

Without loss of generality, we assume $\alpha = \beta$ and $P_f = P_m$ to balance false alarm or missed detection errors. As a result, λ can be written as a function of n:

$$\lambda = \frac{\sqrt{1+2\gamma}+1+\gamma}{\sqrt{1+2\gamma}+1}n, \quad (31)$$

and $E\{\widehat{T}_d\}$ solely depends on n:

$$E\left\{\widehat{T}_d\right\} = nT + \frac{(1-2\alpha)\log\left((1-\alpha)/\alpha\right)RT}{\left[1-2Q\left(\sqrt{2n}\cdot\gamma/2\left(\sqrt{1+2\gamma}+1\right)\right)\right]\log\left(1/Q\left(\sqrt{2n}\cdot\gamma/2\left(\sqrt{1+2\gamma}+1\right)\right)-1\right)}. \quad (32)$$

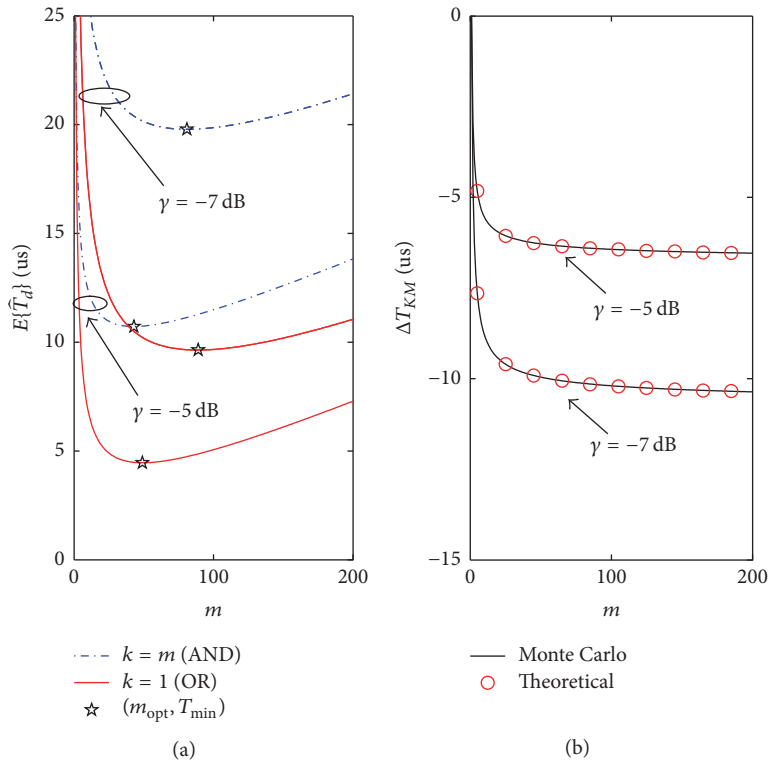

FIGURE 2: Average detection time and detection time difference of counting rule based CED versus SU number for $\gamma = -5, -7$ dB.

The optimal sample number to minimize $E\{\widehat{T}_d\}$, namely, n_{opt}, can be easily derived from (32), with which the speed of ST based CED is consequently maximized.

5. Numerical Results

This section provides some simulation results to verify the theoretical derivations above. Simulation settings are listed as follows: $T = 0.046459$ us [18], $R = 1$, $\alpha = \beta = 1\%$, and $P_0 = P_1$.

In order to test the detection accuracy of fast counting rule based CED, Monte Carlo simulations are conducted with different numbers of SUs ($m = 10, 50, 100, 150, 200$) for $\gamma = -5$ dB. Given a specific m, if $k = m$, parameters n and λ are chosen according to (17) and (18), respectively, and the accuracy results (Q_f and Q_m) are recorded in Table 1. If $k = 1$, parameters n and λ are derived from (22) and (23), respectively, and the corresponding results are demonstrated in Table 2. It can be seen from both tables that, no matter how m changes, the global false alarm and missed detection probabilities always remain constant and practically equal 1%. Therefore, the proposed fast counting rule based CED is able to meet the accuracy constraints.

Since the accuracy constraints have been satisfied, we focus on the performance metric of detection time in Figure 2. Considering $k = m$ and $k = 1$, Figure 2(a) plots the average detection time curves of counting rule based CED versus the number of SUs for $\gamma = -5, -7$ dB. As shown in this subfigure, all curves are concave regardless of k and γ. In other words, there exists an optimal number of SUs to minimize the average detection time. Implementing numerical search according to (20) and (24), the theoretical optimal number of SUs m_{opt} and the minimal average detection time T_{min} are obtained and plotted. Note that each point of $(m_{\text{opt}}, T_{\text{min}})$ agrees well with the bottom of corresponding detection time curve. This phenomenon shows the effectiveness of our method to achieve the highest detection speed. Moreover, to dig into the special cases of $k = m$ and $k = 1$, Figure 2(b)

TABLE 1: Detection accuracy of counting rule based CED with $k = m$ for $\gamma = -5$ dB.

m	n	λ	Q_f	Q_m
10	261	253.32	0.99%	0.99%
50	201	173.63	0.95%	1.00%
100	187	153.88	1.02%	0.95%
150	180	144.60	1.02%	1.03%
200	176	138.81	1.02%	1.02%

TABLE 2: Detection accuracy of counting rule based CED with $k = 1$ for $\gamma = -5$ dB.

m	n	λ	Q_f	Q_m
10	142	193.68	0.97%	1.00%
50	66	106.01	1.02%	0.96%
100	48	84.64	0.98%	0.99%
150	40	74.65	1.03%	0.97%
200	36	68.43	0.97%	0.97%

Table 3: Detection accuracy of ST based CED for $\gamma = -5$ dB.

n	λ	Q_f	Q_m
50	46.94	0.82%	0.62%
	56.94 ($P_f = P_m$)	0.32%	0.33%
	66.94	0.56%	0.90%
100	103.88	0.61%	0.30%
	113.88 ($P_f = P_m$)	0.76%	0.75%
	123.88	0.35%	0.61%

depicts their average detection time difference versus the number of SUs for $\gamma = -5, -7$ dB. In this subfigure, the Monte Carlo curves are derived from Monte Carlo simulations, and the theoretical curves are calculated by (26). As two types of curves are overlapping and always below 0, the correctness of (26) is verified. So the average detection time of counting based CED with $k = 1$ is smaller than that with $k = m$. In other words, OR rule based CED is faster than AND rule based CED.

Aiming to verify the accuracy of fast ST based CED, we perform Monte Carlo simulations with various sample numbers ($n = 50, 100$) for $\gamma = -5$ dB, and record the global false alarm as well as missed detection probabilities in Table 3. Given each n, three values of the local threshold λ are involved: the value calculated by (31) to guarantee $P_f = P_m$ ($\lambda = 56.94, 113.88$), and the calculated value with ± 10 offsets. As shown in Table 3, both Q_f and Q_m are always smaller than 1%, indicating that the proposed fast ST based CED satisfies the accuracy constraints well.

Finally, Figure 3 plots the average detection time curves of counting rule based CED and ST based CED versus the sample number for $\gamma = -5$ dB. In counting rule based CED, both $k = m$ and $k = 1$ are investigated. As shown in this figure, the curve of $k = 1$ is fairly lower, and thus the superiority of OR rule over AND rule is verified again. In ST based CED, $P_f = P_m$ is considered, the Monte Carlo curve is obtained by Monte Carlo simulation, and the theoretical curve is calculated by (32). Three phenomena should be emphasized here: (1) Monte Carlo and theoretical curves agree well with each other, which demonstrates the validity of (32); (2) the curves of ST based CED are even lower than that of counting rule based CED with $k = 1$, which shows that ST based CED is faster; (3) the ST curves are concave, and thereby it is possible to find an optimal sample number to minimize the average detection time. Furthermore, we perform numerical search according to (32) and derive the optimal sample number n_{opt} as well as the corresponding minimal detection time $T_{\min}$. Note that the point of $(n_{\text{opt}}, T_{\min})$ is located at the bottom of Monte Carlo curve. Therefore, by properly selecting a sample number as suggested, the proposed ST based CED is able to minimize the average detection time and achieve the highest detection speed.

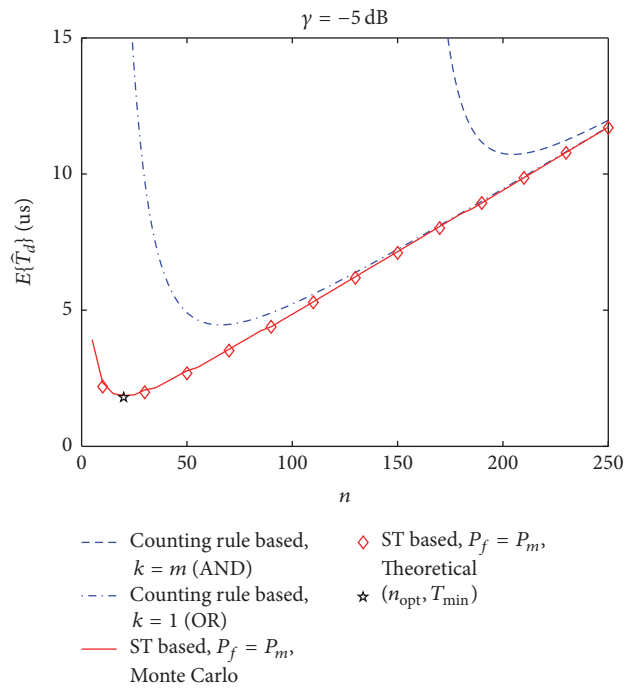

Figure 3: Average detection time of counting rule and ST based CED versus sample number for $\gamma = -5$ dB.

6. Conclusion

This paper has jointly considered two performance metrics of CED and realized fast CED via minimizing the detection time under the constraints on detection accuracy. Some well-proved tools of CED were employed. The counting rule based CED algorithm was discussed. Its detection accuracy and detection time were analyzed. Considering the special cases of counting rule (AND rule and OR rule), we illustrated that the minimal detection time could be achieved by appropriately choosing the number of SUs. Moreover, we proved that, under the same accuracy constraints, OR rule consumed less detection time and was faster than AND rule. Then, by replacing counting rule with ST, the ST based CED algorithm was proposed. This algorithm inherited the benefit of ST and was able to complete PU detection even faster. Its detection time was also analyzed. Via minimizing the detection time, an optimal sample number was deduced, with which ST based CED could obtain the highest detection speed while guaranteeing the desired detection accuracy.

It should be pointed out that although this paper merely illustrates how to combine the detection results of multiple SUs in CR networks, our approach can be applied to the multiantenna scenarios, and how to appropriately combine the outputs of multiple antennas to achieve fast detection is also worth investigating.

Moreover, since the computational complexity of CED also depends on the sample number and the number of SUs, it can be similarly modeled as in (1). Consequently, the performance of computational complexity is similar to that of detection time; that is, ST based CED is the best, and AND rule based CED is the worst.

Conflicts of Interest

The authors declare that there are no conflicts of interest regarding the publication of this paper.

Acknowledgments

This research is supported by the National Natural Science Foundation of China (nos. 61201264, 61362018), China Scholarship Council (no. 201508350023), Fundamental Research Funds for the Central Universities (no. 2242015R20003), Jiangsu Province Postdoctoral Scientific Research Project of China (no. 1402041B), and Huaqiao University (no. 13BS101).

References

[1] S. Filin, T. Baykas, H. Harada, F. Kojima, and H. Yano, "IEEE Standard 802.19.1 for TV white space coexis tence," *IEEE Communications Magazine*, vol. 54, no. 3, pp. 22–26, 2016.

[2] I. F. Akyildiz, W. Lee, M. C. Vuran, and S. Mohanty, "NeXt generation/dynamic spectrum access/cognitive radio wireless networks: a survey," *Computer Networks*, vol. 50, no. 13, pp. 2127–2159, 2006.

[3] R. Tandra and A. Sahai, "SNR walls for signal detection," *IEEE Journal on Selected Topics in Signal Processing*, vol. 2, no. 1, pp. 4–17, 2008.

[4] J. Unnikrishnan and V. V. Veeravalli, "Cooperative sensing for primary detection in cognitive radio," *IEEE Journal on Selected Topics in Signal Processing*, vol. 2, no. 1, pp. 18–27, 2008.

[5] I. F. Akyildiz, B. F. Lo, and R. Balakrishnan, "Cooperative spectrum sensing in cognitive radio networks: a survey," *Physical Communication*, vol. 4, no. 1, pp. 40–62, 2011.

[6] J. Ma, G. Zhao, and Y. Li, "Soft combination and detection for cooperative spectrum sensing in cognitive radio networks," *IEEE Transactions on Wireless Communications*, vol. 7, no. 11, pp. 4502–4507, 2008.

[7] W. Han, J. Li, Z. Li, J. Si, and Y. Zhang, "Efficient soft decision fusion rule in cooperative spectrum sensing," *IEEE Transactions on Signal Processing*, vol. 61, no. 8, pp. 1931–1943, 2013.

[8] W. Choi, M.-G. Song, J. Ahn, and G.-H. Im, "Soft combining for cooperative spectrum sensing over fast-fading channels," *IEEE Communications Letters*, vol. 18, no. 2, pp. 193–196, 2014.

[9] W. Zhang, R. K. Mallik, and K. B. Letaief, "Cooperative spectrum sensing optimization in cognitive radio networks," in *Proceedings of the IEEE International Conference on Communications (ICC '08)*, pp. 3411–3415, May 2008.

[10] Y. Zou, Y.-D. Yao, and B. Zheng, "A selective-relay based cooperative spectrum sensing scheme without dedicated reporting channels in cognitive radio networks," *IEEE Transactions on Wireless Communications*, vol. 10, no. 4, pp. 1188–1198, 2011.

[11] S. Atapattu, C. Tellambura, and H. Jiang, "Energy detection based cooperative spectrum sensing in cognitive radio networks," *IEEE Transactions on Wireless Communications*, vol. 10, no. 4, pp. 1232–1241, 2011.

[12] A. Jamshidi, "Performance analysis of low average reporting bits cognitive radio schemes in bandwidth constraint control channels," *IET Communications*, vol. 3, no. 9, pp. 1544–1556, 2009.

[13] Y.-C. Liang, Y. Zeng, E. Peh, and A. T. Hoang, "Sensing-throughput tradeoff for cognitive radio networks," *IEEE Transactions on Wireless Communications*, vol. 7, no. 4, pp. 1326–1337, 2008.

[14] Y. Zou, Y.-D. Yao, and B. Zheng, "Outage probability analysis of cognitive transmissions: Impact of spectrum sensing overhead," *IEEE Transactions on Wireless Communications*, vol. 9, no. 8, pp. 2676–2688, 2010.

[15] Q. Zou, S. Zheng, and A. H. Sayed, "Cooperative sensing via sequential detection," *IEEE Transactions on Signal Processing*, vol. 58, no. 12, pp. 6266–6283, 2010.

[16] S. Peng, X. Yang, S. Shu, P. Zhu, and X. Cao, "Adaptive sequential cooperative energy detection scheme for primary user detection in cognitive radio," *IEICE Transactions on Communications*, vol. E94-B, no. 10, pp. 2896–2899, 2011.

[17] A. Wald, "Sequential tests of statistical hypotheses," *Annals of Mathematical Statistics*, vol. 16, no. 2, pp. 117–186, 1945.

[18] Y. Zeng and Y.-C. Liang, "Covariance based signal detections for cognitive radio," in *Proceedings of the 2nd IEEE International Symposium on New Frontiers in Dynamic Spectrum Access Networks*, pp. 202–207, IEEE, Dublin, Ireland, April 2007.